Targeting Redox Metabolism of *Leishmania* Parasite for Potential Chemotherapy of Leishmaniasis

A Thesis
Submitted in Partial
Fulfillment of the Requirements for the Degree of

DOCTOR OF PHILOSOPHY

By

Anil Kumar Shukla

Department of Biotechnology
Indian Institute of Technology Guwahati
Guwahati-781039, Assam, India

June, 2012

Dedicated
to
My parents and my mentors

TH-1101_08610603

INDIAN INSTITUTE OF TECHNOLOGY GUWAHATI

DEPARTMENT OF BIOTECHNOLOGY

CERTIFICATE

I hereby declare that the matter embodied in this thesis entitled "***Targeting redox metabolism of Leishmania parasite for potential chemotherapy of Leishmaniasis***" is the result of investigations carried out by me in the Department of Biotechnology, Indian Institute of Technology Guwahati, India under the supervision of Dr. Vikash Kumar Dubey (Supervisor) and Dr. Sanjukta Patra (Co-supervisor).

Keeping with the general practice of reporting scientific observations, due acknowledgements have been made wherever the work of other investigators are referred.

Mr. Anil Kumar Shukla

June, 2012

Roll No: 08610603

TH-1101_08610603

INDIAN INSTITUTE OF TECHNOLOGY GUWAHATI

DEPARTMENT OF BIOTECHNOLOGY

CERTIFICATE

It is certified that the work described in this thesis entitled "***Targeting redox metabolism of Leishmania parasite for potential chemotherapy of Leishmaniasis***" by **Mr. Anil Kumar Shukla (**Roll No: 08610603), submitted to Indian Institute of Technology Guwahati, India for the award of degree of Doctor of Philosophy, is an authentic record of results obtained from the research work carried out under our supervision at the Department of Biotechnology, Indian Institute of Technology Guwahati, India and this work has not been submitted elsewhere for a degree.

Dr. Vikash Kumar Dubey
(Supervisor)

Dr. Sanjukta Patra
(Co-supervisor)

TH-1101_08610603

Acknowledgement

I am thankful to Indian Institute of Technology Guwahati, India and its Department of Biotechnology for providing me the best facilities to carry out my doctoral research. I am also thankful to Indian Institute of Technology Guwahati for research fellowship. I express my sincere thanks to my research supervisors Dr. Vikash Kumar Dubey and Dr. Sanjukta Patra for their valuable guidance throughout my research work. I am indeed indebted to them for giving me an opportunity to work in a very interesting and imperative area of research on "Leishmaniasis". Their continuous encouragement, patience and suggestions gave me a lot of inspiration to carry out my research. I would like to thank them for spending their precious time for discussion by which I have gained immense skills of knowledge. I am fortunate to work under their esteemed guidance as their immense thinking and knowledge made my work fruitful without which this dissertation would not have been possible.

I am thankful to the other members of my Doctoral Committee, Dr. L. Sahoo, Prof. Arun Goyal and Dr Anil Verma for their valuable suggestions and advices which enabled me to improve my work. I am grateful to Dr. Amogh Sahasrabuddhe, CDRI Lucknow and Dr. Hemanta K Majumder, IICB, Kolkata for providing me Leishmania culture and valuable suggestions. I also acknowledge Drs. Andrea Ilari and Gianni Colotti, Università "La Sapienza" Rome, Italy for providing us clone for TR used in the study.

I am grateful to the successive Heads of Department of Biotechnology, Indian Institute of Technology Guwahati, Prof. Pranab Goswami and Prof. Arun Goyal, for providing me with the departmental facilities to carry out my research work. I would also like to thank the technical staff of the department for their help and assistance.

I am thankful to my lab members Dr. Nandini Sarkar, Abhay, Manjeet, Rajesh, Saudagar, Sushant, Shyamali, Mousumi, Shalini, Kavita, Ruchika and Preety as well as ex-lab members Neha and Deblina for their help and co-operation and also for providing a healthy working environment in the lab. I am also thankful to Santhosh, ex-JRF, for his help with the docking studies.

TH-1101_08610603

I owe my special thanks to Swati for helping me with various experiments, providing valuable suggestions and being my motivation. My other friends at IITG especially Amrita, Kumar Pallav, Hanif, A. T. Mostako and Atul deserve special mention for making my stay in the campus lively and enjoyable. Their love and affection has been a constant source of motivation that helped me sail through difficult times.

Last but not the least; I owe personal gratitude to my parents and family members for their endless love, support and encouragement.

Anil Kumar Shukla

June' 2012

TH-1101_08610603

Abbreviations

ATP	:	Adenine triphosphate
Ala	:	Alanine
ANS	:	8-anilino-1-naphthalene sulfonate
cAMP	:	Cyclic Adenine monophosphate
CD	:	Circular dichroism
cGMP	:	Cyclic Guanine monophosphate
CL	:	Cutaneous Leishmaniasis
CM-H_2DCFDA	:	(5-(and-6)-chloromethyl-2,7-dichlorodihydro-fluorescein diacetate acetyl ester)
DCM	:	Dichloro methane
DMEM	:	Dulbecco's minimal essential medium
DMSO	:	Dimethyl Sulfoxide
DTNB	:	(5,5-dithiobis-(2- nitrobenzoic acid)
EDTA	:	Ethylene-diamine-tetraacetic acid
FACS	:	Fluorescence activated cell sorter
FAD	:	Flavin adenine dinucleotide
FBS	:	Fetal bovine serum
FESEM	:	Field emission scanning electron microscopy
FITC	:	Fluorescein isothiocyanate
FTIR	:	Fourier Transform Infrared Spectroscopy
GLX	:	Glyoxalase
Gly	:	Glycine
GR	:	Glutathione reductase
GSH	:	Glutathione
GuHCl	:	Guanidine hydrochloride
HEPES	:	(4-(2-hydroxyethyl)-1-piperazineethanesulfonic acid)
HIV	:	Human Immunodeficiency Virus
HXK	:	Hexokinase
IMP	:	Inosine monophosphate
MALDI	:	Matrix-assisted laser desorption ionization

TH-1101_08610603

MCL	:	Mucocutaneous Leishmaniasis
MG	:	Molten globule
MPEG-PLA	:	Methoxy poly-ethylene glycol-poly lactide
MQ	:	Macrophage
MTT	:	3-(4,5-dimethyl thiazol-2-yl)-2,5-diphenyl tetrazolium bromide
NADPH	:	Nicotinamide adenine di-nucleotide phosphate
NMR	:	Nuclear magnetic resonance
NP	:	Nanoparticle
PFK	:	Phosphofructokinase
PI	:	Propidium iodide
PKDL	:	Post Kala Azar Dermal Leishmaniasis
PMNs	:	Polymorphonuclear cells
PRTase	:	Phosphoribosyl transferase
QR	:	Quinone reductase
RMSD	:	Root Mean Square Deviation
ROS	:	Reactive oxygen species
$T(SH)_2$	:	Trypanothione
TEM	:	Transmission electron microscopy
Px	:	Tryparedoxin peroxidase
TR	:	Trypanothione reductase
TrX	:	Tryparedoxin
VL	:	Visceral Leishmaniasis
WHO	:	World Health Organization
XMP	:	Xanthine monophosphate
XRD	:	X-Ray diffraction

TH-1101_08610603

Contents

TH-1101_08610603

TH-1101_08610603

TH-1101_08610603

TH-1101_08610603

Chapter I

Review of literature on Leishmaniasis: Introduction, Current scenario and Future prospects*.

1.1 Abstract

Leishmaniasis is a life threatening tropical disease caused by *Leishmania sp.*, a protozoan parasite. Leishmaniasis has been ignored for many years mainly because it plagues remote and poor areas. However, recently it has drawn attention of several investigators and active research is going on for antileishmanial drug discovery. The drugs available currently have high failure rates and significant side effects. Recently, liposomal preparations of amphotericin B have been developed and proved to be a better drug, but are very expensive. Miltefosine is one of the few orally administered drugs that are effective against *Leishmania*. However, it has exhibited teratogenicity, hence, should not be given to pregnant women. Thus, the search for novel and improved antileishmanial drugs continues. A rational approach to design and develop new antileishmanials can be implemented to identify several metabolic and biochemical differences between host and parasite that may be exploited as drug target. Moreover, many natural products also have significant antileishmanial activity and are yet to be exploited.

---

*Part of the chapter has been published in ***Applied Biochemistry and Biotechnology***, **2010**, 160, 2208–2218

TH-1101_08610603

1.2 Review of Literature

1.2.1 Leishmaniasis: Overview

Leishmaniasis is mainly a poverty-related disease caused by 20 species of genus *Leishmania*; protozoa transmitted by the bite of a 2 to 3-mm long insect vector female sandfly. In 1901, Leishman identified certain organisms in smear taken from the spleen of a patient who died from "dum-dum fever". At that time "Dum-dum", a town not far from Calcutta, was considered to be particularly unhealthy. The disease was malaria-like, characterized by general weakness, irregular and repetitive bouts of fever, severe anaemia, muscular atrophy and excessive swelling of the spleen. Cunningham, Borovsky, Leishman, Donovan, Wright and Lindenberg separately identified *Leishmania* parasite in different clinical cultures. The link between the disease and kinetoplastids was established by Major Ross (Ross, 1903), who named them *Leishmania donovani.* In 1904, Cathoire and Laveran identified *Leishmania* in children suffering from infantile splenic anaemia. Nicolle named this parasite as *Leishmania infantum*. In 1912, Carini identified *Leishmania* in mucosal lesions of patients with Leishmaniasis in Brazil whereas Bramachari described PKDL (Post kala azar dermal Leishmaniasis) in India in 1922.

The only proven vectors of human disease are the two sandfly species *Phlebotomus* in the Old World and *Lutzomyia* in the New World. Leishmaniasis can be transmitted by blood transfusion, congenitally from mother to infant and by shared syringes among intravenous drug users but, these modes of transmission are rarer than vector-borne transmission. Dogs, sloths, fox and rodents serve as reservoirs for the parasite. This disease was formerly known as Oriental Boil, Baghdad Boil, Black fever, Sand fly disease, Dum-Dum fever, or Espundia (Myler and Fasel, 2008). Figure 1.1 shows geographical distribution of Leishmaniasis. As per World Health Organization statistics, Leishmaniasis currently threatens 350 million men, women, and children in 88 countries around the world. The vector condition for spreading of this disease is most favorable in some parts of Third World countries due to poor living conditions and bad sanitation (Alvar et al., 2006). Over 90% of the cases of Leishmaniasis occur in different parts of India, Bangladesh, Nepal, Sudan and Brazil (Murray, 2002). In India, the state of Bihar accounts for more than 90% of the total reported cases (Bora, 1999). However, human migration and climate change has broadened the ecological niche of *Leishmania*'s vector and currently, human infections are found in 16 countries in Europe including France, Italy, Greece, Malta, Spain and Portugal (Dujardin et al., 2008).

TH-1101_08610603

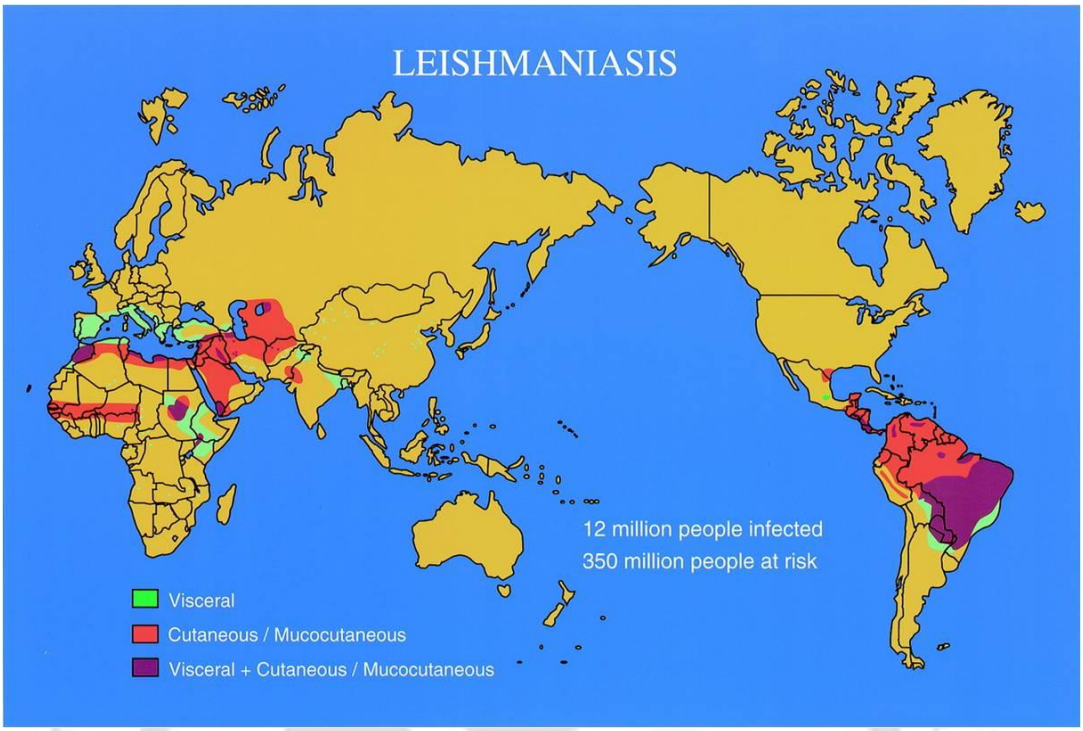

Figure 1.1 Geographical distribution of visceral (green spots) and cutaneous/mucocutaneous (red spots) Leishmaniasis: According to current World Health Organization (WHO) statistics there are 12 million people currently affected by Leishmaniasis in 88 countries on five continents i.e. Africa, Asia, Europe, North America and South America with a total of 350 million people at risk. More than 90% of the visceral Leishmaniasis cases in the world are reported from Bangladesh, Brazil, Sudan, Nepal and India. WHO has placed it in Emerging and Uncontrolled Category I (Adopted with permission from ***Clin Microbiol Rev,*** 2001, 14, 229-243).

In many of the endemic areas, dogs are considered as the major reservoir for human disease, while in other regions, people are the principal reservoir for further human infections (Slappendel and Ferrer, 1998). Dogs appear naturally resistant to this parasite and may remain asymptomatic despite infection (Grosjean et al., 2003).

There are several factors responsible for spread of this disease such as socioeconomic factors, malnutrition, population movements, environmental changes and climatic change. Poverty increases the risk for Leishmaniasis in several ways like poor living habitats (i.e. open sewage, spread of waste and poor sanitary conditions) which provide perfect condition for sandfly breeding. Due to poverty, a large number of people live in small area, which attracts sandflies by providing large amount of blood meals. Protein, iron, vitamin A and zinc deficient nutrition increases the risk of infection by *Leishmania*. Deficiency in these elements leads to failure of the lymph node barrier and

TH-1101_08610603

increased early visceralization of the parasite (WHO/TRS/949, 2010). About 40% of all Leishmaniasis cases in India and Nepal occur in the districts bordering the two countries. Cross border movements of infected population is the primary factor for spread of the disease. Leishmaniasis is a climate-sensitive disease and is critically affected by changes in rainfall, atmospheric temperature and humidity. *Leishmania* co-infection with HIV is non-curable and intensifies the burden of visceral and cutaneous Leishmaniasis by causing severe forms that are more difficult to manage. *Leishmania* leads to infection-mediated immunosuppression and inhibits host defence system due to a massive parasite burden. Cell-mediated immune hypersensitivity due to *Leishmania* infection produces disfiguring chronic mucosal and cutaneous disease whereas reticuloendothelial hyperplasia occurs in case of visceral Leishmaniasis. Both *Leishmania donovani* and *Leishmania infantum* affect all the lymphatic tissues including spleen, liver, mucosa of the small intestine, bone marrow, lymph nodes and other lymphoid tissues. The lifespan of leukocytes and erythrocytes is reduced causing granulocytopenia and anaemia. Diarrhoea may occur as a result of intestinal parasitization and ulceration or secondary enteritis. Advanced stage of infection causes pneumonia, dysentery and tuberculosis.

1.2.2 Types of the disease

Depending on the infecting species, three different forms of Leishmaniasis occur in human being (Figure 1.2). Each of these forms exhibits a diverse and wide range of clinical symptoms. These forms are Cutaneous (CL), Mucocutaneous (MCL) and Visceral Leishmaniasis (VL). The VL, also known as kala-azar, is caused by *Leishmania donovani* and *Leishmania infantum* and is fatal if untreated. In case of VL, the parasites reside in the liver, spleen and bone marrow causing a severe systemic disease. Other two forms, CL and MCL, are not fatal and cause ulcers on the face, arms and legs. They heal slowly but leave scars or cause disfiguring. The causative *Leishmania* species of CL are *Leishmania major, Leishmania tropica, Leishmania ethiopica, Leishmania braziliensis, Leishmania panamensis, Leishmania amazonensis* and *Leishmania mexicana* (Croft and Coombs, 2003).

1.2.2.1 Cutaneous form: This form of the disease is characterized by skin ulcers on the exposed parts of the body such as the face, arms and legs. There may be large number of lesions, sometimes up to 200, causing serious disability and invariable scars which lead to social prejudice (Reithinger et al., 2007).

TH-1101_08610603

1.2.2.2 Mucocutaneous form: MCL produces lesions causing partial or total destruction of the mucous membranes of the nose, mouth and throat cavities. This form of Leishmaniasis can result in victims being humiliated and neglected from society.

1.2.2.3 Visceral forms: This is the most lethal form of the disease, also known as kala azar, dum fever, espundia etc. and is characterized by irregular bouts of fever, substantial weight loss, swelling of the spleen and liver and anaemia. Darkening of the skin of face, hands, feet and abdomen is typically found in India (the Hindi name, kala-azar, means 'black fever' or 'deadly fever'). If left untreated, person may die quickly. About 50% of patients with kala-azar develop PKDL (Post kala azar dermal Leishmaniasis) in all areas endemic for *Leishmania donovani* mostly in East Africa and on the Indian subcontinent.

Figure 1.2 Types of Leishmaniasis: (A) Cutaneous Leishmaniasis and **(B)** Mucocutaneous Leishmaniasis (Adopted with permission from ***Lancet Infect Dis***, 2007, 7, 581–596), **(C)** Visceral Leishmaniasis (WHO/TDR/Crump, 2010).

Leishmaniasis also occurs in dogs (termed as canine Leishmaniasis) and its clinical symptoms include loss of hair, weight loss, fever, anorexia, cutaneous lesions and death (Lindsay and Zajac, 2002)

1.2.3 Life Cycle of Leishmania parasite

The life cycle of *Leishmania* parasite involves two forms, promastigote and amastigote. Promastigote stage of parasite is injected into the human host by infected sandfly. The promastigotes are first phagocytosed by macrophages where they get transformed into amastigote, multiplied and then released into systemic circulation (Figure 1.3). The amastigote form is circular, about 5 microns in diameter, has a nucleus, kinetoplast and rudimentary flagellum. It repeatedly multiplies by binary fission until the host cell is destroyed. When sandflies bite an infected host, it intakes amastigotes.

TH-1101_08610603

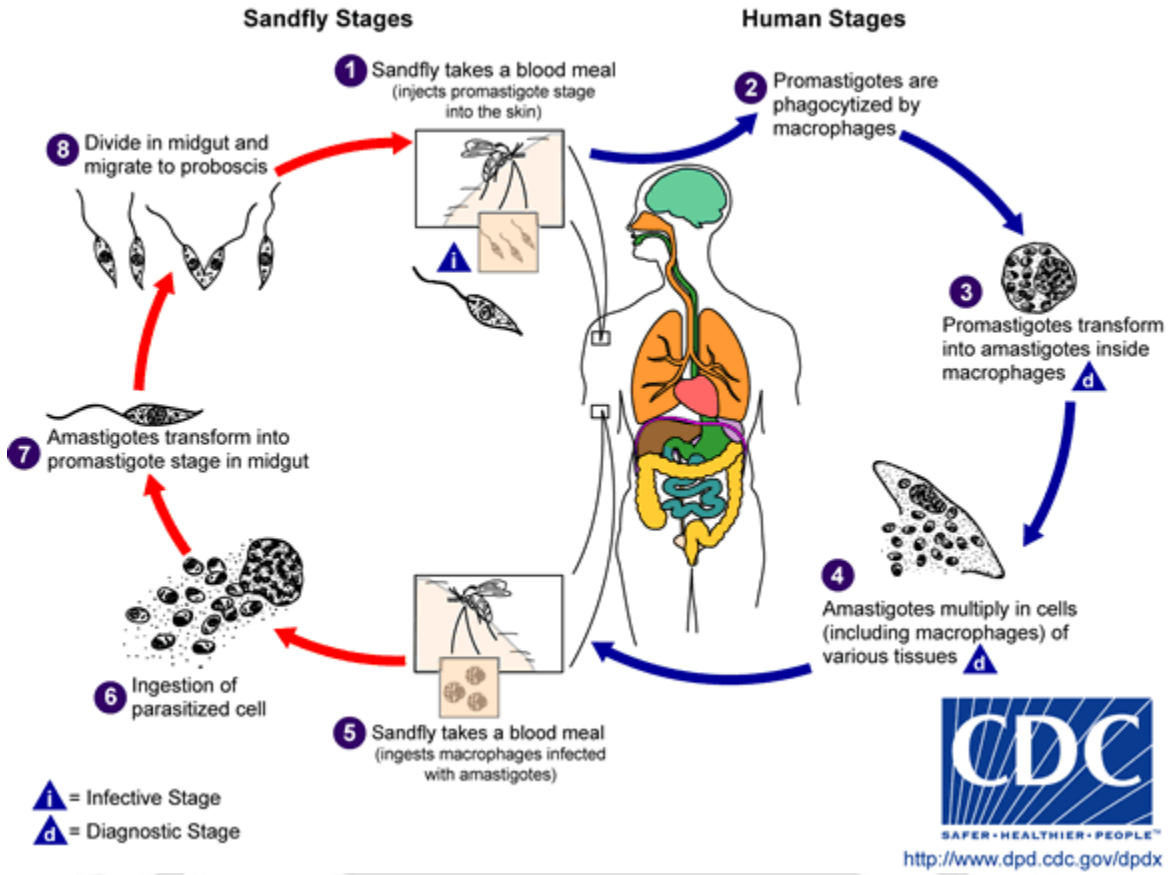

Figure 1.3 Life Cycle of *Leishmania*: Elongated and flagellar promastigote stage resides inside *Phlebotamine* midgut. It injects promastigotes into the blood; they enter into phagocytes (macrophages) and get converted to non-motile amastigote stage. Amastigotes multiply by binary fission until cell ruptures and are recycled to sandfly (http://www.dpd.cdc.gov/dpdx).

These parasites differentiate into so-called promastigote form in the vector's midgut which multiplies and finally migrates to the fly's proboscis (Pearson and de Queiroz, 1996). Thus the main cellular forms of *Leishmania sp*. as defined by cell shape, flagellum and basal body, kinetoplast and nucleus are promastigote and amastigote. In general, the promastigote form of digenetic trypanosomatid is found in the vector and the amastigote form is intracellular (Figure 1.4).

1.2.3.1 Promastigote stage: Promastigote lives in the midgut of sand flies. Fusiform, elongated (14.3-20 µm by 1.5-1.8 µm) with flagellum extending forward as a locomotory organelle.

1.2.3.2 Amastigote stage: Amastigote (Leishmania form or Leishman-Donovan body) is 2.9-5.7 µm by 1.8-4.0 µm in size, round, non-flagellated form, lives within macrophages

TH-1101_08610603

and other mononuclear phagocytes of human body (spleen, liver, bone marrow and lymph nodes).

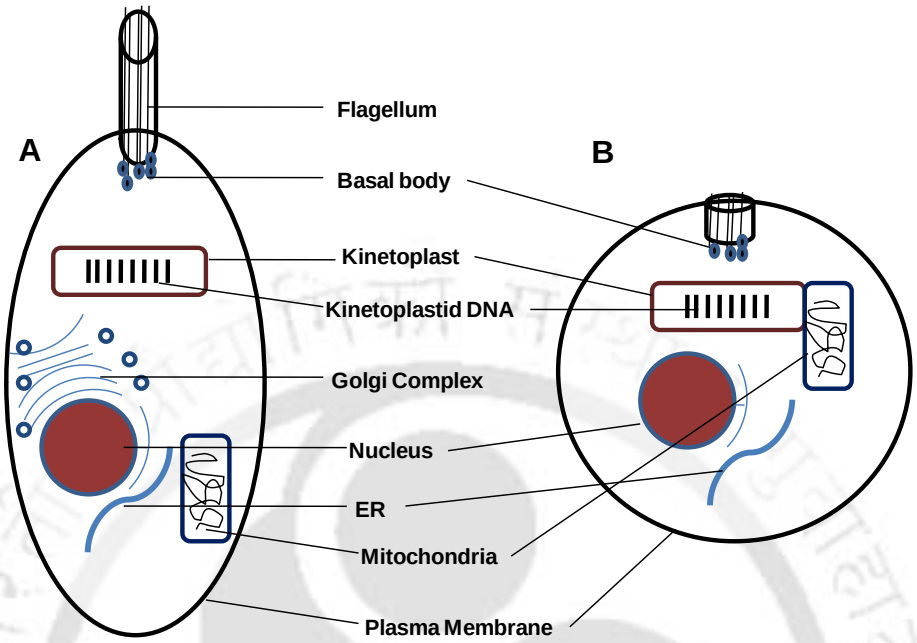

Figure 1.4 Life stages of *Leishmania*: (A) Ultra-structure of promastigote stage of *Leishmania sp.*: It resides inside midgut of the sandfly and has flagellum, DNA, kinetoplast, mitochondria, nucleus etc. **(B)** Ultra-structure of amastigote stage of *Leishmania sp.*: It resides inside macrophages and has spherical shape with same cellular components as promastigote stage except locomotary flagellum.

Therefore, promastigote is the infective stage whereas, amastigote stage inactivates macrophage's defense mechanism

1.2.4 Current therapeutic approaches

The treatment of Leishmaniasis strongly relies upon pentavalent antimonials, sodium stibogluconate (Pentostam) and meglumine antimoniate (Glucantime), which were introduced in the first half of the century for treatment of cutaneous and mucocutaneous Leishmaniasis by Vianna in Brazil (Da Silva, 2005) and for visceral Leishmaniasis by Di Cristina and Caronia in Italy (Di Cristina and Caronia, 1915). Bramachari identified urea stibamine as a pentavalent antimonial drug in 1922 for treatment of all forms of Leishmaniasis. Sodium stibogluconate (10% Sb) and meglumine antimoniate (8.1% Sb) are chemically similar. They are given as intramuscular or intravenous injections and have risk of subsequent thrombosis. They are also administered intralesionally for the treatment of cutaneous Leishmaniasis. Several side-effects are associated with these

TH-1101_08610603

pentavalent drugs like abdominal pain, headache, anorexia, vomiting, nausea, metallic taste, lethargy and serious and fatal cardiac arrhythmia. In 1970s patients infected with visceral Leishmaniasis stopped responding to pentavalent treatment. The clinical isolates of *Leishmania* from those patients proved their resistance against antimonial compounds.

Amphotericin B emerged as a second line of drug. It also includes several life threatening side effects like infusion reactions and fever with rigor and chills. Thrombophlebitis of the injected vein and nephrotoxicity is also common, leading to frequent interruption of treatment in some patients. Some other serious toxic effects of amphotericin B are hypokalaemia and myocarditis. Paromomycin is another drug given as intramuscular injection. It causes severe pain at the injection site, hepatotoxicity and renal toxicity. The mechanism of action of these drugs is not clearly understood, but they are reported to have significant side effects (Mattock, 1999). Pentostam is the recommended treatment for visceral Leishmaniasis but is toxic and parasite has developed resistance against it (Croft, 1988; Grogl et al., 1992). Moreover, failure rates of these drugs are quite high (approximately 10–25% in all cases), except in state of Bihar (India), where the failure rate is >60%.

The new and first ever oral drug is Miltefosine, a phosphocholine analog, which was originally developed as an antimalignant drug. It has been found to be highly active against *Leishmania in vitro* as well as in animal model. However, miltefosine induces gastrointestinal side-effects such as vomiting, anorexia, nausea and diarrhoea. It is also potentially teratogenic and should not be given to pregnant women. Miltefosine and Amphotericin B appear to be better treatment options, but problem of resistance and side effects remain uncracked (Sinha et al., 2006). High cost precludes the use of miltefosine and the latter, Amphotericin B is also teratogenic, thus not recommended for pregnant women (Berman, 2003). Paromomycin sulfate (Humatin) is another drug which has been approved recently and has achieved curing rates similar to those with amphotericin B in patients with VL with similar side effects (Sundar et al., 2007). Strucutres of few commonly available drugs are shown in Figure 1.5.

Several attempts have been made to develop first generation and second generation vaccines with whole killed parasites or extracts and recombinant proteins respectively.

TH-1101_08610603

The results have been inconclusive or negative for prophylaxis. The above discussion is indicative of the urgent need to identify new antileishmanial compounds.

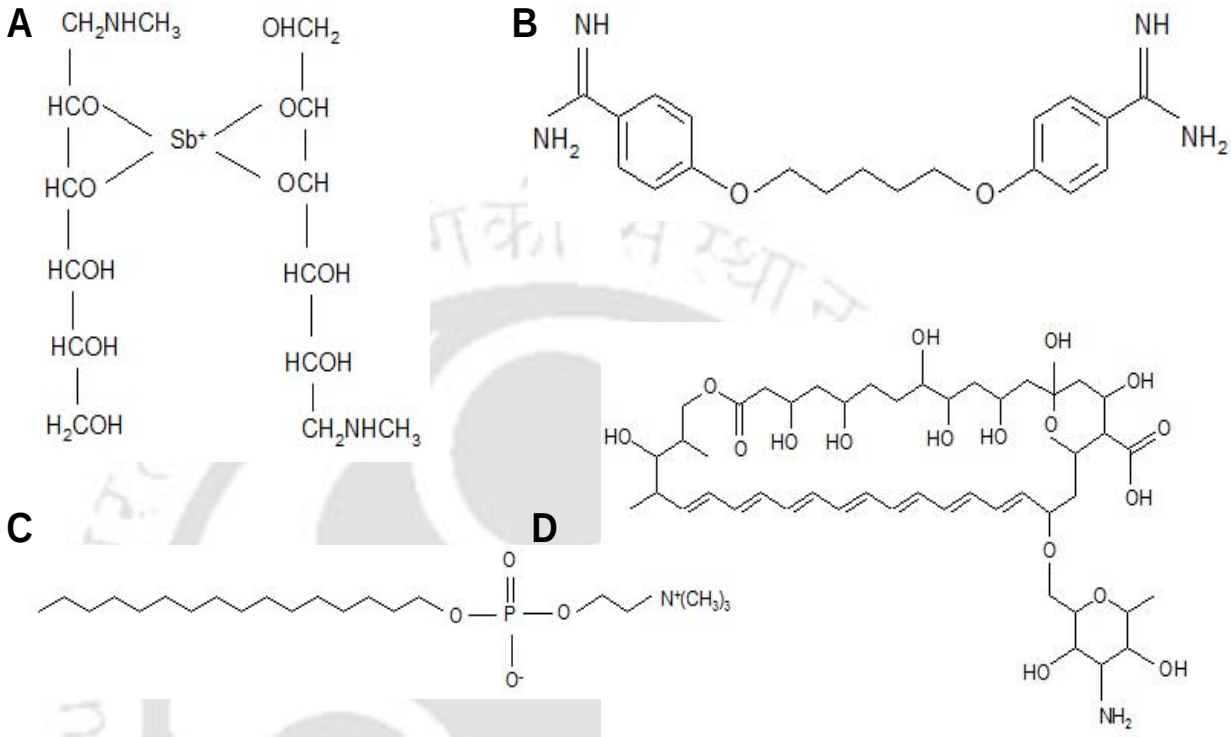

Figure 1.5 Current pharmacological treatments for Leishmaniasis: (A) Meglumine antimoniate (Glucantime), **(B)** Pentamidine, **(C)** Miltefosine (hexadecylphosphocholine) and **(D)** Amphotericin B. Current therapeutics against Leishmaniasis are mainly dependent upon antimony based drugs (e.g. meglumine antimoniate). Parasite has developed resistance against antimonials. Moreover, current drugs are toxic (e.g. Amphotericin B) and expensive (e.g. Miltefosine).

1.2.5 Antileishmanial drug discovery by targeting various metabolic pathways

1.2.5.1 Trypanothione Metabolism of Leishmania parasite: A rational approach to design and develop new antileishmanials has identified several metabolic and biochemical differences between host and parasite which may be exploited as drug target. One such validated drug target is trypanothione reductase (Dumas et al., 1997).

TH-1101_08610603

In mammals, glutathione (γ-glutamyl-cysteinyl-glycine; GSH) metabolism is the principle route of removal of reactive oxygen intermediates such as the superoxide anion radical (O_2^-), hydrogen peroxide (H_2O_2), peroxynitrite ($ONOO^-$), and the hydroxyl radical (HO^-) produced by cellular respiratory process or by external agents (Figure 1.6).

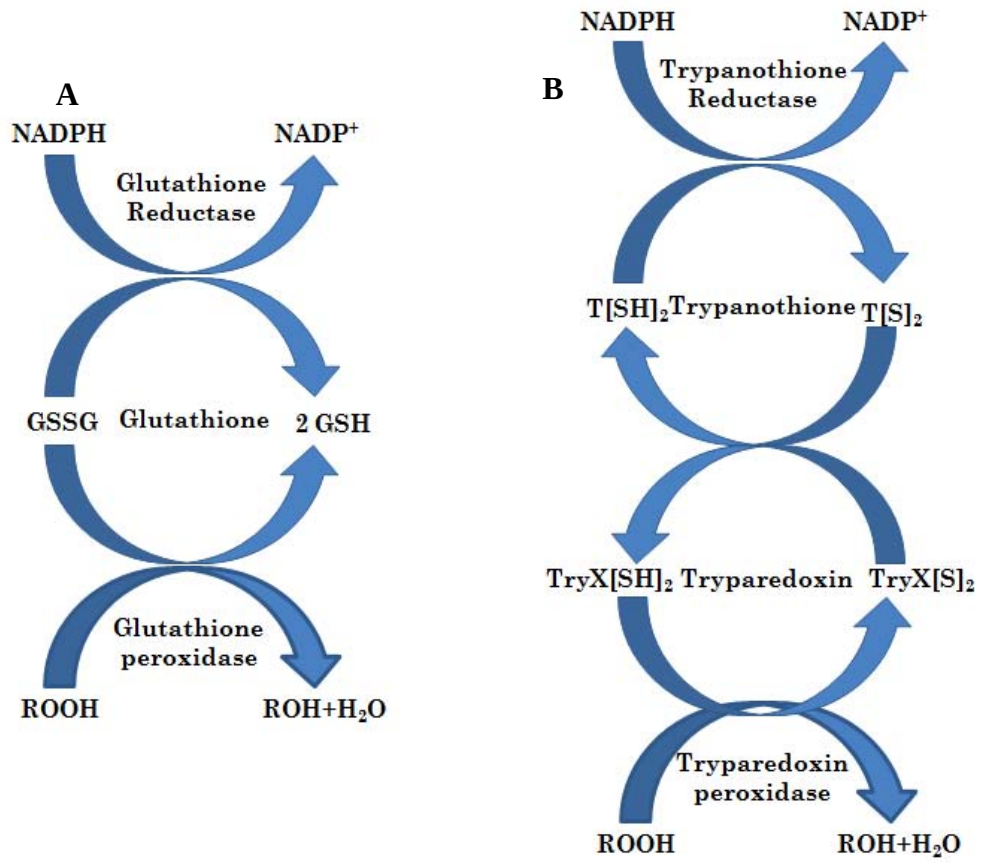

Figure 1.6 Differences between redox metabolism of host and parasite: (A) Glutathione metabolism in mammalian hosts**, (B)** Trypanothione metabolism in parasite. The principle route of removal of oxygen-reduction intermediates in mammalian cells involves selenium dependent glutathione peroxidase (EC 1.11.1.9) working in concert with reduced glutathione, glutathione reductase and NADPH (Flohe et al. 1999). However, the protozoan parasites of genera *Leishmania* rely on cascade of three enzymes: trypanothione synthetase (TryS), trypanothione reductase (TR) and tryparedoxin peroxidase (Px) working in concert with trypanothione (N^1, N^8-bis(glutathionyl)-spermidine), tryparedoxin (TryX) and NADPH .

Glutathione synthetase (GS) is one of the important enzymes involved in synthesis of glutathione. The enzyme that reduces glutathione (GSH), nicotinamide adenine dinucleotide phosphate (NADPH) dependent glutathione reductase (GR), is constitutively active and inducible upon oxidative stress. Oxidized GSH is reduced immediately and is found mainly in its reduced form. Selenium-dependent glutathione peroxidase reduces

TH-1101_08610603

reactive oxygen intermediates and converts GSH to GSSH (Flohe et al., 1999). However, *Leishmania* parasite lacks this antioxidant defense mechanism and relies on cascade of three enzymes: trypanothione synthetase (TryS), trypanothione-recycling flavoprotein trypanothione reductase (TR) and tryparedoxin-recycling enzyme tryparedoxin peroxidase (Px), working in concert with trypanothione {$T(SH)_2$} (N^1, N^8-bis (glutathionyl)-spermidine), tryparedoxin (TrX) and NADPH. TryS catalyzes $T(SH)_2$ synthesis from GSH and spermidine. The $T(SH)_2$ occurs exclusively in parasitic protozoa of the order kinetoplastida such as trypanosomes and leishmania.

$T(SH)_2$ is a reductant of thioredoxin (TrX) and tryparedoxin (TXN), small dithiol proteins, which in turn deliver reducing equivalents for the synthesis of deoxyribonucleotides as well as for the detoxification of hydroperoxides by different peroxidases. $T(SH)_2$ is maintained in reduced form by TR in presence of NADPH, which in turn reduces TXN followed by reduction of Px (Figure. 1.7) (Krauth-seigel and Comini, 2008). The active Px is then used to catalyze the reduction of hydrogen peroxide and organic hydro-peroxides to water and alcohol (Alphey et al., 2000).

The trypanothione system is central for any thiol regeneration and TR has been shown to be an essential enzyme in these parasites. TR and Px are analogous to mammalian GR and glutathione peroxidase (GPX) whereas TryS is analogous to glutathione synthetase (GS). They are the novel targets for development of new drugs by rational inhibitor design. The crystal structure of different proteins, involved in redox system of *Leishmania*, is given in Figure 1.8. Dumas et al. (1997) have investigated further the physiological role of TR in *Leishmania* and tried to create TR-knockout mutants by gene disruption in *Leishmania donovani* and *Leishmania major* strains using the selectable markers neomycin and hygromycin phosphotransferases. The experiment has established that the enzyme is essential for survival of the parasite.

A lot of research has been focussed on identification of specific inhibitors of TR. However, most of the research is concentrated on other trypanosomal species and may not be inhibitory against TR from *Leishmania sp.* due to minute difference in structure. Bonse et al. (1999) have evaluated series of 9-amino and 9-thioacridines as inhibitors of TR from *Trypanosoma cruzi*.

TH-1101_08610603

The compounds are structural analogs of the acridine drug mepacrine (quinacrine), which is a competitive inhibitor of TR, but not of human GR. 9-Aminoacridines are competitive inhibitors of TR with more than one binding site, while 9-thioacridines inhibit TR with mixed-type kinetics (Bonse et al., 1999).

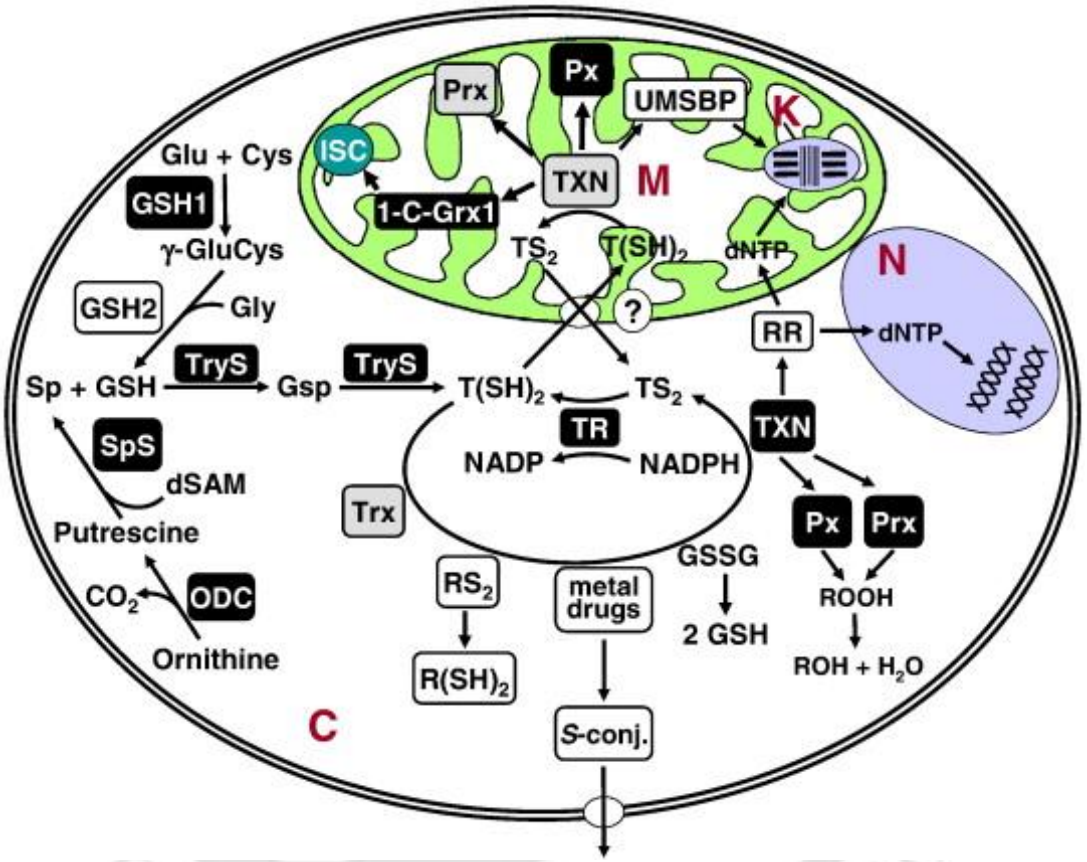

Figure 1.7 Trypanothione Metabolism in *Leishmania*: In presence of trypanothione synthase (TryS) enzyme, two glutathione moieties are linked together with spermidine linkage to form trypanothione {$T(SH)_2$}. Trypanothione reductase (TR) maintains reduced {$T(SH)_2$} which is responsible for detoxification of hydroperoxides and synthesis of DNA precursors through tryparedoxin protein. (Adopted with permission from ***Biochim Biophys Acta,*** 2008, 11, 1236-1248)

Recently, quaternized analogs of the 2-chlorophenyl sulfides are also reported to be antileishmanial and suggested to be the inhibitor of TR (Parveen et al., 2005). The bisbenzylisoquinoline alkaloids were also investigated as potent inhibitors of TR and trypanocidal agents (Fournet et al., 1993).

TH-1101_08610603

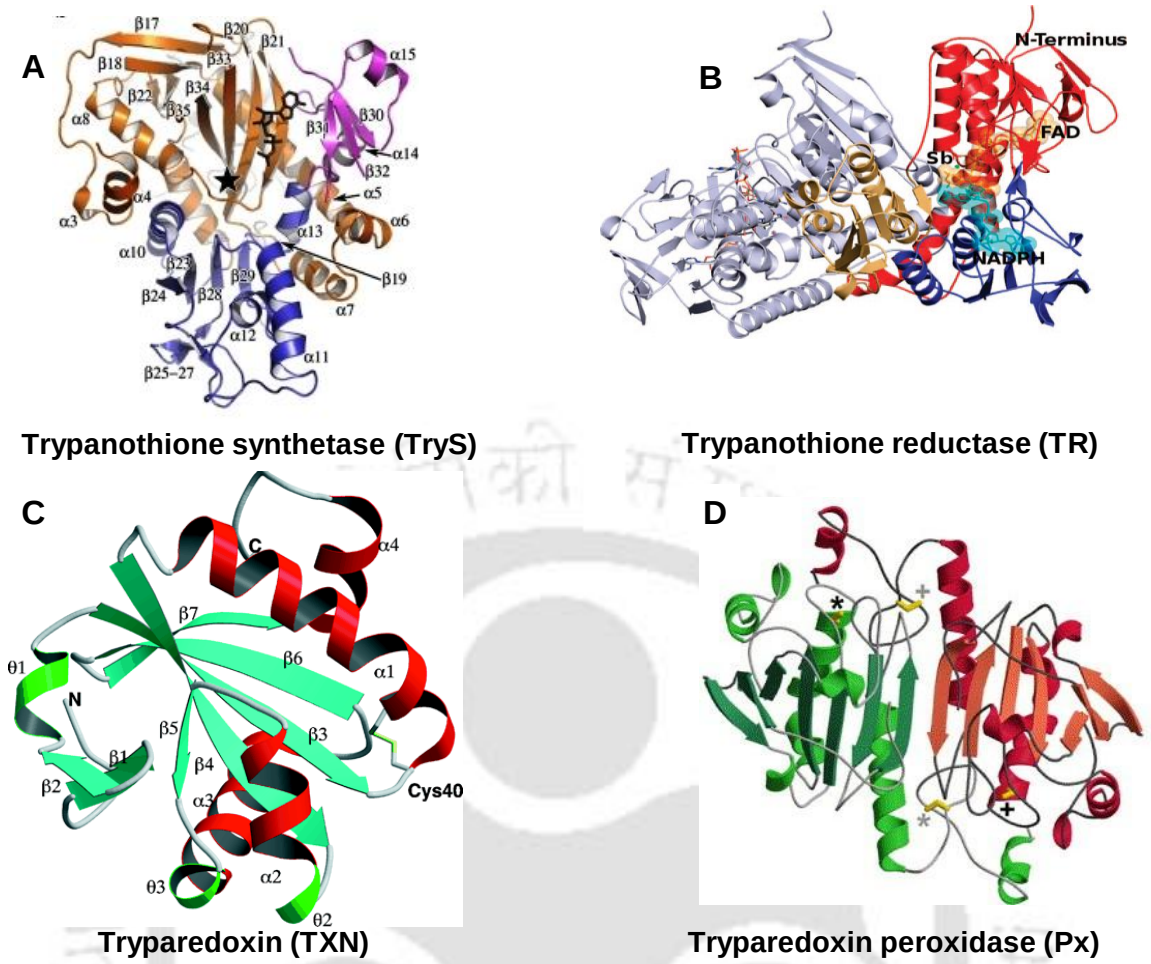

Figure 1.8 Structures of proteins involved in thiol metabolism of *Leishmania:* (A) Crystal structure of trypanothione synthetase (TryS) (Adopted with permission from ***J Biol Chem,*** 2008, 283, 17672-17680). **(B)** Crystal structure of trypanothione reductase (TR) (Adopted with permission from ***J Med Chem,*** 2009, 52, 2603–2612**). (C)** Crystal structure of tryparedoxin protein (TXN) (Adopted with permission from ***J Biol Chem,*** 1999, 274, 25613-25622). **(D)** Crystal structure of tryparedoxin peroxidase (Px) (Adopted with permission from ***J Struct Biol,*** 2005, 150, 11-22).

Antimicrobial chlorhexidine {1, 1′-hexamethylenebis [5-(4-chlorophenyl) biguanide]} is also known to be an inhibitor of TR (Meiering et al., 2005). Only few animal studies have been reported on these compounds. It has been found that only phenothiazines and related tricyclic antidepressants are shown to reduce parasitic burden in infected mice. Most of the other compounds are not effective, most likely because they get metabolized in the body. Thus, search for new class of TR inhibitor is still on. Moreover, inhibitory effect of these compounds against *Leishmania* TR needs to be evaluated.

1.2.5.1.1 Trypanothione Reductase enzyme: A potential drug target: TR (E.C. 1.6.4.8) and GR (E.C. 1.6.4.2) both belong to the protein family of FAD-dependent NADPH oxido reductase (Williams, 1992) and share close structural and mechanistic similarities.

TH-1101_08610603

TR is a dimeric protein with monomeric molecular mass of 52 kDa. TR comprises of FAD-binding domain, NADPH-binding domain and interface domain (Figure 1.9) forming two identical active sites. Active site involves FAD, NADPH and central domains of one monomer and the interface domain of the other (Khan, 2007). TR is a NADPH-dependent flavoprotein unique to protozoan parasites from the genera *Trypanosoma* and *Leishmania*. Mammals use their most abundant thiol, the tripeptide glutathione (L-γ-glutamyl-L-cysteinyl glycine; GSH), to regulate intracellular reducing environment and protect biological molecules from oxidative stress by getting oxidized to glutathione disulfide (GSSG) via flavoenzyme GR (Meister, 1989). Glutathione is not the principal thiol in trypanosomes and these protozoa do not possess GR. Instead, the metabolites $T(SH)_2$, N^1-glutathionyl- spermidine (GspdSH) and the auxiliary enzyme TR maintain the reducing environment in protozoan cells. TR and GR both catalyze transfer of electrons from NADPH to their specific substrates via FAD prosthetic group and a redox-active cysteine disulfide (Ghisla and Massey, 1989a; Borges et al., 1995; Fairlamb et al. 1985; Shames et al. 1986; Benson et al. 1992; Hunter et al. 1992; Schirmer et al. 1995).

Although TR and GR are analogous enzymes and they perform same physiological function and they have 40% of sequence similarity, yet several characteristic differences account for the selectivity of inhibitors against these two enzymes such as charge difference of their active sites, different amino acid residues as well as size of the active site. In trypanosomatids, $T(SH)_2$ differs from GSSG by the presence of a spermidine cross-link between the two glycyl carboxyl groups (Fairlamb and Cerami, 1992).

There are also several differences in the active site of GR and TR such as TR possesses a negatively charged active site with an overall charge of -2 due to presence of an extra protonated amino group in $T(SH)_2$. Whereas, GR has positively charged active site due to two extra carboxylate groups in GSSG. The amino acid residues, playing major role in substrate specificity, are also different i.e. Ala34 of GR is replaced by Glu19 in TR, Arg37 by Trp22, Arg347 by Ala343, and Asn117 by Met114. Moreover, TR has a larger active site compared to GR in order to accommodate its bulkier substrate (Figure 1.10).

TH-1101_08610603

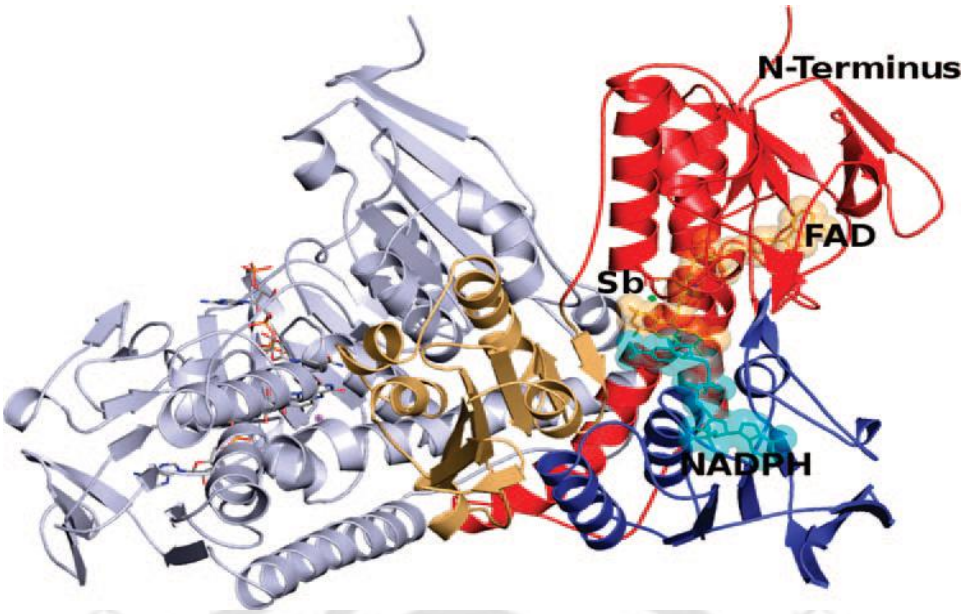

Figure 1.9 Crystal Structure of *L. infantum* TR in oxidized form: One monomer of the dimer is colored grey. In the other monomer, the FAD binding domain (residues 1-160 and 291-360) is red, the NADPH binding domain (residues 161-290) is blue and the interface domain (361-488) is yellow-orange. The FAD and NADPH cofactors are indicated in stick, and Sb (III) is indicated as a green sphere**.** (Adopted with permission from ***J Med Chem,*** 2009, 52, 2603–2612**)**

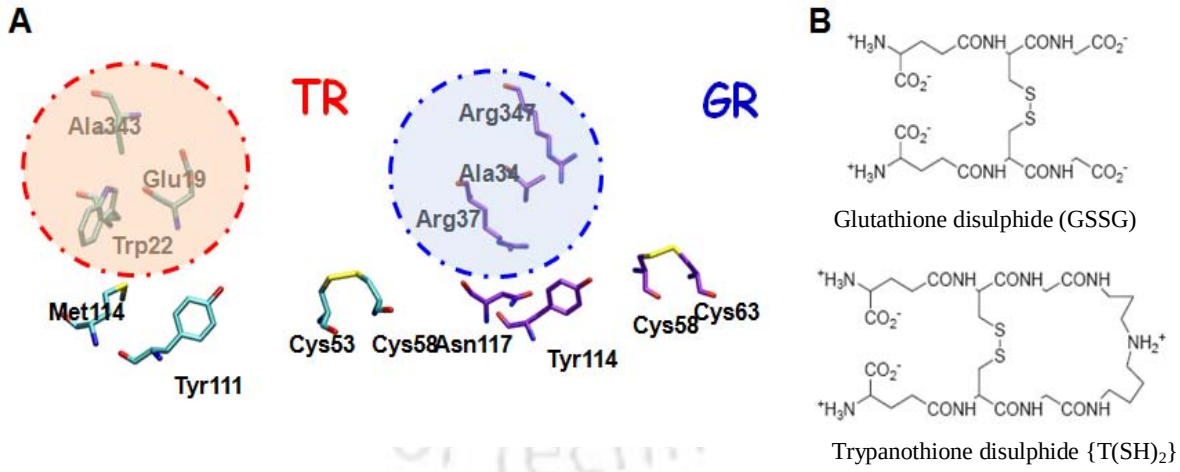

Figure 1.10 Differences in active site and substrate specificity of Trypanothione reductase (TR) and Glutathione reductase (GR): **(A)** Differences in active site residues of TR and GR, Ala343 Glu19 and Trp22 in TR is substituted with Arg 347, Ala34 and Arg 37 in GR. **(B)** Structure of glutathione (GSSG), substrate for GR and trypanothione $\{T(SH)_2\}$, substrate for TR. $T(SH)_2$ is having overall positive charge whereas GSSG is negatively charged. Thus, active site of TR is negative whereas that of GR is positive.

TH-1101_08610603

Thus, due to these fundamental differences, TR may be proposed and amplified further as a target for rational designing of antitrypanosomal and antileishmanial drugs without interfering with the biological function of GR. Several inhibitors of TR have been reported such as tricyclic antidepressants (Benson et al., 1992; Garforth et al., 1997), polyamine conjugates (O'Sullivan et al., 1997), substrate analogues (Tromelin et al., 1993) and chemically synthesized peptide inhibitors (Dixon et al., 2005), but most of these drugs have limited use due to their toxicity, high cost and parasitic resistance.

1.2.5.2 Methylglyoxal metabolism: Methylglyoxal, a highly active dicarbonyl glycolytic byproduct, causes mutagenesis and cytotoxic effects by reacting with nucleophilic centers of RNA, DNA and proteins. In all mammalian cells, the detoxification of methylglyoxal solely depends on an universal glyoxalase system which involves a sequential action of glyoxalase I (Glx1; EC 4.4.1.5) and glyoxalase II (Glx2; EC 3.1.2.6) in concert with a tripeptide glutathione as cofactor (Thronalley et al., 1996). However, trypanosomatids rely on an analogous trypanothione-dependent glyoxalase system in which Glx1 catalyzes formation of S-D lactoyltrypanothione from the hemithioacetal which is formed non-enzymatically from methylglyoxal and reduced trypanothione. In the next step, Glx2 catalyzes an irreversible hydrolysis of S-D-lactoyltrypanothione to D-lactate and regenerates trypanothione (Vickers et al., 2004). Although the trypanosomatids and their mammalian host, both have similar glyoxalase system, yet difference in their substrate specificity indicates that Glx1 or Glx2 could be a potential target for antitrypanosomatid chemotherapy. Moreover, the glyoxalase system has already been proposed as an interactive target for anticancer (Thronalley et al., 1996) and antimalarial (Vickers et al., 2004) chemotherapy. Thus, the inhibition of the trypanothione-dependent glyoxalase pathway of *Leishmania sp.* may be a possible solution for antileishmanial chemotherapy.

1.2.5.3 Parasite Glycolysis: The energy metabolism of trypanosomatids solely depends on the available carbon sources in their hosts. The amastigote form of *Leishmania sp.* uses glucose of mammalian bloodstream and fatty acids of lysosomal compartment of macrophages as energy source. The insect stage of *Leishmania sp.* (promastigote) encodes an amylase to obtain energy from amino acid catabolism and a sucrase-like protein for digestion of disaccharides taken in by the sand flies feeding on nectar or honeydew. The metabolic adaptation to the rapid environmental changes caused by transmission of parasite between vertebrate host and insect is regulated by peroxisomes-

TH-1101_08610603

like organelles called glycosomes (Bringaud et al., 2006). The net APx production in glycolytic pathway from glucose to pyruvate results in autocatalysis of hexokinase (HXK) or phosphofructokinase (PFK) that in-turn causes accumulation of hexose phosphate intermediates to lethal levels. In trypanosomatids, the unique compartmentalization of glycolysis within glycosomes regulates HXK and PFK catalysis in order to avoid the negative side effect of autocatalytic design of glycolysis. In other organisms, this is performed by a feedback inhibition of HXK and PFK (Haanstra et al., 2008).

Glycosomes contain seven glycolytic enzymes catalyzing conversion of glucose to 3-phosphoglycerate and the consumption and production of APx is balanced. The net APx synthesized in cytosolic portion of remaining glycolytic pathway is inaccessible through glycosomal membrane for HXK or PFK. Hence, the compartmentalization of glycolysis provides an alternative mechanism to prevent accumulation of toxic level of glycolytic intermediates such as glucose 6-phosphate, fructose 6-phosphate and fructose 1, 6-bisphosphate (Michels et al., 2006). This unique organization of glycolytic pathway in *Leishmania sp.* and its large evolutionary distance to mammalian host indicates the occurrence of unique structural and functional features of intermediate enzymes in parasite. Thus, these enzymes could be potential targets for antileishmanial drug.

1.2.5.4 Purine Salvage Pathway: Purines and pyrimidines are very important components of metabolism for all living organisms. They perform many vital functions inside the cell such as APx provides energy for different cellular processes, purine and pyrimidine nucleotides help in synthesis of both carbohydrates and lipids, cAMP and cGMP are key second messenger molecules, several vitamins having nucleotide moiety work as cofactors and nucleoside triphosphates are the immediate precursors for DNA and RNA synthesis. All parasitic protozoa, including *Leishmania sp.*, lack the ability to synthesize purine nucleotides *de novo* and absolutely rely on an unique salvage pathway to obtain purine bases from their mammalian hosts. In *Leishmania sp.*, in the first step of this process, purine bases are transported across parasite membrane by two kinds of nucleoside transporters, LdNT1 and LdNT2, present on cell surface (Datta et al., 2008). LdNT1 is present in both promastigote and amastigote stages of the parasitic life cycle and transports adenosine/ pyrimidine nucleoside, while LdNT2 is present in amastigote stage and specifically transports only purine nucleosides (Aronow et al., 1987). Since

TH-1101_08610603

these purine transporters have an important role in nucleoside transportation within cells, they could be a potential route for delivery of analogous cytotoxic drug in *Leishmania sp*.

The enzymes adenine deaminase and guanine deaminase catalyze the conversion of adenine and guanine to hypoxanthine and xanthine respectively, which in turn are converted to inosine monophosphate (IMP) and xanthine monophosphate (XMP) by phosphoribosyl transferase (PRTase) activity of adenine phosphoribosyl transferase (APRTase), hypoxanthine-guanine phosphoribosyl transferase (HGPRTase) and xanthine phosphoribosyl transferase (XPRTase). Adenylosuccinate synthetase and adenylosuccinate lyase convert IMP to AMP, whereas XMP is converted to GMP by GMP synthetase (Glew et al., 1988).

Moreover, it has also been reported that *Leishmania sp.* contains trace amount of nucleoside kinase, which can directly convert nucleosides to mononucleotides. The formation of nucleotides of hypoxanthine and xanthine are the initial steps of purine salvage in *Leishmania donovani.* While purines are efficiently conserved by this parasite, the salvage of pyrimidines is not so dramatic (Lafon et al., 1985). Thus, various alternative purine salvage pathways exist in the parasite and inhibition of a single enzyme would not be lethal for them. Therefore, a chemotherapeutic agent that can inhibit more than one enzyme of purine salvage pathway could be an alternative solution of antileishmanial chemotherapy.

TH-1101_08610603

Table 1.1 Summary of studies on various pathways/targets for antileishmanial compounds.

Sr. No.	Pathway	Targets	Inhibitors/compounds	Mode of Inhibition	Reference
1	Trypanothione metabolism	Trypanothione reductase	Pentavalent antimonial compounds, e.g., sodium stibogluconate and meglumine antimoniate	It boosts IFN gamma and T-cell production inducing a strong Th1 response,	Singh et al., 2009
			Melarsoprol	Melarsoprol forms covalent complex with trypanothione reductase thus inactivating it and exposing parasite to oxidative stress.	Croft and Coombs, 2003
			Kukoamine A (a natural hypertensive agent) , isolated from *Lycium chinense*	Mixed-type inhibition of trypanothione reductase (TR)	Khan, 2007
			Acridine drug mepacrine (quinacrine)	Competitive inhibitor of TR	Bonse et al., 1999
			9-Aminoacridines and 9-thioacridines	9-Aminoacridines are competitive inhibitors of TR with more than one binding site while 9-thioacridines inhibit TR with mixed-type kinetics	Fournet et al., 1993
			Clomipramine	Competitive inhibitor of TR	Benson et al., 1992
			Altenusin (a biphenyl from *Alternaria sp*.)	Inhibitor of TR	Cota et al.,2008
			Iridoid glucosides from *Nyctanthes arbortristis*	Competitive inhibitors of TR	Shukla et al., 2010a
			Doxorubicin and Mitomycin C	Competitive inhibitors of TR	Shukla et al., 2010b
2	Cell signal transduction	Phospholipids and sterols	Miltefosine	Inhibition of phospholipid and sterol biosynthesis	Croft and Coombs, 2003
3	Polyamine biosynthesis	Ornithine decarboxylase	Pentamidine (Pentam-300)	Interacts with trypanosomal kinetoplast DNA	Delfin et al., 2009
4	Cell growth and proliferation	Protein and phospholipids	Nebulizer	Nebulizer inhibits incorporation of nucleic acids into RNA and DNA, causing inhibition of protein and phospholipid synthesis	Croft and Coombs, 2003
5	Microbial respiration	Fumarate reductase	Licochalcone A	Inhibits the conversion of fumarate to succinate and disrupts ultrastructure of mitochondria of amastigote stage of *Leishmania* lifecycle	Chen et al., 2001
6	Ergosterol biosynthesis	Sterols	2′,6′-dihydroxy-4′-methoxychalcone	Alters the sterol composition	Torres-santos et al., 2009
7	DNA Replication	DNA topoisomerase II	Flavonoids (e.g., 8-prenylmucronulatol, lyasperin H, and smiranicin)	Inhibits DNA topoisomerase II catalytic activity	Salem and Werbovetz, 2005
8	Immune system	-	KMP-11 DNA vaccine	Elevates levels of IFN-gamma	Bhaumik et al., 2009
9	Other oxidative pathway	Amastigotes	Redox active dinitrodiphenylthioethers	Generation of reactive oxygen species in MQ	Delfin et al., 2009

TH-1101_08610603

1.2.6 Natural products as antileishmanial agents

Natural products have played an important role in the drug discovery processes. Several medicinal plants have been traditionally used for treatment of Leishmaniasis. Although many compounds were isolated from plant sources and found to have antileishmanial activity, yet the exact mechanism of action of these plants extract against *Leishmania sp.* remains unclear. It is likely that these natural products may have inhibitory effect on one or more parasite specific enzymes whose mammalian counterpart is significantly different. A variety of aromatic ketones (known collectively as chalcones) which form the central core for many biological compounds, are reported to have antileishmanial activity. Licochalcone A is one of such compounds which is isolated from the roots of licorice (*Glycyrrhiza inflate)*. This compound strongly inhibits amastigote stage of *L. major*. It has also been demonstrated that licochalcone A alters the ultrastructure and function of mitochondria of *Leishmania* parasites. Licochalcone A is also reported to inhibit parasite-specific fumarate reductase enzyme (Chen et al., 2001). Another chalcone, 2′,6′-Dihydroxy-4′-methoxychalcone was purified from the dichloromethane extract of *Piper aduncum* and showed significant activity against promastigotes and intracellular amastigotes of *L. amazonensis* (Torres-Santos et al., 2009). The antileishmanial activity of 2′, 6′-dihydroxy-4′-methoxychalcone was further enhanced after encapsulation in polymeric nanoparticles. Recently, Torres-Santos et al. (2009) have shown that this compound alters the sterol composition of *L. amazonensis* and suggested that the target site is different from other known sterol inhibitors. Two chalcones, 2,2′,4′-trihydroxy-6′-methoxy-3′,5′-dimethylchalcone and 2′,4′- dihydroxy-6′-methoxy-3′,5′-dimethylchalcone, from methanolic extract of *Psorothamnus polydenius* have also shown to have antileishmanial activity (Salem and Werbovetz, 2005).Three isoflavans, isolated from the Iranian plant *Smirnowia iranica* (Fabaceae), namely 8-prenylmucronulatol, lyasperin H and smiranicin inhibited the growth of *Leishmania donovani* promastigotes. *S. iranica* appears to have a rich source of antileishmanial isoflavans. However, these compounds also show host cell toxicity which limits their pharmaceutical value.

The antileishmanial activity of these flavonoids was correlated to minicircle linearization in parasites and inhibition of leishmanial topoisomerase II catalytic activity (Salem and Werbovetz, 2005). Similarly, several other plant secondary metabolites are shown to have antileishmanial activity and are listed in Table 1.2.

TH-1101_08610603

Table 1.2 Various natural products shown to have antileishmanial activity.

S. No	Compound	Comments	Plant	Reference
1.	Argentilactone	Lactones	*Annona haematantha* (Annonaceae)	Akendengue et al., 2002
2.	Klaivanolide	Lactones	*Uvaria klaineana* (Annonaceae)	Akendengue et al., 2002
3.	Rolliniastatin-1	Acetogenins	*Rollinia emarginata* (Annonaceae)	Fevrier et al., 1999
5.	Sylvaticin	Acetogenins	*Rollinia emarginata* (Annonaceae)	Fevrier et al., 1999
6.	Quamocin	Acetogenins	*Rollinia emarginata* (Annonaceae)	Fevrier et al., 1999
7.	Minquartynoic acid	Acetylenes	*Minquartia guianensis*	Marles et al., 1989
8.	Actinodaphnine*	Alkaloid	*Cassytha filiformis* (Lauraceae)	Hoet et al., 2004
9.	Sarachine	Aminosteroid	*Saracha punctata* (Solanaceae)	Moretti et al., 1998
10.	2-n-Propylquinoline	Quinoline Alkaloids	*Glipea longiflora* (Rutaceae)	Fournet et al., 2000
11.	Chimanine B	Quinoline Alkaloids	*Glipea longiflora* (Rutaceae)	Fournet et al., 2000
12.	Chimanine D	Quinoline Alkaloids	*Glipea longiflora* (Rutaceae)	Fournet et al., 2000
13.	Canthin-6-one-alkaloids	Alkaloids	*Ailanthus excelsa*	Thouvenel et al., 2002
14.	Amarogentin**	Secoiridoid Glycoside	*Picrorhiza kurrooa*	Ray et al., 1998
15.	liriodenine	Alkaloid	*Stephania dinklagei* (Menispermaceae)	Camacho et al., 2002
16.	N-methylliriodendronine	Alkaloid	*Stephania dinklagei* (Menispermaceae)	Camacho et al., 2002
17.	Xylopine	Alkaloid	*Guatteria amplifolia* (Annonaceae)	Montenegro et al., 2003
18.	Benzoquinolizidine cephaeline	Alkaloid	*Psychotria klugii*, Rubiaceae,	El-On et al., 1984
19.	Pendulone	Quinones	*Millettia pendula*	Takahashi et al., 2004
20.	Hydroxybenzoisochromanquinone	Quinones	*Psychotria* (Cephaelis) camponutans	Del et al., 2004
21.	Benzo [g]isoquinoline-5,10-dione	Anthranoid	*Vismia orientalis* (Clusiaceae)	Mbwambo et al., 2004
22.	Emodin	Anthranoid	*Vismia orientalis* (Clusiaceae)	Mbwambo et al., 2004
23.	Vismione D	Anthranoid	*Vismia orientalis* (Clusiaceae)	Mbwambo et al., 2004
24.	3-geranyloxy-6-methyl-1,8-dihydroxyanthraquinone	Anthraquinones	*Vismia orientalis* (Clusiaceae)	Mbwambo et al., 2004
25.	Diospyrin***	Naphthoquinones	*Diospyros montana*	Ray et al., 1998
26.	Yuccasaponin MC3	Saponin	*Yucca filamentosa* (Agavaceae)	Plock et al., 2001
27.	3-Oxotirucalla-7,24Z-dien-26-oic acid	Triterpene Carboxylic acid	*Celaenodendron mexicanum*	Saeidnia et al., 2004
28.	Isoiguesterin	Triterpenes	*Salacia madagascarienis* (Celasteraceae)	Theim et al., 2005
29.	Simalikalactone D	Triterpenes	*Simaba orinocensis* (Simaroubaceae)	Muhammad et al., 2004

* The alkaloid was shown to interfere with the catalytic activity of DNA topoisomerases

** Inhibits the activity of DNA-topoisomerase I.

*** Selective inhibition of topoisomerase I (does not inhibit topoisomerase II)

TH-1101_08610603

The chloroform fraction of *Peschiera australis* has been shown to have antileishmanial activity (Delorenzi et al., 2001). Aqueous onion extracts shows antileishmanial effect against many *Leishmania sp.* (Saleheen et al., 2004). Hexane, dichloromethane, ethyl acetate, and methanol extracts of Warburgia ugandensis (Canellaceae), a Kenyan medicinal plant also show strong antileishmanial activity (Ngure et al., 2009). Crude ethanolic extract of Indian medicinal plant, *Desmodium gangeticum*, also shows significant activity against *Leishmania* (Singh et al., 2005). Diospyrin, a naphthoquinones from *Diospyros montana*, and amarogentin, a secoiridoid glycoside from *Picrorhiza kurrooa*, are selective inhibitor of topoisomerase I of the parasite. Moreover, the compound vasicine or peganine, isolated from *Peganum harmala*, has been tested *in vitro* against the promastigote stage of *Leishmania donovani*. It was shown that this compound induces apoptosis in *Leishmania* promastigotes. Peganine hydrochloride dehydrate is more safe and induces apoptosis in all stages of life cycle of *Leishmania donovani* by disturbing transmembrane potential of mitochondria (Mishra et al., 2008). Moreover, betulinic acid, a naturally occurring pentacyclic triterpenoid, and Luteolin, a flavonoid isolated from *Salvia tomentosa*, are also found to inhibit topoisomerase of *Leishmania* (Chowdhury et al., 2002a; Chowdhury et al., 2002b). An anticarcinogen, 3, 3′-diindolylmethane which is derived from indole-3-carbinol found in *Brassica* vegetables exerts antileishmanial activity by inhibition of F^0F^1-APx synthase (Roy et al., 2008).

1.3 Scope of current research

Several metabolic pathways like trypanothione metabolism, methylglyoxal metabolism, parasite glycolysis, purine salvage pathway and target enzymes/molecules of these pathways have been identified for antileishmanial drug discovery. Extensive research is being carried out to identify compounds which can interfere with parasite-specific pathways and can be further developed as drugs against Leishmaniasis. Several plants contain antileishmanial compounds. However, exact mode of action of these plant products is not known as yet. Few of the compounds from plant origin have been studied in detail and mode of action/or target molecule is also known. Aqueous or alcoholic extract of large number of plant species have been extensively investigated and reported to have antileishmanial activity (Fournet and Muñoz, 2002; Rocha et al., 2005; Salem et al., 2006) but the mechanism of action of these natural products remains elusive and require further investigations. If several plant extracts are having antileishmanial activity, then what is their mode of action? This was one of the questions I investigated during my

TH-1101_08610603

PhD research. We hypothesized that these plant extracts contain inhibitors of key enzymes of redox metabolism of *Leishmania sp.* Systemic screening of inhibitory effects of these plant extracts against TR (and other target enzymes) is necessary for identification of lead candidate compounds for their antileishmanial activity. It can be obtained by selectively targeting parasite's specific metabolic pathways without interfering with host's metabolic pathways. These studies made us more curious to do research on identification of novel drugs and evaluation of their mechanism of action for possible chemotherapy against Leishmaniasis. Additionally, identification of commercially available drugs, known to have antitumor activity, was also our prime focus of research for therapeutic approaches directed against Leishmaniasis.

Interestingly, we found some antitumor agents which are tricyclic quinone derivatives like doxorubicin and mitomycin C and they efficiently inhibit TR enzyme from *Leishmania sp.*The present study also describes the mode of action of few compounds from plant origin like iridoid glucosides from *Nyctanthes arbortristis,* a well known Indian medicinal plant. Furthermore, we extensively studied these compounds to clearly identify their mode of antileishmanial activity like inhibition studies on the key enzymes of redox metabolism, estimation of oxidative stress (monitored by flow cytometric analysis and fluorescence spectroscopy) by using specific dye against several reactive oxygen species, apoptosis assay etc. *In vitro* antileishmanial activity was measured by cytotoxicity assay (MTT) on promastigotes and axenic amastigotes. Inhibition of TR leads to decrease in reduced $T(SH)_2$ level, which was estimated by measuring reduced thiol content by DTNB. Safety measurements of these compounds were performed on different mammalian cell lines like Human embryonic kidney cell line (HEK293), mouse macrophages (J774.1A) and RBC.

We have also formulated biodegradable polymeric nanospheres encapsulating these antileishmanial agents for efficient and localized delivery to macrophages (the parasitic home) for increased efficiency, slow release and less toxicity. Polymeric nanoparticles of MPEG-PLA were synthesized by nanoprecipitation method and characterized by several techniques like TEM, FE SEM, BET, XRD, IR etc. Intracellular drug release was performed on mouse macrophages (J774.1A). Finally, we have investigated biophysical and folding parameters of TR from *Leishmania infantum*

TH-1101_08610603

Thus, the work embodied in this thesis is divided into the following chapters containing the following specific objectives:

I. *Evaluation of selected antitumor agents as subversive substrate and potential inhibitor of trypanothione reductase: an alternative approach for chemotherapy of Leishmaniasis*

After extensive computational analysis, we found some antitumor agents (Doxorubicin and Mitomycin C) showing significant inhibition of TR activity. *In vitro* inhibition studies indicated these compounds as competitive inhibitors and subversive substrates of TR enzyme. As quinone reductase (QR) and TR both belong to the same family NADPH oxido-reductase and have NADPH as cofactor, so TR may reduce quinone moiety of these compounds to hydroquinone which further gets re-converted to quinone in presence of O_2 similarly as QR. This mechanism leads to generation of superoxide free radical and oxidative stress in parasite. This hypothesis was validated by time dependant FT-IR analysis. These candidate drugs were further screened for their mode of action (inhibition studies, ROS generation, cytotoxicity studies etc.).

II. *PEGylated nanospheres encapsulating antileishmanial drugs for their specific macrophage targeting, reduced toxicity and deliberate intracellular release*

Numerous techniques (liposomal formulations, micelles, emulsions and nanoparticles) have been implicated to administer drugs to several target tissue and have met with failures because of their characteristic of being identified by PMNs (polymorphonuclear cells) and macrophages which leads to their phagocytosis. However, this phagocytic mechanism facilitates drug delivery to target site in case of Leishmaniasis i.e. macrophage itself. The biodegradable diblock co-polymer MPEG-PLA (methoxypoly (ethylene glycol)-b-poly (lactic acid)) nanoparticles are expected to be the most appropriate for antileishmanial drug delivery due to their amphiphilic, biodegradable behavior and increased half life in blood stream. Doxorubicin and mitomycin C loaded polymeric MPEG-PLA nanoparticles were prepared by nanoprecipitation method and characterized by TEM, FESEM, XRD and BET surface area analyzer. *In vitro* release profile of drugs suggested fairly slow release. These polymeric nanoparticles were efficiently capable of delivering drug at low pace inside macrophages which was

TH-1101_08610603

monitored by fluorescent microscopy using intrinsic fluorescence of doxorubicin. Cytotoxicity profile suggested that encapsulation of doxorubicin and mitomycin C into NPs nullifies cellular toxicity on Human embryonic kidney cell line (HEK-293) and mouse macrophages (J774.1A).

III. *Deciphering molecular mechanism underlying antileishmanial activity of Nyctanthes arbortristis, an Indian medicinal plant*

We isolated iridoid glucosides from seed kernel of *Nyctanthes arbortristis*, a widely used medicinal plant and explored them for inhibition studies on TR. Docking studies revealed that iridoid glucosides bind at the active site of TR with high docking energy. Therefore, further evaluation of inhibition parameters (Ki, IC_{50}), antileishmanial activity (via MTT assay), ROS generation (fluorescense studies and flow cytometry using CM-H_2DCFDA dye), safety evaluation (on HEK 293 and J774A.1) and other experiments (apoptosis mechanism and killing of intra-macrophageal amastigotes) were performed.

IV. *Biophysical and Folding Parameters of Trypanothione Reductase from Leishmania infantum*

As TR, a key enzyme of trypanothione metabolism of the parasite, was extensively explored as drug target during my research, therefore we carried out experiments to gather significant knowledge about biophysical and intrinsic properties of this enzyme (unfolding studies, activity modulation in presence of denaturants and at effect of different pH conditions). These studies would be helpful for better understanding of drug-target interactions.

TH-1101_08610603

Chapter II

Evaluation of selected antitumor agents as subversive substrate and potential inhibitor of trypanothione reductase: An alternative approach for chemotherapy of Leishmaniasis*.

2.1 Abstract

Trypanothione reductase (TR) is a validated drug target against Leishmaniasis. Using integrated computational and experimental approaches, the chapter reports doxorubicin and mitomycin C, known antitumor agents, as novel inhibitors of TR of Leishmania parasite. Interestingly, these compounds also act as subversive substrates and subvert the physiological function of enzyme by converting it from an anti-oxidant to a pro-oxidant. Possible mechanism of subversive substrate is investigated using various spectroscopic and biochemical techniques. Both doxorubicin and mitomycin C show significant effect on redox homeostasis of the parasite and high antileishmanial activity. The results suggest that the parasite death is apoptotic in nature. The toxicity studies as well as available toxicity data in literature indicate these compounds have acceptable toxicity in limited dose.

---

* Part of the work has been published in ***Molecular and Cellular Biochemistry,*** 2011, 352, 261-270

TH-1101_08610603

2.2 Introduction

Trypanosomatids cause various lethal forms of tropical human diseases including Leishmaniasis, which is caused by over twenty different species of *Leishmania* parasite (e.g. *Leishmania donovani*, *Leishmania infantum*, *Leishmania major*, *Leishmania mexicana* etc.). There are mainly three forms of the disease namely cutaneous, visceral and mucocutaneous. Out of these three forms, cutaneous Leishmaniasis is the most common form while visceral Leishmaniasis is the lethal form. Leishmaniasis causes several clinical disabilities like disseminated visceral infection (Kala azar), ulcerative skin lesions and destructive mucosal inflammation which impose a great social burden (especially for women), impair economic productivity and impede social development. Vector for the disease is female *Phlebotomine* sandfly, a dipteran, which transmits the parasite to human body during blood sucking (Myler and Fasel, 2008). *Leishmania* exists mainly in two life cycle forms namely promastigote in sandfly and amastigote in human macrophage. According to current WHO statistics about 12 million people living in 88 countries, mainly of 5 continents i.e. Asia, Europe, Africa, South America and North America are suffering from Leishmaniasis with 1.5-2 million new cases annually (Desjeux, 1992). This disease is endemic in low income population of Central and South American countries (Tempone et al., 2005). Commonly available drugs for Leishmaniasis have several drawbacks such as high cost, low efficacy and drug resistance (Shukla et al., 2010). Thus, there is an urgent need for new and less toxic treatments for Leishmaniasis.

Post genomic era of research has identified several differences in metabolic pathways between parasite and mammalian host which may be exploited as drug target. The glutathione/glutathione reductase system is the basis of redox balance in the mammalian host. Glutathione is the major thiol in human beings and is maintained in reduced form by glutathione reductase (GR). This reduced glutathione helps in removal of reactive oxygen species. In marked contrast to mammalian cells, TR is the key enzyme of thiol metabolism in trypanosomatids i.e. Glutathione/Glutathione reductase system is replaced by an analogous Trypanothione/Trypanothione reductase system in the parasite. Trypanothione molecule, consisting of two glutathione moieties linked by a spermidine linkage, serves as the substrate for TR (Fairlamb and Cerami, 1992). Trypanothione is maintained in reduced form by TR, which finally removes ROS by detoxification of hydroperoxides into alcohol and water via tryparedoxin protein (Krauth-Seigel and Comini, 2008). In-spite of similar physiological function, GR and TR are quite specific

TH-1101_08610603

towards their substrates due to difference in their respective active sites (Henderson et al., 1987b; Singh et al., 2008). Therefore, trypanothione reductase is considered to be a selective target for antiparasitic agents. Doxorubicin and mitomycin C are quinone derivatives and well known antitumor agents. Doxorubicin is also reported to have antileishmanial activity (Kole et al., 1999). However, mechanism of action for antileishmanial activity of doxorubicin has been a matter of debate for long. Some groups have reported its mode of action by interacting with base pairs of nuclear DNA (Sett et al., 1992), while others have reported the inhibition of topoisomerase II of the parasite (Singh and Dey, 2007). A recent report suggests that doxorubicin may exert its action by binding to parasite-specific antigen on macrophage (Mukherjee et al., 2004). So far, no study is reported on the effect of doxorubicin on redox homeostasis of parasite. Also, mitomycin C has not been studied as a leishmanicidal agent. Therefore, we have evaluated antileishmanial effect of doxorubicin and mitomycin C and clearly demonstrated their mode of action. These results unambiguously show that doxorubicin and mitomycin C disturb redox homeostasis and increase ROS concentration by acting as inhibitors as well as subversive substrates of TR. Crystal structure of TR from *Leishmania infantum* is already reported; hence, TR from *Leishmania infantum* has been used for computational studies as well as enzymatic assays. However, efficacy of these compounds has been tested on most lethal species of parasite, *Leishmania donovani*.

2.3 Materials & Methods

2.3.1 Materials

Doxorubicin, mitomycin C and DTNB were purchased from Sigma-Aldrich. Trypanothione reductase gene inserted in the unique NdeI-HindIII site of pET28b Novagen, in frame with N-terminal His-tag was generously donated by Dr. Andrea Ilari and Dr. Gianni Colotti, Università "La Sapienza" Rome, Italy. Cell permeant probe CM-H_2DCFDA was procured from molecular probe (Invitrogen). DMEM culture medium, FBS and gentamicin were obtained from Invitrogen. Trypanothione was purchased from Bachem, Switzerland. All other chemicals used were of analytical grade and were purchased from Sigma Aldrich, USA.

2.3.2 Leishmania parasites and cultures

Leishmania donovani (DD8) promastigotes were maintained in DMEM with 10% heat inactivated fetal bovine serum, 40µg/ml gentamicin antibiotic and 25 mM HEPES buffer

TH-1101_08610603

at 26^0 C. Axenic amastigotes were generated from promastigote stage by altering the pH of growth medium from 7.4 to 6.0, temperature to 37^0C and providing 5% CO_2 (Sereno and Lemerse, 1997)

2.3.3 In silico docking studies

Leishmania infantum TR structure (PDB ID 2JK6) was used for docking study. Docking was done using AutoDock 4.2.2.1 by implementing Lamarckian genetic algorithm, which is considered as one of the best docking methods available in AutoDock (Morris et al., 1998; Huey et al., 2007). Docking was performed after the removal of cofactors, SO_4^{2-} and water molecules from the protein manually. Polar hydrogens were added, Gasteiger charges were calculated, atom types were assigned using AutoDock tools interface (Shukla et al., 2010b). The rotatable bonds and torsions of the ligand were set by TORSDOF, grid maps were generated using the AutoGrid utility with 120 × 120 × 102 points with a grid spacing of 0.375Å. The X, Y and Z coordinates were fixed at -1.0, 30.0 and 15.0 respectively, with the knowledge of the active site. ga_pop_size (initial population size), 300; ga_num_evals (number of energy evaluations), 2500000; and ga_run (number of GA runs), 100, the remaining docking parameters were set to default. The active site of receptor was kept rigid and non flexible docking was carried out because no significant conformational change was observed at the active site during binding of native substrate in *T. cruzi* which shares a significant similarity with the TR of *Leishmania infantum* (Baiocco et al., 2009a). The docked confirmations of each ligand were clustered on the basis of Root Mean Square Deviation (RMSD). All the clusters were visually observed for their interaction with the active site residues. Ligplot was employed to make the hydrogen bonding and hydrophobic interactions map between the compounds and active site residues (Wallace et al., 1995).

2.3.4 Enzyme expression, purification and activity assays

Recombinant *Leishmania infantum* TR was expressed in *E. coli* using M9 medium. Expressed 6x His-tagged TR was purified in 50 mM phosphate buffer (pH-7.5) using Ni-affinity chromatography. To further purify native TR, 6xHistag was removed by on-column thrombin cleavage (Baicco et al., 2009b). Finally, native TR was obtained without 6xHistag. 6xHistag removal was further confirmed by MALDI analysis. Enzyme was stored at 4^0C in phosphate buffer (pH-7.5). Enzymatic assay was carried out on Tecan spectrophotometer using DTNB as an indicator for reduced thiol groups (Hamilton

TH-1101_08610603

et al., 2003). The final assay mixture (250 µl) contained TR (1 m unit), 40 mM HEPES (pH-7.5), 15 mM NADPH, 1 mM EDTA, 25 µM DTNB and different concentrations of Trypanothione {$T(S)_2$} ranging from 0.5 to 50 µM and 2.5 µl of 10 µM and 20 µM inhibitors. Enzyme mixture was pre-incubated with NADPH for 5 mins at 26^0C. The reaction was started by the addition of substrate followed by the inhibitor. Enzyme activity was monitored at 412 nm to detect the conversion of DTNB into yellow coloured TNB. Lineweaver–Burk plot (double reciprocal plot) was generated for calculation of K_m and V_{max}.

For evaluation of doxorubicin and mitomycin C as subversive substrates of TR, same enzymatic assay was performed in absence of DTNB while doxorubicin and mitomycin C were used as substrates (range 2.5 to 100 µM) in place of trypanothione. Enzyme activity was monitored as decrease in absorbance of NADPH at 340 nm.

2.3.5 Infrared spectroscopy (IR) studies

IR is a very important tool to identify the functional groups present in any compound. Therefore, we have performed IR studies to define the changes in basic structure of antitumor agents. IR spectra were taken in stretching frequency range from 4000 cm^{-1} to 450 cm^{-1} for two samples; one was complete assay mixture as described above for subversive substrate with 100 µM of doxorubicin and without TR and the second sample was with TR. IR spectrum was also collected after few minutes to estimate back conversion of hydroquinone to quinone moiety due to atmospheric oxidation. The graphs were plotted between stretching frequency (cm^{-1}) and %T.

2.3.6 Estimation of decrease in the level of reduced thiol

Inhibition of TR causes decrease in reduced trypanothione level which was estimated via microtitre plate assay using DTNB. Leishmania promastigotes and axenic amastigotes were grown in 1 ml culture medium for 12, 24, 36 and 48 h in presence of various concentrations (1.562, 3.125, 6.25, 12.5, 25, 50 and 100 µM) of compounds. Cells were centrifuged, dissolved in 10 mM Tris-HCl buffer (pH-2.5) and sonicated for 2 min. Acidic pH was used during sonication to prevent oxidation of free thiol groups. Cell debris was removed by centrifugation. 100 µl of supernatant and 100 µl of 500 mM phosphate buffer (pH-7.5) were taken in each microtitre well followed by addition of 20 µl of DTNB (1 mM) to each well. Absorbance was measured at 412 nm.

TH-1101_08610603

2.3.7 Measurement of ROS level elevation in Leishmania promastigotes/axenic amastigotes

Intracellular ROS levels were measured in presence of quinone derivatives using cell permeant probe CM-H_2DCFDA (Balasubramanyam et al., 2003). *Leishmania* cells were incubated with different concentrations of doxorubicin and mitomycin C (0, 5, 10 and 20 μM) for different time intervals (0, 3, 12, 24 and 48 h), centrifuged, washed and resuspended in PBS (pH-7.4). These cells were loaded with 10 μM CM-H_2DCFDA probe in dark for 45 min. ROS levels were measured by monitoring the conversion of non-fluorescent dye to highly fluorescent 2',7'- dichlorofluorescein in presence of proper oxidant using excitation wavelength of 488 nm and emission wavelength of 530 nm.

2.3.8 Flow cytometry studies:

Leishmania cells were investigated for morphological changes due to ROS elevation using flow cytometry (BD FACScaliber). After treatment of leishmania promastigotes and axenic amastigotes with 20 μM of doxorubicin and mitomycin C, cells were stained with CM-H_2DCFDA for 45min in dark and flow cytometric analysis was done for both treated and untreated cells using 488 nm laser and 530 nm emission filter.

2.3.9 Calculation of IC_{50} values of Quinone derivatives against Leishmanial promastigotes / axenic amastigotes

MTT assay was performed for estimation of viability of promastigotes and axenic amastigotes in presence of different concentrations of compounds (Mossman, 1983). Both promastigotes ($1x10^6$ cells/ml) and axenic amastigotes ($1x10^5$ cells/ml) in logarithmic phase were grown in microtitre plate for 24 h and then incubated in presence of different concentrations of quinone derivatives (1 μM-100 μM) for 48 h. After addition of MTT for 4 h, purple coloured formazan complex was formed which was dissolved in DMSO. The absorbance was measured at 570 nm for calculation of % cell viability. The absorbance is a measure of living cells and IC_{50} is the concentration of quinone derivatives which causes death of 50% cells.

2.3.10 Flow cytometric determination of apoptosis using Annexin V-FITC PI kit

Apoptosis causes rapid alterations in phospholipids of cell membrane leading to exposure of phosphatidyl serine on cell surface (early apoptosis) which can be detected by using

TH-1101_08610603

fluorescein isothiocyanate (FITC) conjugated Annexin V. Necrotic cells also bind with Annexin V-FITC but also get stained with Propidium Iodide (PI). Flow cytometric detection of apoptosis was performed in promastigotes using Annexin V-FITC apoptosis detection kit (Calbiochem) according to manufacturer's protocol (Paris et al, 2004; Debrabant et al., 2008; Das et al., 2008). Briefly, promastigotes ($1x10^6$ cells/ml) were incubated with 20 µM of doxorubicin and mitomycin C for 24 h. Cells were centrifuged at 1000g for 5 min, washed twice with PBS, suspended in 0.5 ml 1X binding buffer followed by addition of 1.25 µl of Annexin V FITC for 15 min at room temperature. The cells were again centrifuged and resuspended in binding buffer followed by addition of 10 µl propidium iodide. Flow cytometer (BDFACS caliber) was used with an argon laser (excitation wavelength 488nm) for detection of Annexin V FITC stained (early apoptotic) cells in FL1 filter (emission wavelength 518 nm) and PI stained(late apoptotic or necrotic) cells in FL2 filter (emission wavelength 620 nm).

2.3.11 Estimation of toxicity on Human Red Blood Cells

RBC haemolysis assay was carried out to evaluate the toxicity of doxorubicin and mitomycin C (Kazi et al., 1994). RBC suspension was prepared in 10 mM PBS (pH-7.4). RBC suspension was incubated with different concentrations of inhibitors ranging from $1xIC_{50}$ upto $32xIC_{50}$ for different time intervals as 1, 3, 6, 12 and 24 h. RBC suspension containing 2% Triton X-100 was taken as positive control while RBC suspension containing PBS was negative control. After incubation, cells were centrifuged at 2000rpm for 5 mins and supernatant was taken in microtitre plate. Absorbance was measured at 541 nm for the estimation of haemolysis as a function of hemoglobin absorbance. Percentage haemolysis was calculated using the following formula-

$$\% \text{ RBC Hemolysis} = \frac{\text{Abs of Sample - Abs of Negative Control}}{\text{Abs of Positive Control}} \text{ X } 100$$

where, sample is supernatant obtained after RBC haemolysis by drugs, negative control is 10 mM PBS buffer (pH-7.4) and positive control is 2% Triton X-100.

TH-1101_08610603

2.4 Results

2.4.1 Doxorubicin and mitomycin C have shown positive inhibition of TR in in-silico docking studies

The *in silico* studies showed that both doxorubicin and mitomycin C (Figure 2.1) bind around the active site of TR. The predicted binding mode was obtained by choosing the largest cluster with highly favourable binding energy. In our docking simulation the tetracyclic moiety of doxorubicin was in hydrophobic interaction with the amino acids of the hydrophobic patch of active site formed by Try21, Met113 whereas, its side chain was in hydrogen bonding with Glu467, which aids in the orientation of active site histidine (Figure 2.2A). On the other hand, mitomycin C binds to the hydrophobic cavity formed by Leu399, Phe396, Pro398 (Figure 2.2B) among which, Leu399 is a conservative substitution in TR from the human counterpart glutathione reductase. 3D plots have also indicated binding of these compounds at the active site of TR (Figure 2.2 C & 2.2D)

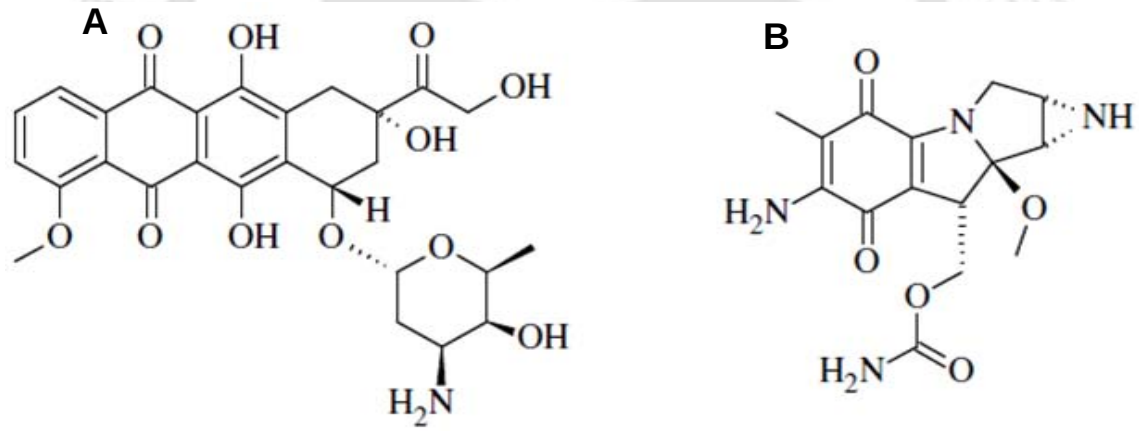

Figure 2.1 Chemical structure of quinone derivatives: (A) Doxorubicin and **(B)** Mitomycin C

2.4.2 Purification of Trypanothione reductase and determination of its kinetic parameters

Recombinant TR enzyme was successfully expressed in *E. coli* (BL21), purified using Ni-affinity chromatography and 6xHistag was removed by thrombin cleavage (Figure 2.3A). 6xHistag removal was further confirmed by MALDI (Matrix assisted Laser Desorption Ionization) analysis (Figure 2.3 B, C). Kinetic parameters like K_m and V_{max} of purified TR were estimated by Line-weaver Burk plot (Figure 2.3 D, E). K_m value of TR was calculated to be 5.44±0.05 µM.

TH-1101_08610603

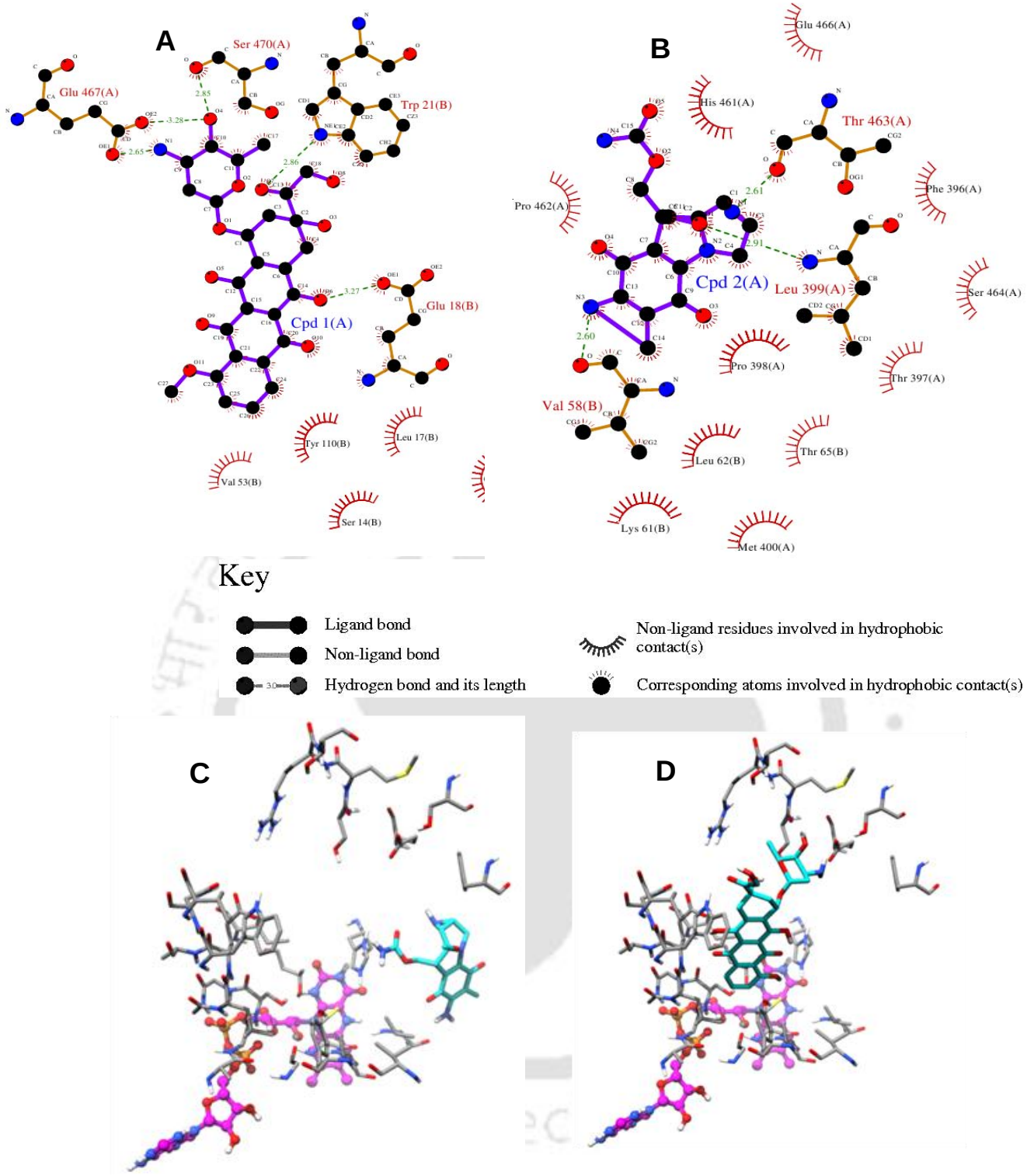

Figure 2.2 **2D Ligplots and 3D plots showing interaction of doxorubicin and mitomycin C with TR active site: (A)** Ligplot of Doxorubicin, **(B)** Ligplot of Mitomycin C, **(C)** 3D plot of doxorubicin-TR interaction **(D)** 3D plot of mitomycin C-TR interaction: These compounds bind to the residues of TR substrate binding cleft and can be potential inhibitors of the enzyme. . In *in silico* docking with TR doxorubicin and mitomycin C showed binding energy -8.63 and -7.01 kcal with K_i values 0.469 and 7.29 µM respectively.

TH-1101_08610603

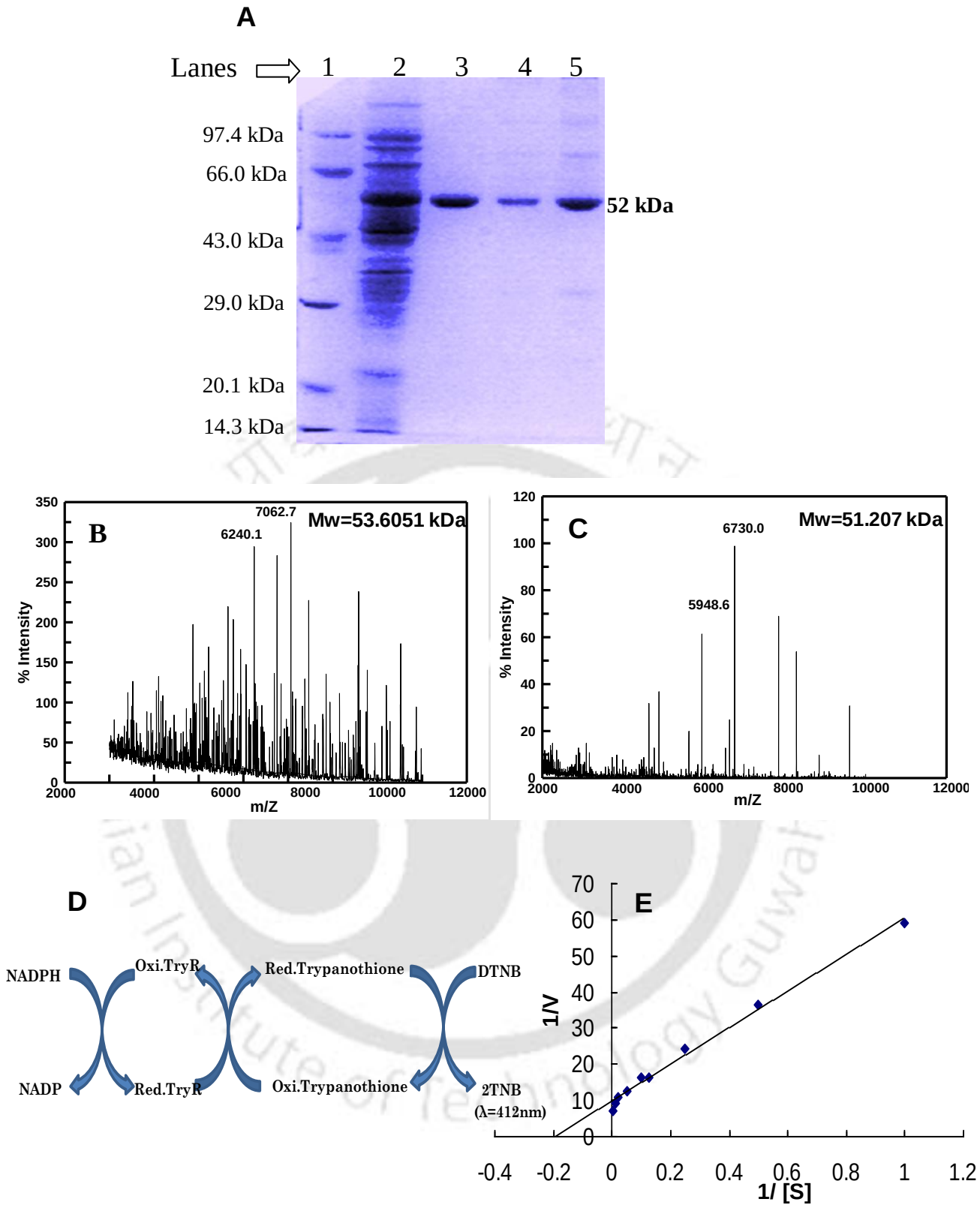

Figure 2.3 Expression, purification and 6xHis tag removal of TR: **(A)** SDS-PAGE showing marker (Lane1), crude TR after expression (Lane2), purified TR with 6xHistag (Lane 3&4) and TR without 6xHistag (Lane 5). **(B)** MALDI spectra of TR with 6xHistag. **(C)** MALDI spectra of TR without 6xHistag. Molecular weight of TR was calculated to be 53.6051 kDa with Histag and 51.207 kDa without Histag from MALDI spectra. **(D)** Schematic representation of enzymatic assay of TR. **(E)** Line-weaver Burk plot of TR enzyme assay.

TH-1101_08610603

2.4.3 Inhibitory effect of doxorubicin and mitomycin C on Trypanothione reductase activity

Doxorubicin and mitomycin C inhibit TR, which is depicted by an increase in K_m value from 5.44±0.14 µM to 23.62±0.25 µM and 10.52±0.15 µM respectively (with 10 µM of inhibitor concentration). The K_i values for doxorubicin and mitomycin C were found to be 3.24±0.05 µM and 12.65±0.04 µM respectively. As V_{max} of the enzymatic reaction remained constant, the compounds are likely to be competitive inhibitors (Figure 2.4). Interestingly, when trypanothione substrate is not added to the reaction mixture, doxorubicin and mitomycin C act as substrates which results in generation of $NADP^+$. The K_m and V_{max} for doxorubicin were found to be 16.89±0.15 mM and 118 µmoles/min respectively. K_m and V_{max} for mitomycin C were calculated to be 66.7±0.18 µM and 100 µmoles/min respectively.

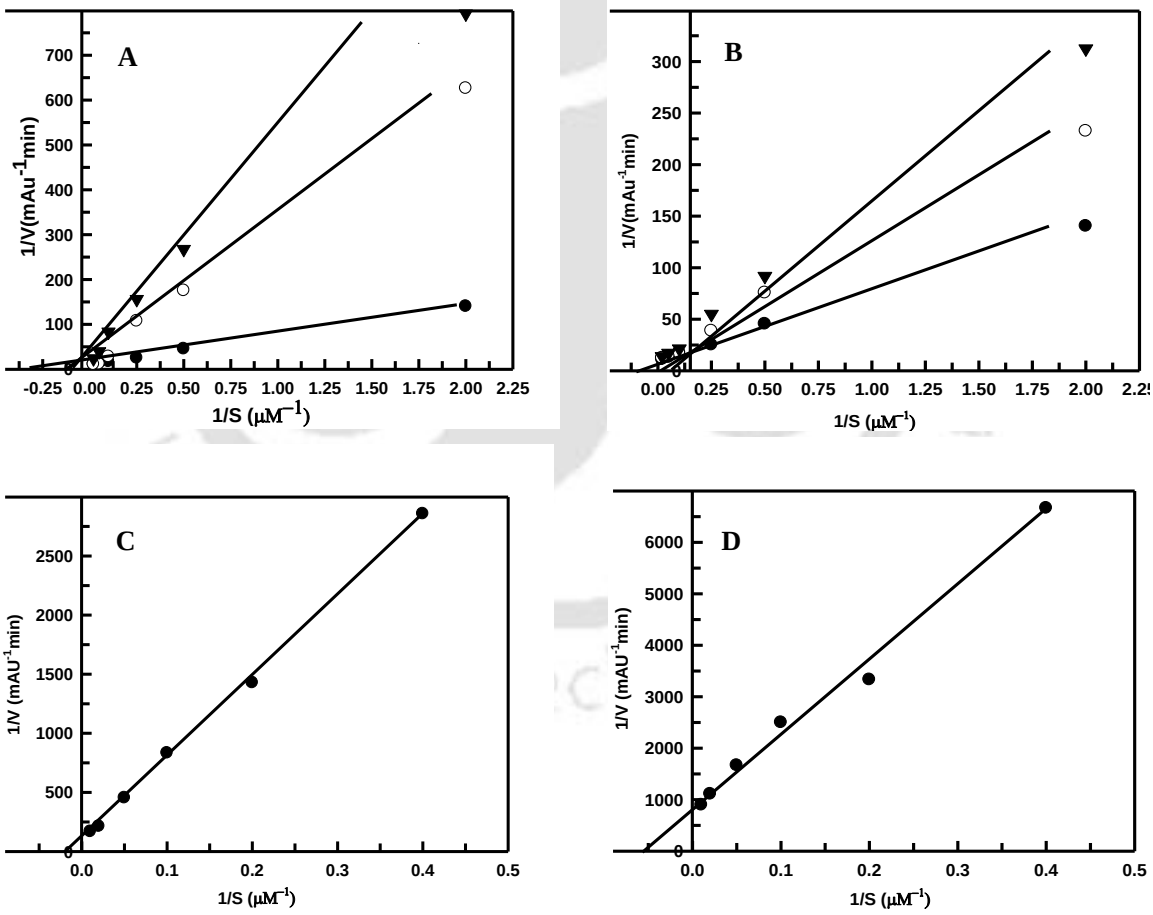

Figure 2.4 Enzymatic assay of TR: **(A)** In presence of 10 and 20 µM doxorubicin. **(B)** In presence 10 and 20 µM mitomycin C. **(C)** Enzymatic assay with different concentrations (ranges 2.5–100 µM) of doxorubicin as subversive substrate. **(D)** Enzymatic assay with different concentrations (ranges 2.5–100 µM) of mitomycin C, as subversive substrate. Triangle, circle and dot represent data with 0, 10 and 20 µM inhibitor concentration.

TH-1101_08610603

2.4.4 Quinone moiety of antitumor agent gets converted to hydroquinone by TR

Infrared spectroscopy results show the conversion of quinone moiety of doxorubicin to hydroquinone when enzymatic reaction was accomplished using TR. Keto-enol tautomerism leads to decrease in stretching frequency (Murthy et al., 1962). IR spectrum of doxorubicin without TR showed a typical peak of quinone ring >C=O with stretching frequency of 1643 cm^{-1}. IR spectrum after reaction in presence of TR, showed stretching frequency at 1632 cm^{-1} which indicated the enolization of >C=O and decrease in stretching frequency (Figure 2.5).

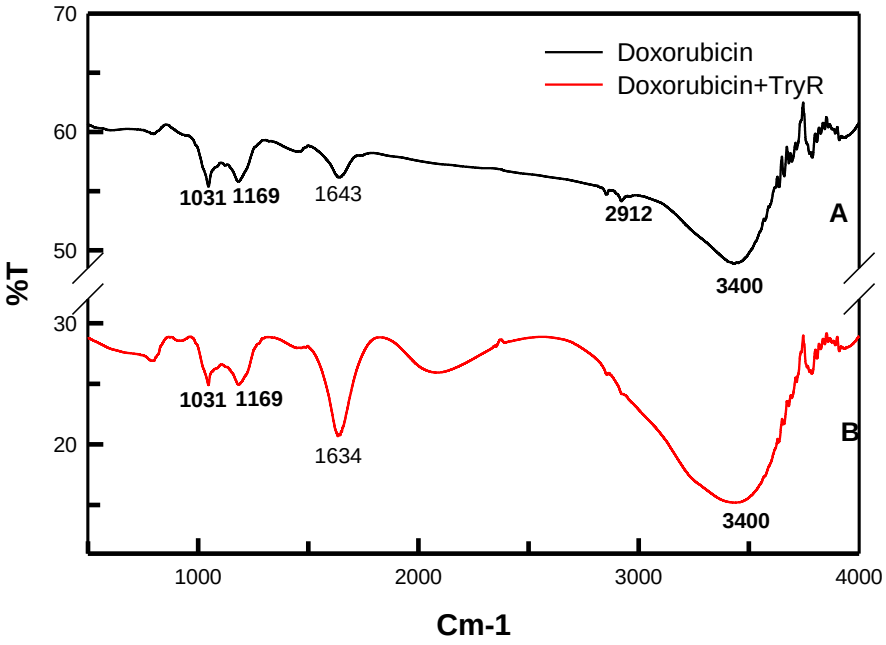

Figure 2.5 Infrared spectroscopic analysis of quinone-hydroquinone conversion in antitumor agents: **(A)** IR spectrum of doxorubicin in reaction mixture without TR enzyme. **(B)** IR spectrum of doxorubicin after reaction in presence of TR. Stretching frequency of >C=O group decreases from 1643 cm^{-1} to 1632 cm^{-1} due to enolization of quinone moiety.

2.4.5 Doxorubicin and mitomycin C lead to decrease in reduced thiol level

The inhibition of TR results in a decrease in reduced trypanothione which is reflected as a decrease in total free thiol as estimated by DTNB assay. There is no simple and specific assay to measure reduced thiol concentration. Hence, we have measured change in total free thiol of cell at different concentrations of doxorubicin and mitomycin C as a function of time (Figure 2.6). Out of all the concentrations taken, 25 µM has shown almost 60% decrease in total thiol after 36 h as compared to control experiment. This decrease is due to the inhibition of TR which can not convert oxidized trypanothione to its reduced form.

TH-1101_08610603

It should be noted that the assay is not specific to reduced trypanothione but to total free thiol (reduced thiol) and trypanothione constitutes the major thiol in parasite cell. Thus, 60% decrease in free thiol concentration due to TR inhibition is quite significant.

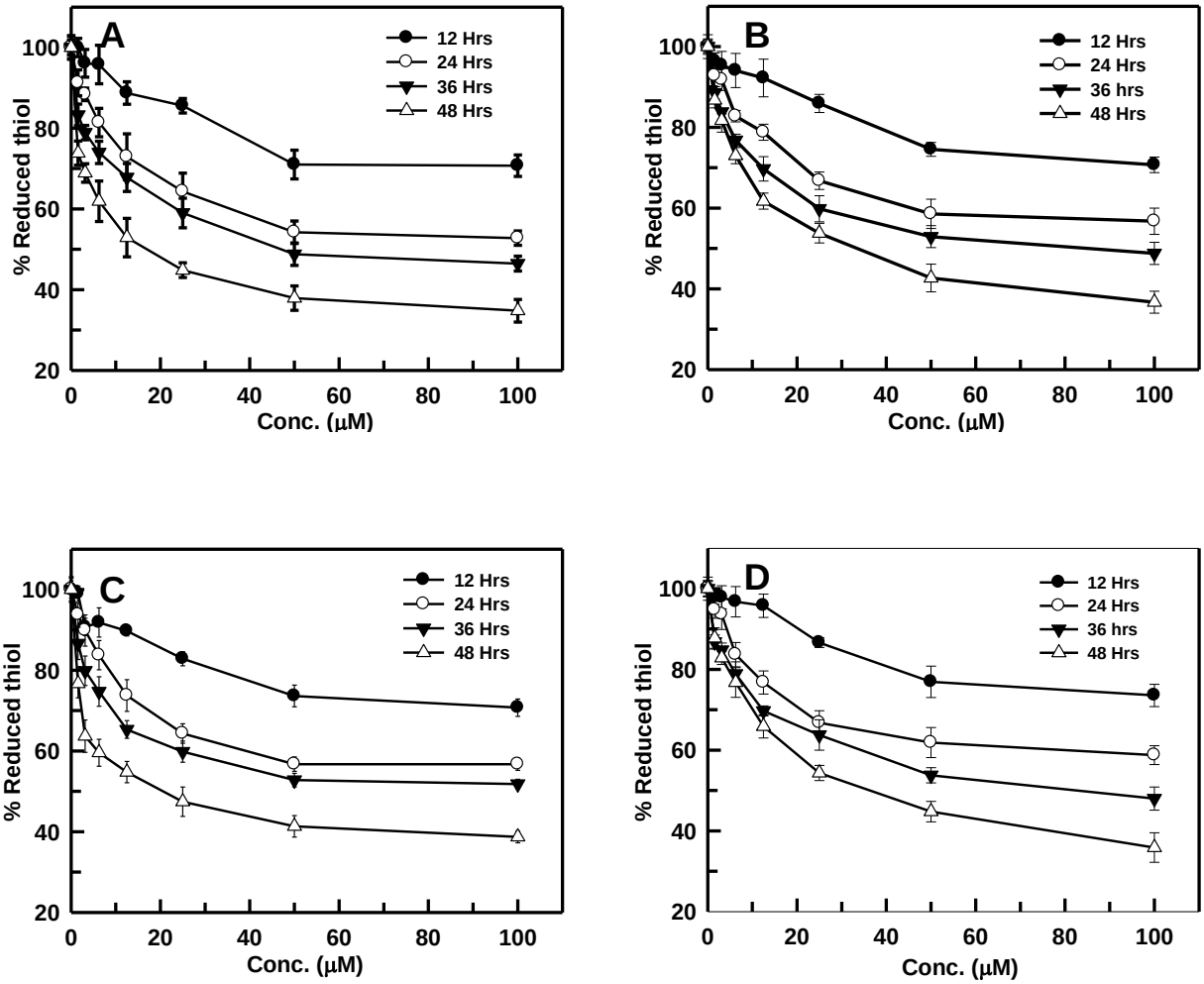

Figure 2.6 Estimation of free thiol levels (reduced thiol): Effect of different concentrations of **(A)** doxorubicin and **(B)** mitomycin C on *Leishmania* promastigotes as a function of time 12, 24, 36 and 48 h. Effect of different concentrations of **(C)** doxorubicin and **(D)** mitomycin C on *Leishmania* axenic amastigotes. As the reduced thiol assay is not specific to reduced trypanothion and also, only small fraction of reduced thiol (free thiol) in parasite is reduced trypanothione, 15% decrease in reduced thiol concentration is very significant.

Thus, these results clearly indicate that inhibition of TR causes decrease in total thiol pool which will cause unavailability of reducing equivalents for removal of reactive oxygen species as well as DNA synthesis.

TH-1101_08610603

2.4.6 Doxorubicin and mitomycin C lead to increase in intracellular ROS levels

Intracellular ROS measurements using CM-H_2DCFDA probe have shown that ROS levels were sufficiently increased when promastigotes were incubated with 20 µM doxorubicin as estimated by an increase in fluorescence intensity from 54.23±0.92 A.U. to 61.06±0.97 A.U. and 90.27±0.65 A.U. after 3 h and 48 h, respectively. Similar effect was found on amastigote stage and fluorescence intensity increases from 54.96±0.83 A.U. to 58.07±0.83 A.U. and 83.79±0.83 A.U. after 3 h and 48 h. 20 µM Mitomycin C also showed similar effect with increase in fluorescence from 54.47±0.67 A.U. to 58.23±0.78 A.U. and 88.92±0.97 A.U. on promastigotes and from 54.33±0.97 A.U. to 60.44±0.92 A.U. and 81.66±0.78 A.U. on amastigotes for 3 h and 48h. This increase in fluorescence intensity with respect to increasing concentration of compounds leads to increased ROS level and oxidative stress (Figure 2.7).

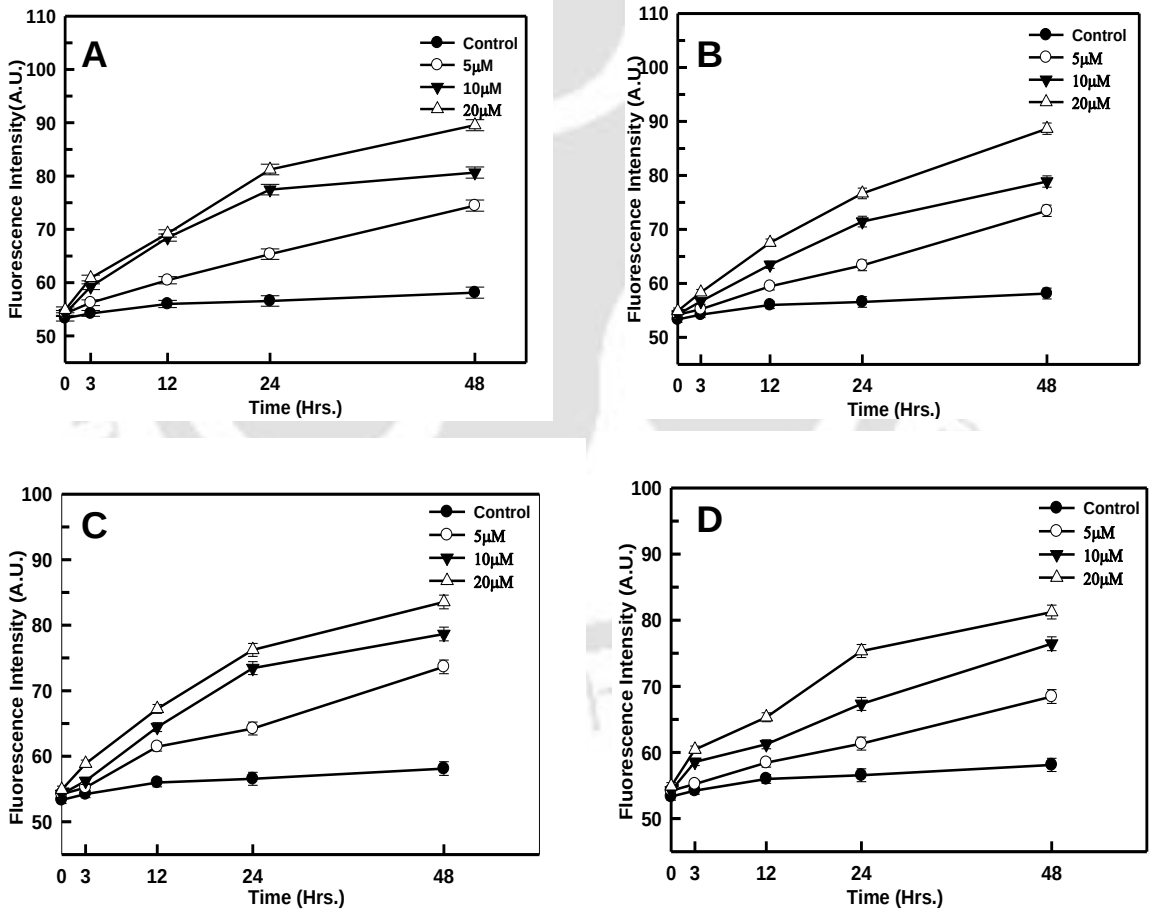

Figure 2.7 Measurements of intracellular ROS levels: Effect of doxorubicin on **(A)** promastigotes and **(B)** amastigotes stages. Effects of mitomycin C on **(C)** promastigotes and **(D)** amastigotes stages are also shown. Cells were treated with CM-H_2DCFDA dye and fluorescence was measured as explained in materials and methods. Results clearly indicate increase in ROS level after drug treatment.

TH-1101_08610603

Oxidative stress exhibited by these compounds was measured by flow cytometry using CM-H_2DCFDA probe. Larger numbers of cells were seen in experimental samples compared to control in density plot of flow cytometry using 530 nm emission filter. Oxidative stress in the parasite leads to morphological changes in the cells and cell death which is observed by flow cytometry using the same dye. FSC-H is a measure of cell size i.e greater the FSC-H, greater will be the cell size and SSC-H is a measure of surface smoothness i.e. greater the SSC-H, greater the roughness. FSC-H is greatly decreased from more than 400 in control cells to less than 200 in case of doxorubicin and mitomycin C treated promastigotes and amastigotes. SSC-H is highly increased from less than 100 in control cells to more than 600 in case of treated promastigotes and amastigotes.

The FL1 filter is specific for 530 nm emission so we have taken density plots using FL1 parameter to specifically observe increase in ROS level. We found that compared to control promastigote and amastigote, a large number of cells showed emission at FL1 filter in treated cells. These results indicate that *Leishmania* cells decrease in size as well as their surface becomes rough after treatment with the above compounds leading to cell death (Figure 2.8).

2.4.7 Doxorubicin and mitomycin C significantly inhibit the growth of Leishmania parasite

Doxorubicin and mitomycin C inhibit the growth of Leishmania when tested *in vitro* against *Leishmania donovani* promastigotes and axenic amastigotes using MTT cell viability assay. IC_{50} values of doxorubicin against promastigotes and axenic amastigotes were found to be 11.76±0.11 µM and 12.02±0.15 µM, respectively. Mitomycin C also showed similar IC_{50} values which were determined to be 12.76±0.20 µM and 11.52±0.15 µM for promastigotes and axenic amastigotes respectively (Figure 2.9).

TH-1101_08610603

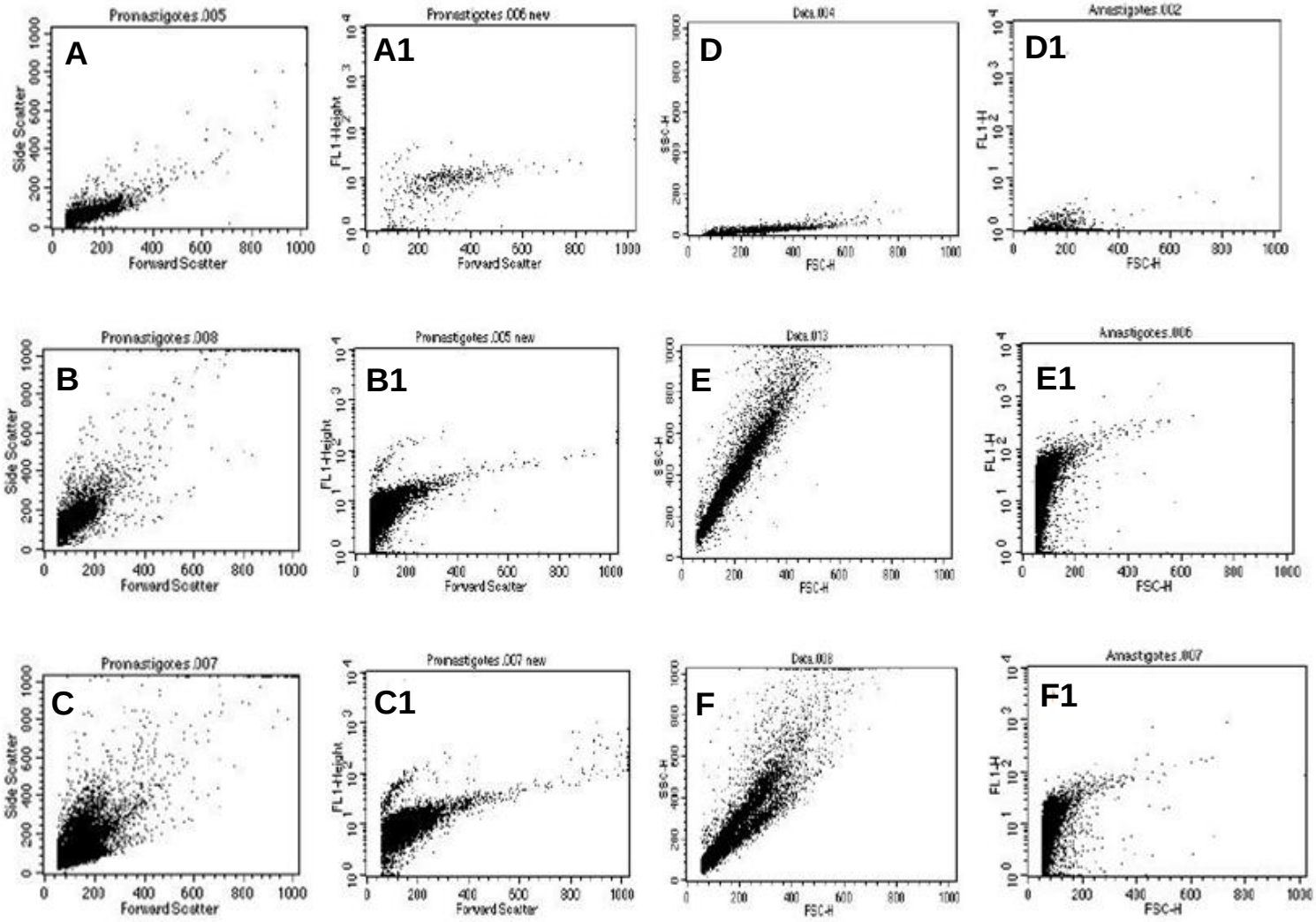

Figure 2.8 Flow cytometric analysis of ROS and morphological changes due to oxidative stress in *Leishmania*: (A)-(C) represent FSC versus SSC acquisition dot plot of control *Leishmania* promastigotes, promastigotes treated with 50 µM doxorubicin and promastigotes treated with 50 µM mitomycin respectively. Similarly **(A1)–(C1)** represent FSC versus FL1 acquisition dot plot of control, doxorubicin treated and mitomycin treated promastigotes respectively. **(D)–(F)** represent FSC versus SSC acquisition dot plot of untreated, doxorubicin treated and mitomycin treated amastigotes respectively. Similarly **(D1)–(F1)** represent FSC versus FL1 acquisition dot plot of control, doxorubicin treated and mitomycin treated amastigotes respectively.

TH-1101_08610603

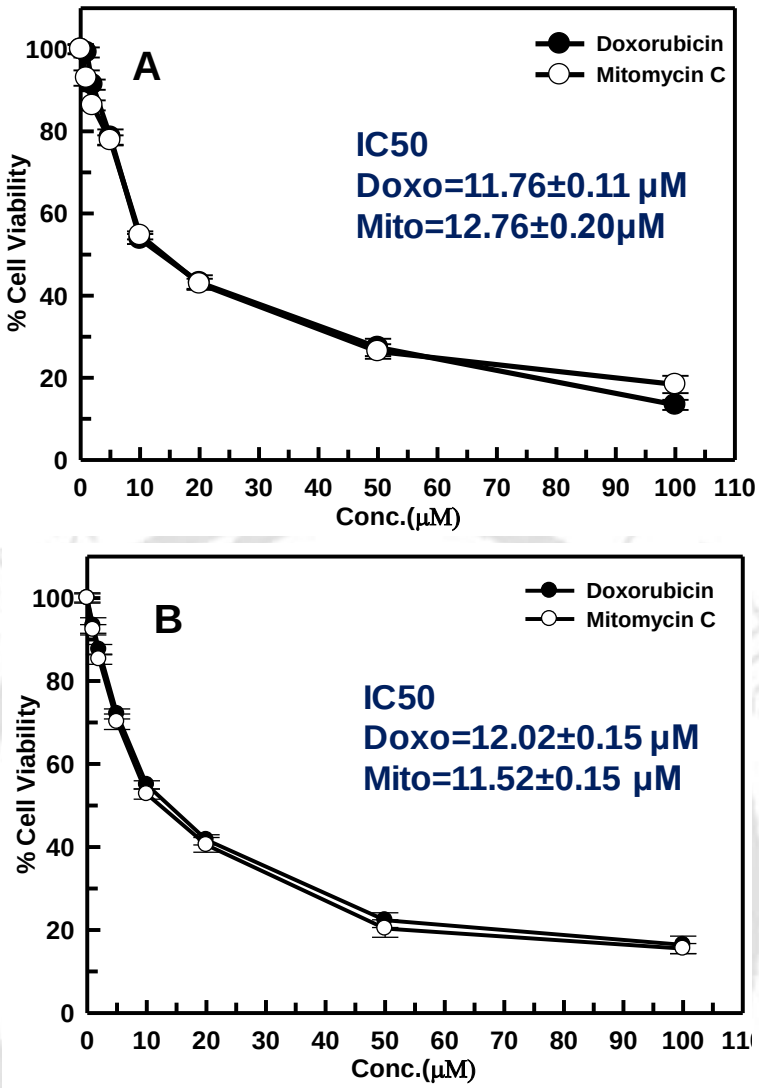

Figure 2.9 MTT cell viability assay: (A) *Leishmania* promastigotes and **(B)** *Leishmania* axenic amastigotes with different concentrations (0, 1, 2, 4, 10, 20, 50 and 100 µM) of doxorubicin and mitomycin C respectively. Both of these have shown quite low IC_{50} values.

2.4.8 Antitumor agents lead to apoptosis of Leishmania promastigotes

Annexin V, a calcium dependent phospholipid binding protein interacts with externalized PS (phosphatidyl serine) by apoptotic cells. Cell impermeable dye, PI (propidium iodide), was used to differentiate between necrotic cells and apoptotic cells as Annexin V also labels necrotic cells but PI does not permeate cells until membrane integrity is lost i.e. necrosis of cell occurs. Acquisition dot plots clearly demonstrate that % of apoptotic and necrotic cells are quite higher in treated cells compared to control cells which may be due to increased ROS level (Fig. 2.10).

TH-1101_08610603

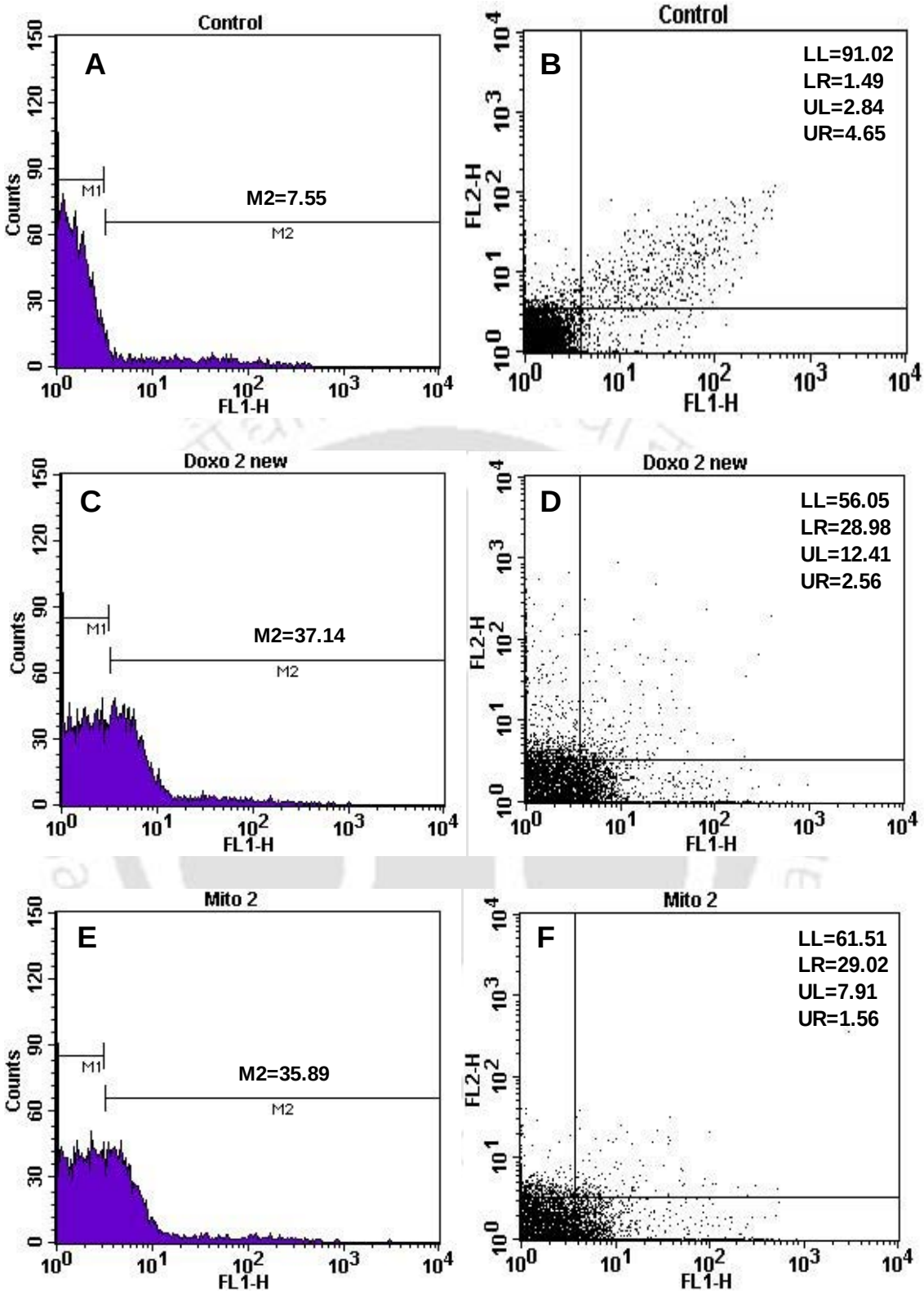

Figure 2.10 Flow cytometric determination of apoptosis using Annexin V-FITC, PI kit: Histogram and respective acquisition plots of **(A)** and **(B)** control promastigotes, **(C)** and **(D)** promastigotes in presence of doxorubicin and **(E)** and **(F)** in presence of mitomycin C. These results show apoptosis of *Leishmania* promastigotes in presence of antitumor agents.

TH-1101_08610603

2.4.9 Doxorubicin and mitomycin C are not toxic to human Red Blood Cells

In RBC haemolysis assay, when these compounds were incubated for 1 h (standard time for haemolysis assay) we found no haemolysis with concentration corresponding to IC_{50} value. Even after a prolonged incubation with higher concentrations, minor haemolysis was found. After 6 h with four times of IC_{50}, only 2.494±0.12% and 2.848±0.12% haemolysis was observed for doxorubicin and mitomycin C respectively, which is in error range. After 24 h of incubation with thirty two times of IC_{50}, we found only 12.746±0.10% and 7.278±0.29% of haemolysis (Figure 2.11). These drugs also have acceptable toxicity on mouse macrophages in limited dose.

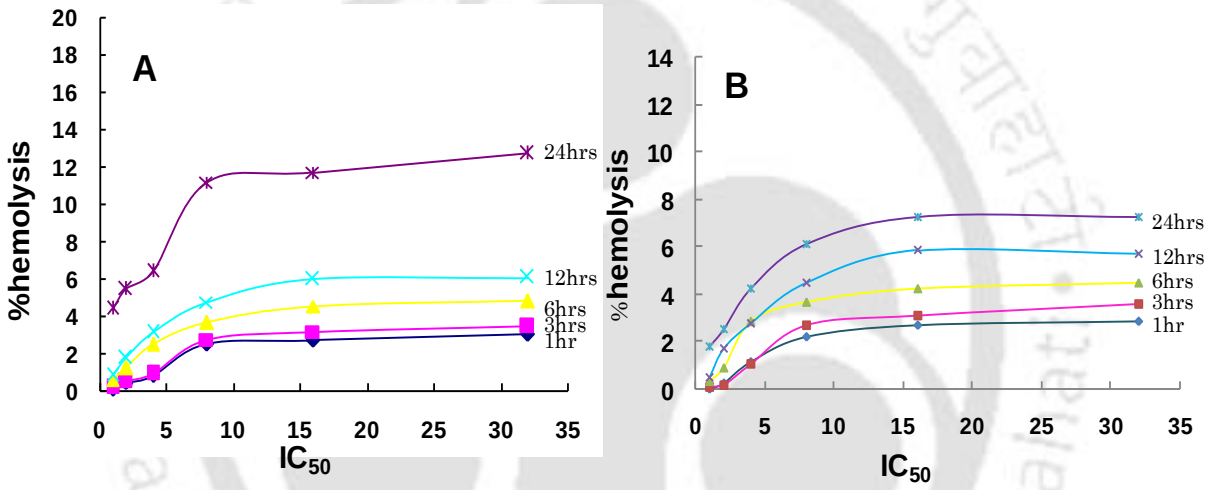

Figure 2.11 Cytotoxicity studies on Human RBC in presence of antitumor agents: (A) RBC haemolysis assay in presence of doxorubicin (concentration upto 32xIC_{50}) **(B)** RBC haemolysis assay in presence of mitomycin C (concentration upto 32xIC_{50}).

Therefore, these cytotoxicity measurements indicate that these antitumor agents namely doxorubicin and mitomycin C can be used as potent antilieshmanial agents. They are supposed to have no toxicity if given in limited doses for antilieshmanial chemotherapy.

TH-1101_08610603

2.5 Discussion

We have investigated the biochemical basis for chemotherapy of Leishmaniasis with the well-documented antitumor agents like doxorubicin and mitomycin C. In our search for novel inhibitor for TR, we found potential napthoquinone antitumor agents which, to the best of our knowledge, haven't been assessed for their action towards trypanothione reductase. Our *in silico* molecular docking studies with these antitumor chemotherapeutic agents i.e. doxorubicin and mitomycin C showed binding energy comparable to potent inhibitors. Thus, these compounds may be potential inhibitors of TR. The *in silico* results prompted us for experimental studies for further evaluation of these compounds. We have clearly demonstrated on recombinant TR protein that these compounds are competitive inhibitors of TR, which results in oxidative stress. The inhibition of TR results in increased concentration of oxidized trypanothione, thus total reduced thiol should decrease. The inhibition of the TR was also confirmed by decreased total free thiol by DTNB assay. It is worth mentioning here that the assay is not specific for reduced trypanothione but total free thiol (reduced thiol) and only small fraction of total free thiol in cell is reduced trypanothione. Thus, 60% decrease in free thiol concentration due to TR inhibition is very significant and this change is due to the inability of parasite to recycle oxidized trypanothione. Moreover, our results show that these compounds also act as subversive substrates and get reduced by TR.

The quinone moieties of these compounds can be reduced by TR and the resulting reduced quinone (hydroquinone) enters the redox cycle. This causes the accumulation of superoxide free radical which kills the parasite (Scheme 1). Thus, these compounds subvert physiological function of enzyme by increasing oxidative stress. The scheme I is supported by our IR data also. The enolization of quinone ring of any compound leads to slight decrease in stretching frequency (Murthy et al., 1962). We found a slight decrease in stretching frequency from 1643 to 1632 cm^{-1} upon addition of TR enzyme. This proves that TR converts quinone moiety of antitumor agents to hydroquinone. Therefore our hypothesis for subversive substrate mechanism is successfully proved by IR studies. This is further accompanied by ROS elevation and apoptosis of parasite which is proved by fluorescence studies and flow cytometric analysis.

TH-1101_08610603

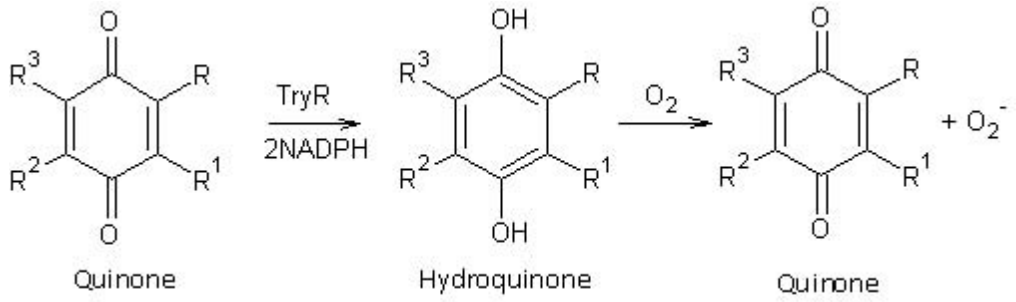

Scheme 1 Mechanism of subversive substrate for quinone derivatives, doxorubicin and mitomycin C: TR reduces quinone derivative to hydroquinone which is re-oxidized by molecular oxygen and generates superoxide free radical.

It is worth mentioning that these compounds show antitumor activity via similar mechanism by acting as substrate for NADPH:quinone oxidoreductase, an enzyme that is reported to be seen in elevated levels in tumor cells. In cancerous cell, upon reduction by the NADPH:quinone oxidoreductase, these compounds are transformed into cytotoxic species by interacting with the biomolecules (Colluci et al., 2008). Both QR and TR belong to FAD oxidoreductase class of enzymes in which $NADPH+H^+$ is the proton donor. The studies using CM-H_2DCFDA fluorescent probe for fluorescence spectroscopy and flow cytometric methods clearly demonstrated increased oxidative stress in presence of these compounds while control did not show any significant change. Moreover, our flow cytometric data shows change in cellular morphology of the parasite due to increase in oxidative stress which is depicted by an increase in SSC-H and decrease in FSC-H. Furthermore, an increase in FL1 emission in density plot indicates increase in ROS levels.

The parasitic viability estimated by MTT assay is correlated with ROS. If these compounds act as inhibitor, ratio of $TS_2/T(SH)_2$ will increase, thus, total free thiol will decrease. Our results have shown that these compounds decrease total free thiol and increase oxidative stress inside the parasite. They bind to the protein molecule in a way which prevents substrate (oxidized trypanothione) binding. Later, these compounds are reduced and act as subversive substrate as discussed earlier. In both the conditions the oxidative stress will increase and the parasite will not be able to survive. TR inhibition exerts different effects on ability of survival of promastigote and amastigote stage (Krauth-seigel and Comini, 2008). However, in our current studies, we found both promastigote and amastigote stages are equally sensitive to TR inhibition.

TH-1101_08610603

This work has led to the discovery that these quinone derivatives work as competitive inhibitors as well as subversive substrates for TR and can be developed as potential drugs against Leishmaniasis. RBC haemolysis assay suggested these compounds to be fairly safe as no significant haemolysis was found even at very high concentrations and with prolonged incubation time. Doxorubicin is shown to have minor cardiotoxicity. However, it has been shown that liposome encapsulation of doxorubicin is highly efficient in increasing the therapeutic value with no cardiotoxicity (Tardi et al., 1996). Thus, a liposome encapsulated doxorubicin appears to be a better antilieshmanial agent. Initially, mitomycin C was suggested to have pulmonary side effects. However, many recent reports have shown mitomycin C to be completely safe in limited doses. Mitomycin C does not increase the generation of oxygen radicals in pre-stimulated granulocytes and cytokines (IL-6, TNF-[alpha] or TGF-[beta]) in culture medium (Dirix et al., 1997). Therefore, both doxorubicin and mitomycin C have acceptable toxicity as drugs, if given in limited dose as their K_i values and IC_{50} values are quite small. The group is also working on other enzymes of the redox metabolism (Singh and Dubey, 2009; Saravanan et al., 2010)

2.6 Conclusion

In summary, we have reported that doxorubicin and mitomycin C, known antitumor agents, act as competitive inhibitors and subversive substrates of TR enzyme of leishmania parasite and they increase intracellular oxidative stress. These compounds show excellent leishmanicidal effect and acceptable toxicity. Thus, these compounds may be developed as unique and novel therapeutics for the treatment of Leishmaniasis and other trypanosomal diseases. It should be noted that the trypanothione/ trypanothine reductase system is common to other trypanosomatids causing Chagas' disease (caused by Trypanosoma cruzi) and African sleeping sickness (caused by Trypanosoma brucei). Mitomycin C and doxorubicin may have potential effect against these parasites as well.

TH-1101_08610603

Chapter III

MPEG-PLA nanospheres encapsulating antileishmanial drugs for their specific macrophage targeting, reduced toxicity and deliberate intracellular release*.

3.1 Abstract

The present chapter focuses on study of biodegradable polymeric nanoparticles (NPs) for encapsulation of doxorubicin and mitomycin C (antileishmanial drugs) and their efficient delivery to macrophages, the parasitic home. The biodegradable polymer MPEG-PLA {methoxypoly (ethylene glycol)-b-poly (lactic acid)} was used to prepare polymeric nanoparticles encapsulating doxorubicin and mitomycin C. The morphology, mean diameter and surface area of spherical NPs were determined by TEM, FESEM and BET surface area analyzer. X-ray diffraction and FTIR were performed to validate drug encapsulation. *In vitro* release profile of drug suggested its fairly slow release. These polymeric NPs were efficiently capable of releasing drug inside macrophages at a slower pace as compared to free drug which was monitored by fluorescent microscopy. Encapsulation of doxorubicin and mitomycin C into NPs decreases cellular toxicity on mouse macrophage (J774.1A) and human embryonic kidney (HEK 293) cell lines.

---

* Part of the work has been published in ***Vector Borne and Zoonotic Diseases***, 2012, Accepted.

TH-1101_08610603

3.2 Introduction

Leishmaniasis, a deadly infectious disease, is caused by a parasitic protozoan *Leishmania* and transmitted to mammals by the bite of Phlebotomine, a sandfly vector (Desjeux, 1992; Myler and Fasel, 2008). Out of the three major forms of infections, visceral Leishmaniasis (also called as "Kala-azar") caused by *Leishmania infantum* and *Leishmania donovani* is lethal and most common in India. Effective vaccines against this disease are still under development. Moreover, the available drugs are considerably toxic, costly and lead to parasitic resistance (Kedziersky et al., 2006; Shukla et al., 2010a). The chemotherapy for Leishmaniasis is primarily dependent upon antimonial compounds as first line of drugs (e.g. Sodium stibogluconate, Meglumine antimoniate etc.). These drugs are extremely toxic due to antimony toxicity. Amphotericin B is a second line drug exhibiting nephrotoxicity and other severe side effects. Miltefosine is the only available oral drug against Leishmaniasis, it is teratogenic and parasite has developed resistance against it. The treatment failure rates are significantly high and enforce the scientific community to develop more efficient drugs. In our previous studies, we have reported mechanism of antileishmanial activity of anticancer quinone derivatives doxorubicin and mitomycin C. These drugs exhibit competitive inhibition and work as subversive substrates for TR enzyme, a redox balancing enzyme of *Leishmania sp.* involved in removal of cellular oxidative stress (Shukla et al., 2011b). Doxorubicin is also shown to have antileishmanial effect on intracellular amastigotes and infected BALB/c mice (Sett et al., 1992). In this chapter, we report formulation of doxorubicin and mitomycin loaded biodegradable NPs to target intracellular *Leishmania* amastigotes.

Leishmania parasite exists in two life forms, long elongated, flagellated promastigote in midgut of sand fly and small, rounded and non-motile amastigotes in macrophage. Macrophages engulf promastigotes via phagocytosis inside phagosomes and these phagosomes fuse with lysosomes to form phagolysosomes where they are converted to amastigotes (Gupta et al., 2010). *Leishmania* is the only known parasite that replicates inside macrophages and resists its own killing by an unknown mechanism (Ofek et al., 1995). Macrophages are the primary cells to evade different kinds of pathogens and act as the first line of defense by phagocytosis of foreign particles (Gordon et al., 1995). This strategy of macrophages can be used to actively deliver a drug directly to the site of infection, thereby reducing toxicity of the drug. Nano-based drug delivery systems have gained enormous attention due to their high stability, lower toxicity and tunable

TH-1101_08610603

hydrophilic-hydrophobic behavior (Frank et al., 2008). Recently, several efforts have been made to develop drug carriers such as peptide-conjugates, micelles, liposomes etc. (Jones and Leroux, 1999; Panyam and Labhasetwar, 2003; Torchilin and Trubetskoy, 1995). Some of these formulations are easily identified by the reticular endothelial system and taken up by macrophages much more effectively than free drug (Bally et. al., 1998; Lundberg et. al., 2004). It improves the efficacy of drug and decreases its toxicity to great extent. Liposomal doxorubicin has reduced toxic effects without losing its efficacy against cancer (Tardi et al., 1996). Major drawback of liposomal formulations is their bigger size and extremely hydrophobic behavior, leading to their accumulation at injected site and poor solubility.

In recent past, biodegradable NPs have been extensively used for clinical administration of several anticancer drugs because of their facilitated extravasation into tumor sites and controlled delivery (Service, 2005; Brigger et al., 2002; Desai et al., 1997). Poly (d, l-lactide) (PLA), a synthetic polymer gets hydrolyzed to nontoxic hydroxyl-carboxylic acid through ester bond cleavage which is finally converted to water and carbon dioxide through citric acid cycle. PLA has been approved by the US Food and Drug Administration (FDA) due to its biodegradability (Xiao et al., 2010). Poly (D, L-lactide) NPs exhibited an enhancement of antileishmanial effect of primaquine (Muriel et al., 1998). MPEG-PLA diblock copolymer has been used for intravenous drug delivery system due to its great biodegradability and non-toxic behavior (Gref et al., 1994).

In our current study, we have intended to formulate these antileishmanial drugs encapsulated inside the polymeric nanospheres of MPEG-PLA copolymer for their decreased toxicity, enhanced and localized delivery, slow release at infection site and increased efficiency. Low molecular weight hydrophilic MPEG (550) and high amount of hydrophobic PLA were chosen to increase overall hydrophobicity of the NPs. This increases absorption of plasma proteins and opsonins on NP surface, thus facilitating phagocytosis by macrophages. The PLA segment of the polymer is hydrophobic enough and forms the inner-core to entrap the doxorubicin and mitomycin C. We have successfully encapsulated doxorubicin and mitomycin C drugs inside these polymer NPs, compared their toxicity level with free drug and optimized delivery of the drug inside macrophage. Thus, a logical strategy has been developed for efficient delivery of antileishmanial drugs using biodegradable polymeric NPs as drug carriers.

TH-1101_08610603

3.3 Materials & Methods

3.3.1 Materials

Doxorubicin, Mitomycin C, Methoxy poly (ethylene glycol) (MPEG, Mw=550), D, L-lactide, Stannous Octoate (Sn $(Oct)_2$), Dimethyl sulfoxide (DMSO), Dichloromethane (DCM) and Acetonitrile were purchased from Sigma Aldrich, USA. DMEM culture medium, FBS and penicillin-streptomycin antibiotic mixture were procured from Gibco (Invitrogen).

3.3.2 Maintenance of Cell lines

Mouse macrophage (J774A.1) was procured from National Centre for Cell Science, Pune, India. The cells were grown in DMEM containing 1.5g/l $NaHCO_3$, 10% fetal bovine serum, penicillin (100UI/ml) and streptomycin (100UI/ml) at 37^0C in 5% CO_2.

3.3.3 Synthesis of MPEG-PLA Block Copolymer

MPEG-PLA diblock biodegradable co-polymer was synthesized using ring opening polymerization method (Zheng et al., 2010; Cheng et al., 2007). In brief, in a three necked round bottom flask, 4 g lactide (3,6-Dimethyl-1, 4-dioxane-2, 5-dione) and 10 g low molecular weight MPEG (550) were mixed in 30 ml distilled toluene (by azeotropic distillation) containing 0.75% $Sn(Oct)_2$ under N_2 flame. The flask was sealed and maintained at 130^0C for 24 h in silicon-oil bath. The polymer synthesized was dissolved in dichloromethane (DCM) and recovered by fractional precipitation using cold methanol. Final co-polymer was filtered and dried at 40^0C in vacuum for 48 h. Synthesized polymer was characterized by ^{1}H-NMR (Varian) and FTIR using Perkin Elmer spectrophotometer (Model: Spectrum).

3.3.4 Formulation of drug encapsulated nanoparticles

The nanoprecipitation method was employed for synthesis of drug encapsulated MPEG-PLA NPs (Fessi et al., 1989; Dong et al., 2004). In brief, 1 mg of drugs (doxorubicin and mitomycin C) and 100 mg of MPEG-PLA block copolymer were dissolved in 10 ml of acetonitrile kept at 50^0C to form organic phase. This organic solution was added drop-wise to deionized water with 0.25% Pluronic F-68 as surfactant under moderate mechanical stirring. After 10 mins, MPEG-PLA block copolymer self assembled into NPs due to diffusion of acetonitrile into water with encapsulation of drug within its

TH-1101_08610603

hydrophobic core. Acetonitrile was evaporated overnight at room temperature. Blank MPEG-PLA NPs were prepared using the same method but without drug.

3.3.5 Characterization of the synthesized nanoparticles

The formulated nanoparticles were characterized for their morphology, size and surface area.

3.3.5.1 Morphology and Size determination

Morphology and size of NPs were determined using FESEM and TEM. A drop of NP suspension, kept on aluminium foil, was dried at 60^0C in an oven and attached on copper tape. After gold coating, NPs were analyzed under FESEM using Sigma Carl-Zeiss microscope operating at 1.3 kV EHT and 59.99 KX magnification. For TEM, sample was coated onto a carbon coated copper TEM grid and air-dried. The sample was analyzed by a high resolution TEM (JEM 2100; Jeol, Peabody, MA, USA) operating at an accelerating voltage of 200 KeV. Surface area, pore volume and pore diameter of NPs were determined by BET surface area analyzer (Beckman Coulter). Dried NPs (50 mg) were analyzed by BET at outgas temperature of 150^0C under N_2.

3.3.5.2 X-ray Diffraction and Infrared Spectroscopy studies

Determination of crystallographic properties and drug encapsulation of NP were done using X-ray diffractometer and FTIR. MPEG-PLA, MPEG-PLA doxorubicin-NP and doxorubicin were dried and analyzed by X–ray powder diffraction (XRD) using Bruker D8 Advance X–ray diffractometer with Cu Kα radiation. FTIR has also been performed on two samples i.e. NPs after encapsulation of drug and NPs without drug.

3.3.6 In vitro drug release

For determination of *in vitro* release kinetics of drug from MPEG-PLA NPs, 2 ml of Doxo-NP solution was diluted to 20 ml with phosphate buffered saline (PBS, pH 7.4) and kept in an orbital incubator shaker at 37^0C at 30 rpm. The tube was taken out at different time intervals, centrifuged at 6000 rpm to pellet out NPs and supernatant was analyzed for drug content by UV-VIS spectrophotometer at 485 nm. Doxorubicin showed absorbance maxima at 485 nm.

TH-1101_08610603

3.3.7 Optimization of intracellular release of encapsulated drug

Mouse macrophage (J774A.1) cells ($1x10^6$ cells/ml) were seeded overnight in 24 well plates in DMEM with 10% FBS. MPEG-PLA encapsulated doxorubicin and free doxorubicin were added to the culture at a final concentration of 10 µM. Fluorescent images of drug loaded macrophages were collected to evaluate doxorubicin concentration diffused inside macrophages. The media was taken out at different time intervals (0, 8, 24, 48, 72 and 96 h), cells were washed twice with PBS (pH-7.4) and analyzed under Epi-fluorescent Microscope (Motic, AE31). Doxorubicin gives red fluorescence when excited at 488nm with an emission maxima at 595 nm. Fluorescence intensity measurements were also performed using Tecan spectrophotometer (Ex. 488 nm, Em. 595 nm).

3.3.8 Cytotoxicity studies

MTT assay was performed to evaluate the effect of encapsulation on cytotoxicity of these antitumor agents on normal human cell lines. The % cell viability was estimated on J774.1A mouse macrophages and HEK 293 (Human embryonic kidney cell line) using free drugs as well as encapsulated drug via MTT assay (Mossman et al., 1983) as described earlier. Briefly, both promastigotes ($1x10^6$ cells/ml) and axenic amastigotes ($1x10^5$ cells/ml) in logarithmic phase were grown in microtitre plate for 24 h and then incubated in presence of different concentrations of free drug and encapsulated drug (1 µM-100 µM) for 48 h. After addition of MTT for 4 h, purple coloured formazan complex was formed which was dissolved in DMSO. The absorbance was measured at 570 nm for calculation of % cell viability. The absorbance is a measure of living cells and IC_{50} is the concentration of quinone derivatives which causes death of 50% cells.

TH-1101_08610603

3.4 Results

3.4.1 Synthesis and characterization of MPEG-PLA diblock co-polymer

The MPEG-PLA diblock co-polymer was synthesized using MPEG and lactide as substrates and highly efficient stannous octoate as a catalyst. The hydroxyl group (-OH) of MPEG interacts with the carboxyl (-COOH) group of opened lactide ring which leads to the formation of MPEG-PLA amphiphilic diblock copolymer (MPEG=hydrophilic core, PLA=hydrophobic core) (Figure 3.1A). The structure of synthesized polymer was determined by ^{1}H-NMR (taking $CDCl_3$ as standard) and FTIR spectroscopy. Peaks at 3.36 and 3.61 ppm correspond to etherial $-CH_3$ and $>CH_2$ groups of MPEG, whereas peaks at 2.14 and 5.16 ppm correspond to $-CH_3$ and >CH- group of PLA in H^{1}-NMR (Figure 3.1B). FT-IR spectra also showed peaks corresponding to different functional groups of MPEG-PLA copolymer i.e. peak a, d correspond to -O- (ether) and $>CH_2$ group of MPEG, c, b and e represent >CO of lactide, $>CH_2$ scissor and free –OH at end of the polymer (Figure 3.1C).

3.4.2 Synthesis and characterization of nanoparticles

The successful synthesis of blank and drug loaded MPEG-PLA NPs was carried out by nano-precipitation method along with solvent evaporation technique. TEM and FESEM pictures showed that synthesized NPs were spherical, smooth with mean diameter of around 70-220 nm (Figure 3.2). The surface area of the particles, analyzed by BET surface area analyzer, was estimated to be 14.491 m^2/g with a total pore volume of 0.0632 ml/g. This shows a very high surface area of the NP along with sufficient pore volume to encapsulate enough quantity of drug.

3.4.3 Encapsulation of antileishmanial drugs

Figure 3.3A shows XRD spectra of (a) free drug (doxorubicin), (b) encapsulated drug and (c) blank MPEG PLA NP. Peaks were obtained at 2θ of 27.19, 31.57 and 45.32 for crystalline doxorubicin, whereas these peaks disappeared in case of drug loaded MPEG-PLA NPs which confirmed the successful encapsulation of drug. In case of blank NPs, some additional peaks at 25.73, 36.05 and 39.59 were obtained due to change in crystal properties upon encapsulation of drug. The nanoparticles encapsulating doxorubicin showed peaks for doxorubicin in FTIR spectra which further confirmed encapsulation of drug (Figure 3.3B).

TH-1101_08610603

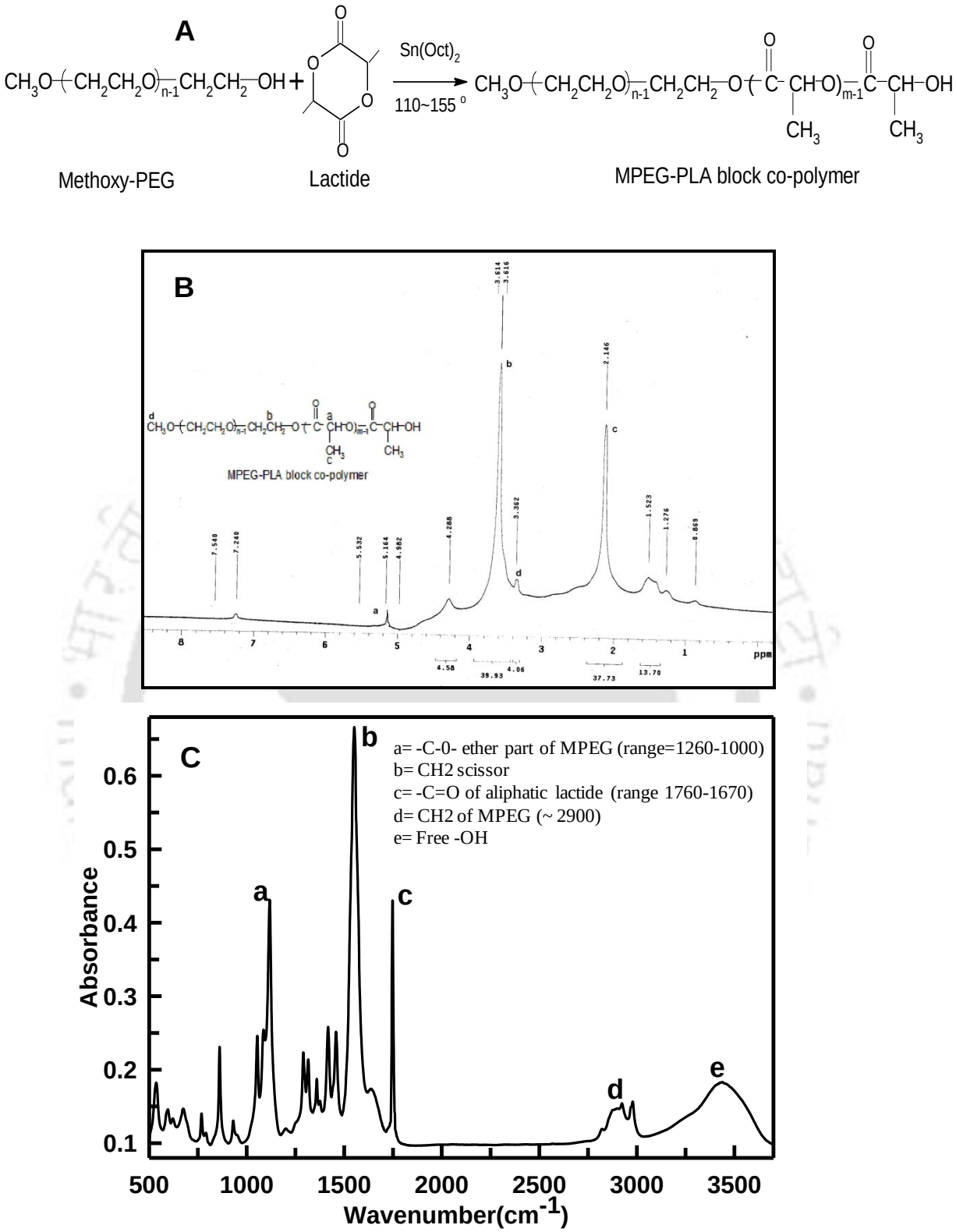

Figure 3.1 **Characterization of MPEG-PLA polymer: (A)** Schematic of MPEG-PLA synthesis. **(B)** H^1-NMR spectra of synthesized MPEG-PLA diblock copolymer and **(C)** FTIR spectra of MPEG-PLA. In NMR, synthesis of the polymer was confirmed by peaks at 3.36 and 3.61 ppm corresponding to etherial -CH_3 and >CH_2 groups of MPEG and peaks at 2.14 and 5.16 ppm corresponding to -CH_3 and >CH- groups of PLA. FTIR spectra also showed peaks of different functional groups.

TH-1101_08610603

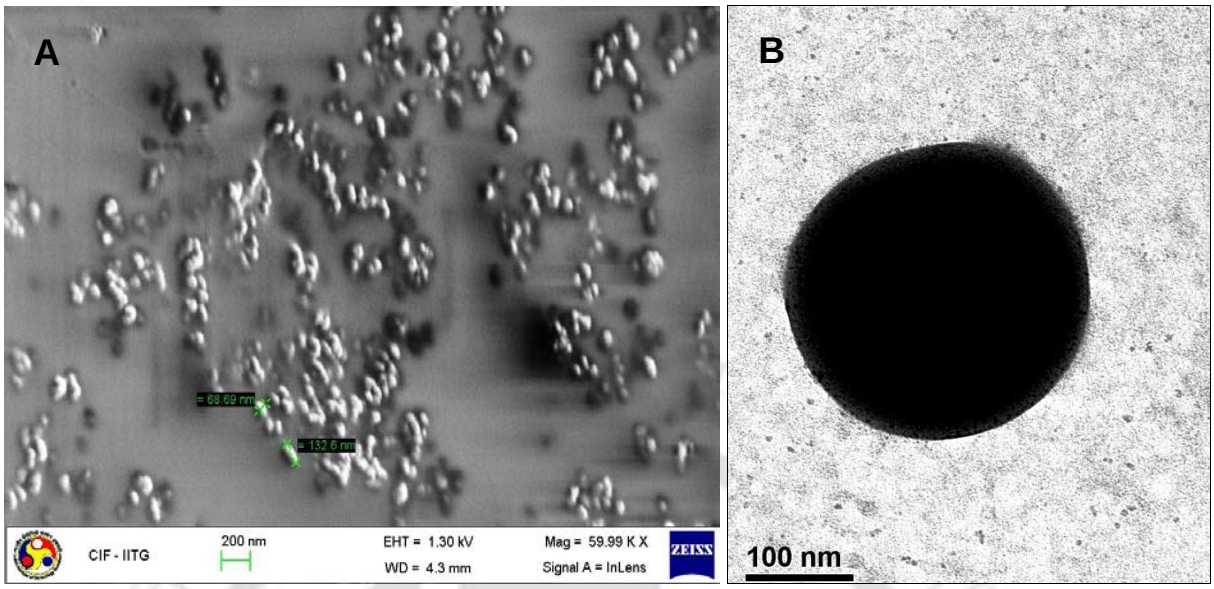

Figure 3.2 Characterization of nanoparticles: (A) FESEM (Field Emission Scanning electron microscopy) and **(B)** TEM (Transmission electron microscopy) images of nanoparticles. FESEM was operated at 1.3 kV EHT and 59.99 KX Magnification and TEM was operated at accelerating voltage of 200 kV. Images show that synthesized nanoparticles were spherical and smooth with mean diameter ranging 70-220 nm.

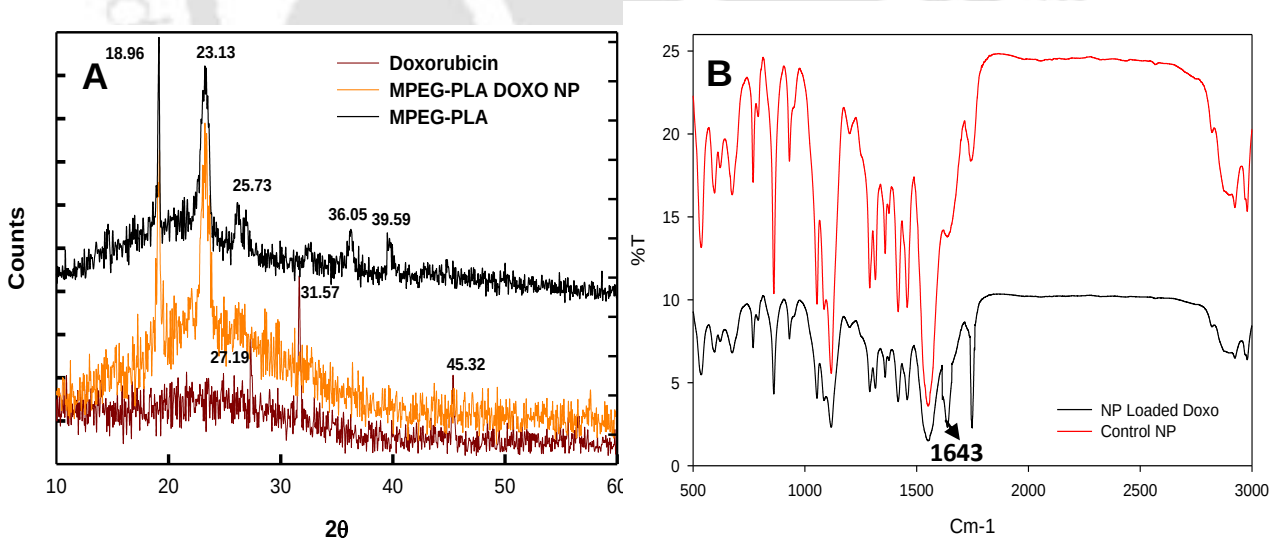

Figure 3.3 Characterization of encapsulated drug: (A) XRD spectra of (a) free drug (doxorubicin), (b) encapsulated drug and (c) blank MPEG PLA NP. Crystalline doxorubicin gives peaks at 2θ of 27.19, 31.57 and 45.32, whereas these peaks disappeared in case of NPs confirming successful encapsulation of drug. Some addition peaks were obtained in case of MPEG-PLA polymer which is because of the change in crystallinity on NP formation. **(B)** FTIR spectra of encapsulated doxorubicin and control NPs. Specific peak of quinone moiety was obtained at 1643cm-1 in case of NPs having drug which was absent in NPs without drug.

TH-1101_08610603

3.4.4 Deliberate intracellular release of encapsulated drug inside macrophage

Doxorubicin was found to give absorption maxima at 485 nm, so the estimation of drug content was done at the same wavelength. *In vitro* release profile of doxorubicin shows moderately slow release of drug with 84.59±7.32% release after 240 h (Figure 3.4).

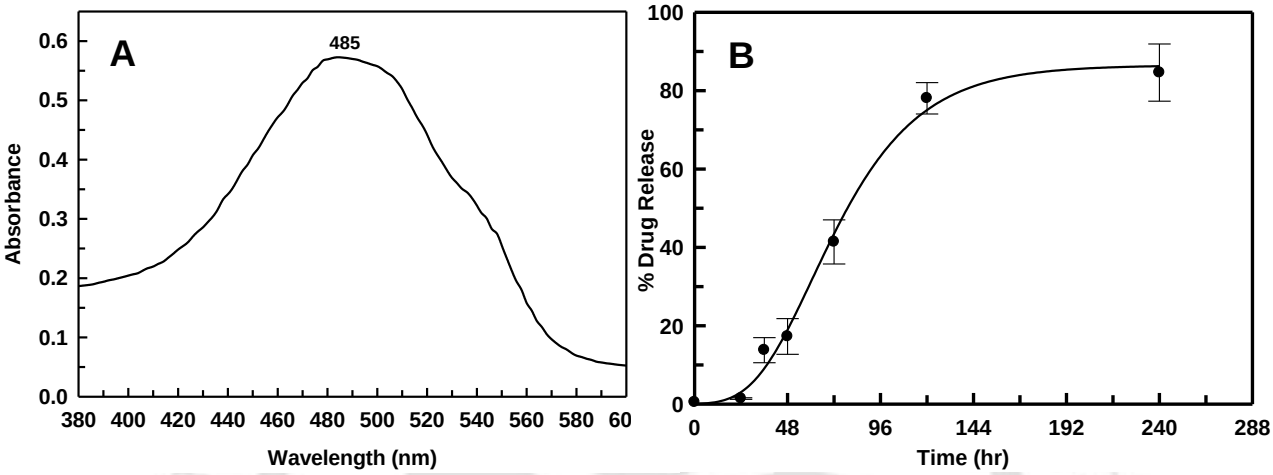

Figure 3.4 ***In vitro*** **drug release: (A)** Absorbance spectra of doxorubicin, **(B)** *In vitro* release profile of doxorubicin. The release profile showed fairly slow release of drug with 84.59±7.32% release after 240 h. The slow release is supposed to increase drug exposure to parasite which will increase its efficiency.

In vitro release profile was also supported by intracellular release of doxorubicin estimated by fluorescence spectroscopy. Epi-fluorescent images of macrophages have shown bright red fluorescence of doxorubicin just after 8 h of incubation with a maximum intensity at 48 h in case of free doxorubicin whereas, in case of encapsulated drug, only about 5% macrophages exhibited fluorescence after 24 h and the maximum intensity of doxorubicin fluorescence was delayed to 96 h (Figure 3.5A-H).

The same pattern was also obtained with fluorescence intensity parameters obtained by fluorescence spectrophotometer (Figure 3.5I). Thus encapsulated doxorubicin is efficiently delivered to macrophages via NPs and the release of the drug was found to be slow compared to native drug. These results indicate that encapsulated drug is released rather slowly inside the targeted cell with long-term exposure to the parasite leading to enhanced efficacy.

TH-1101_08610603

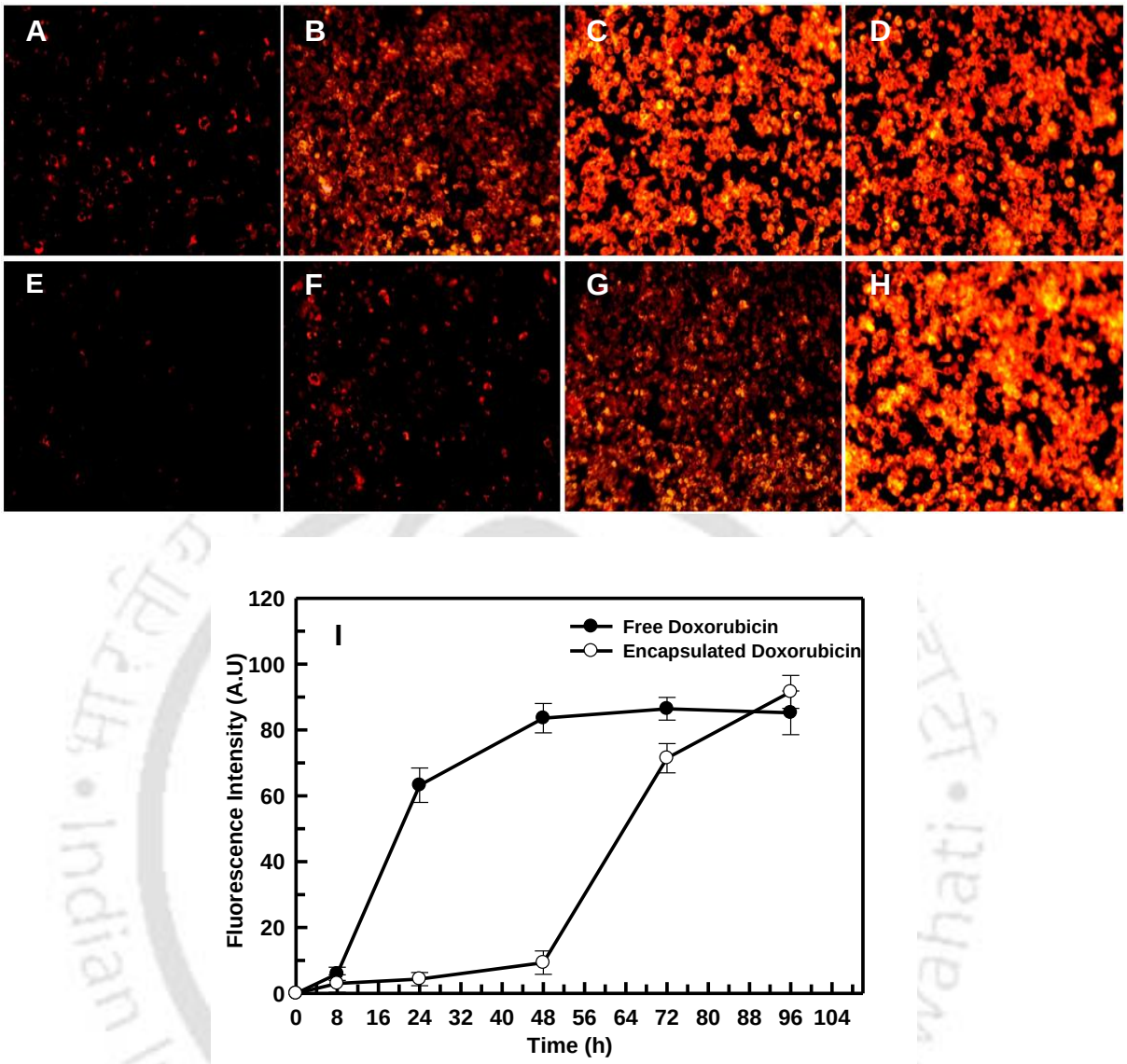

Figure 3.5 Fluorescent microscopic images of macrophage at different time intervals: (A), (B), (C) and **(D)** at 8, 24, 48, 72 h after incubation with free doxorubicin. **(E), (F), (G)** and **(H)** at 24, 48, 72 and 96 h of incubation with encapsulated doxorubicin (Magnification 100X). Images show bright red fluorescence of doxorubicin after 8h of incubation with a maximum intensity at 48 h in presence of free drug, whereas in case of encapsulated drug, only ~5% macrophages give fluorescence after 24 h and maximum intensity is delayed to 96 h. The same pattern was also obtained with fluorescence intensity parameters obtained by fluorescence spectrophotometer **(I).**

3.4.5 Cellular toxicity and safety evaluation

Doxorubicin is shown to have minor cardio toxicity. Initially, mitomycin C was suggested to have pulmonary side effects. Mitomycin C does not increase the generation of oxygen radicals in pre-stimulated granulocytes and cytokines (IL-6, TNF-[alpha] or TGF-[beta]) in culture medium (Dirix et al., 1997). Macrophages are the parasite proliferation site and therefore are the main target for drug delivery. NP mediated delivery is specific for

TH-1101_08610603

macrophages hence it is extremely important to evaluate the cytotoxicity of these formulations on macrophages itself. The cytotoxicity experiments were conducted on mouse macrophages (J774.1A) and HEK 293.The results showed that drug toxicity fairly reduces after encapsulation. The % viability of mouse macrophage (J774.1A) cell lines at 1.56 µM of free doxorubicin was 65.45±9.88 whereas at the same concentration of encapsulated drug it was 78.87±6.99 (Figure 3.6). In case of mitomycin C these values were found to be 83.82±16.14 and 92.78±4.92. Similar results were obtained on HEK293. Thus, it can be concluded that polymeric encapsulation of doxorubicin and mitomycin C decreases their toxicity with increased therapeutic value.

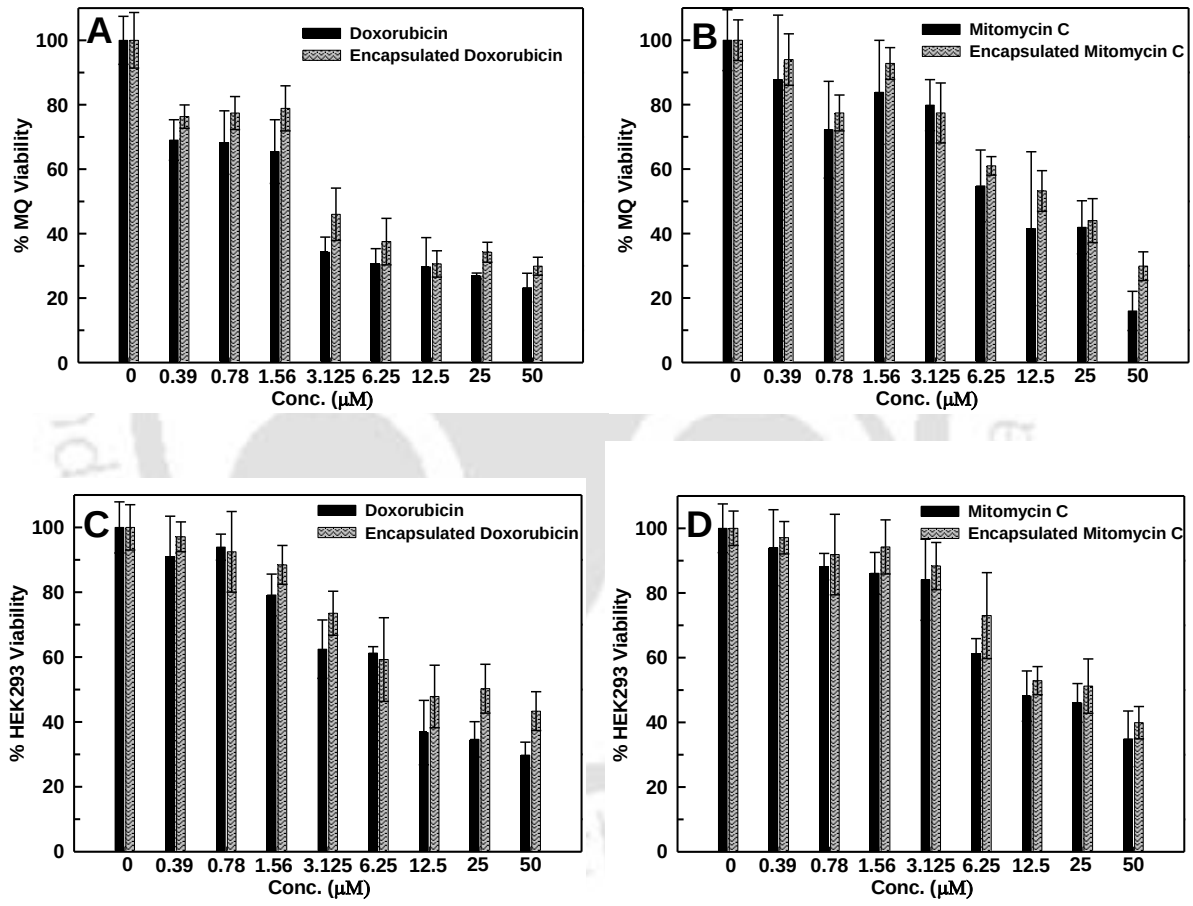

Figure 3.6 **Cytotoxicity assay of free and encapsulated drug (A)** doxorubicin and **(B)** mitomycin C on mouse macrophage (J774.1A). **(C)** doxorubicin and **(D)** mitomycin C on HEK293.The cells were incubated with different concentrations of free and encapsulated drugs (0-50 µM).

TH-1101_08610603

3.5 Discussion

Numerous techniques (liposomal formulations, micelles, emulsions and NPs) have been implicated over the last decade in order to administer drugs to targeted tissues (Gref et al., 1995). Unfortunately, most of these modes of administration met with failure because of identification by PMNs (polymorphonuclear cells) and macrophages and were quickly phagocytozed. However, this mechanism facilitates antileishmanial drug delivery to target site i.e. macrophage itself. The biodegradable polymer MPEG-PLA (methoxypoly (ethylene glycol)-b-poly (lactic acid)) seems to be appropriate for antileishmanial drug delivery due to its amphiphilic and biodegradable behavior. Therefore, this idea prompted us to encapsulate doxorubicin and mitomycin C inside MPEG-PLA polymeric NP and evaluate their delivery to macrophage. Doxorubicin is known to form Doxo-Doxo dimer in solution by chemical reaction between 3'-NH_2 and C^9-α Ketol side chain and Π-Π stacking of their planer ring (Yokoyama et al., 1998; Menozzi et al., 1984; Mclennan et al., 1985). Dimeric form of doxorubicin is hydrophobic in nature which enhances entrapment of doxorubicin in hydropobic PLA fraction (Figure 3.7A).

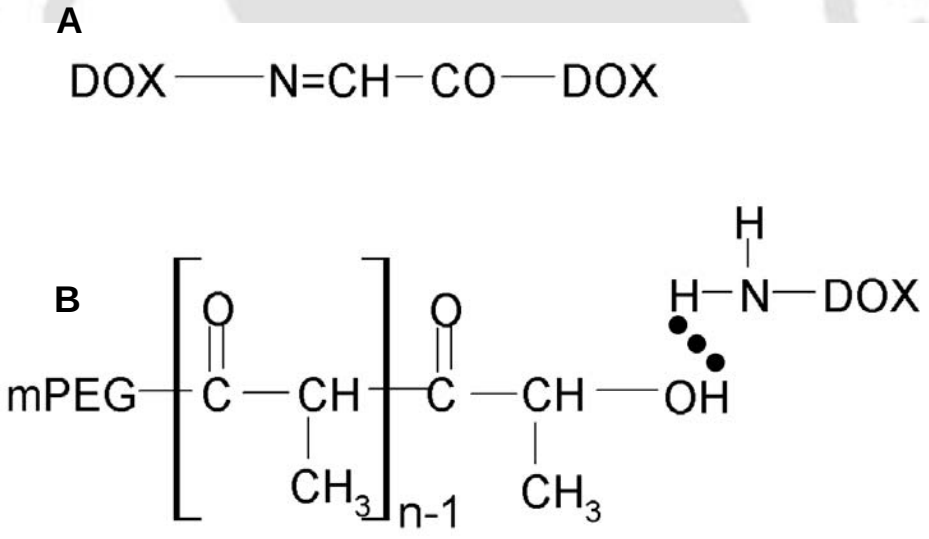

Figure 3.7 Doxorubicin dimer formation and hydrogen bonding: (A) Doxorubicin dimer formation (Dox-Dox). **(B)** Hydrogen bonding between -NH_2 of doxorubicin (or mitomycin C) and –OH of poly (D, L-lactide) segment. Dimer formation makes doxorubicin hydrophobic and hydrogen bonding increases its encapsulation inside the PLA core of the polymer micelle.

Alternatively, doxorubicin and mitomycin C are overall cationic molecules (due to –NH_2 groups) whereas PLA is an ester having terminal –OH group. This will contribute to the hydrogen bonding between drugs and PLA (Figure 3.7B) thus enhancing entrapment of drugs in the core of the micelle. An important criterion to increase entrapment of these

TH-1101_08610603

drugs in the micelle is to increase interaction between drug and PLA core which can be accomplished by increasing the amount of both drug and the PLA. Therefore we have used MPEG-PLA polymer with less fraction of PEG and more of PLA. Doxorubicin gets protonated at its 3'-NH_2 position and exists as 3'-NH_3^+which can interact with electronegative groups (Yi et al., 2005). According to previous study (Righetti, 1979), protonated behavior of glycosidic amine is retained up to pH 7 and gets deprotonated above pH-7. Once the polymer enters inside macrophages, 3'-NH_2 of drugs will get protonated due to acidic pH of lysosomal compartment. This should facilitate the release of drug due to conversion of dimeric Doxo-Doxo to monomer Doxo.

3.6 Conclusion

When drugs are administered into the body, only a small fraction reaches the macrophage where amastigote form of the parasite resides and multiplies. Thus, for better efficacy of drug generally higher doses are required, which may result in toxic side effect. Thus, preferential delivery of drug to macrophage is desired after systemic or localized administration. The study reports potential application of biodegradable polymer MPEG-PLA nanoparticles loaded doxorubicin and mitomycin C as a method for targeted drug delivery to macrophage. MPEG-PLA nanoparticles loaded doxorubicin and mitomycin C show targeted slow delivery to macrophage with lower side effects.

TH-1101_08610603

Chapter IV

Deciphering molecular mechanism underlying anti-leishmanial activity of *Nyctanthes arbortristis*, an Indian medicinal plant *¥.

4.1 Abstract

We report here the effect of iridoid glucosides (Compound a, b and c), non-toxic natural compounds, isolated from *Nyctanthes arbortristis* on redox homeostasis of *Leishmania* parasite. These compounds led to an increase in reactive oxygen species (ROS) by inhibiting TR, one of the crucial enzymes of redox metabolism of the parasite. Our experiments on *Leishmania* promastigotes and axenic amastigotes clearly showed that these compounds are highly active as antilieshmanial agents. *In vitro* experiments on intra-macrophageal amastigotes showed significant killing of parasite even at very low concentration. Determination of mechanism of action of iridoid glucosides showed that increased ROS level leads to oxidative stress, cell membrane damage and apoptosis of *Leishmania sp*. Our cellular toxicity assays on human embryonic kidney (HEK293) and mouse macrophage (J774A.1) cell lines showed these compounds to be very safe for therapeutic application. The current study points out towards potential application of iridoid glucosides as non-toxic and affordable antileishmanial agents.

---

* Part of the work has been published in ***Journal of Ethnopharmacology***, 2011, 134, 996-998
¥ Part of the work has been published in ***European Journal of Medicinal Chemistry***, 2012, DOI: 10.1016/j.ejmech.2012.04.034

TH-1101_08610603

4.2 Introduction

Nyctanthes arbortristis L. (Oleaceae) is widely used in the traditional medicine of India. Seeds, flowers and leaves of the plant are reported to have immunostimulant, hepatoprotective, antileishmanial, antiviral and antifungal activities (Puri et al., 1994). The leaves have been used in ayurvedic medicine to treat sciatica, arthritis, fever and are also used as a laxative (Saxena et al., 2002**)**. Flower of *Nyctanthes arbortristis* is shown to have antibacterial activity against many gram-positive and gram-negative microorganisms (Khatune et al., 2001). Three iridoid glucosides, arbortristoside a, b and c, used in the current study, were tested to be biologically active for antileishmanial activity on hamster (Tandon et al., 1991). However, the molecular mechanism underlying antileishmanial activity of these compounds remains elusive.

Leishmaniasis is a tropical disease caused by more than 30 species of protozoan *Leishmania* parasite (e.g. *Leishmania donovani, Leishmania infantum, Leishmania major, Leishmania mexicana* etc.) which is a trypanosomatid belonging to the order kinetoplastida. It affects about 88 countries and 12 million cases are found in tropical and subtropical areas with 1.5-2 million new cases each year (Desjeux, 1992). *Leishmania sp.* is transmitted to humans by the bite of a female sandfly *Phlebotomine* (Myler and Fasel, 2008*)*. This disease is still common in rural areas and is endemic in central and south American countries (Tempone et al., 2005). There are mainly three types of the Leishmaniasis, namely cutaneous, visceral and mucocutaneous. Out of which visceral Leishmaniasis is the most common and lethal form. The classical treatment of Leishmaniasis is toxic pentavalent antimonials discovered 60 years back. Other available drugs like amphotericine B, paromomycin, miltefosine and pentamidine also have their own drawbacks in terms of high cost, resistance development and low efficacy or other side effects. So far, best available drug is miltefosine which is unaffordable for general population due to high cost. Moreover, it is teratogenic and not suitable for pregnant women (Shukla et al., 2010a). Vaccines for the disease have been tested unsuccessfully so far (Kedzierski et al., 2006). Thus, search for a better anti-leishmanial drug is still on. Metabolic pathways essential for parasitic survival which are absent in mammalian host are attractive targets for drug discovery. All the trypanosomatids possess a unique thiol metabolism for the homeostasis to overcome the oxidative stress (Figure 4.1).

TH-1101_08610603

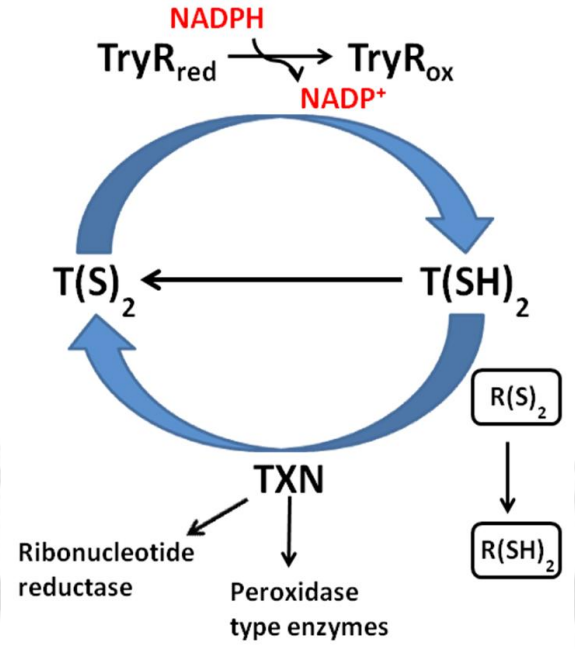

Figure 4.1 Trypanothione metabolism in leishmania parasite: Oxidised trypanothione {$T(S)_2$}is reduced by TR. Reduced trypanothone{$T(SH)_2$} passes reducing equvalent to Tryparedoxin (TXN) which transfers it to ribonuclease reductase and various peroxidases for DNA synthesis and detoxification of hydroperoxides..

Trypanothione {$T(SH)_2$}/Trypanothione reductase (TR) metabolism is unique in the parasite and TR is the key enzyme of the pathway. The TR is involved in homeostasis of redox metabolism. $T(SH)_2$ molecule consists of two glutathione moieties linked together by spermidine and is a substrate for TR (Fairlamb and Cerami, 1992; Fairlamb et al., 1985). TR helps in maintaining the redox balance by detoxification of hydroperoxides, formation of DNA precursors by NADPH dependent reduction of trypanothione. Neither $T(SH)_2$ nor TR is found in mammalian host, so TR is considered to be selective target for antiparasitic agents. In the current chapter, we have identified inhibitors of TR from *Nyctanthes arbortristis* which may be further developed as affordable drugs. We have clearly evaluated the effect of iridoid glucosides from *Nyctanthes arbortristis* on redox homeostasis of *Leishmania* using several techniques. We have also estimated sustainability of parasite to increased ROS and redox imbalance. Finally, safety measurements of these compounds have also been evaluated on cell lines for their use as potential antileishmanials.

TH-1101_08610603

4.3 Materials & Methods

4.3.1 Materials

Plant (*Nyctanthes arbortristis*), known as night-flowering jasmine, is very common in India. Stem, leaf and flowers of the plant were collected from IIT Guwahati. Iridoid glucosides were isolated from *Nyctanthes* seed-kernel by column chromatography of different solvent fractions using silica gel (60-120), followed by elution with acetate-methanol and chloroform-methanol. Cell permeant probe CM-H_2DCFDA {5-(and -6)-chloromethyl-2, 7 -dichlorodihydro-fluorescein diacetate acetyl ester}, DMEM culture medium, FBS and gentamicin were procured from molecular probe (Invitrogen). Oxidized trypanothione {$T(S)_2$} was purchased from Bachem, DTNB and all other chemicals of high grade were purchased from Sigma Aldrich, USA.

4.3.2 Leishmania parasites and cultures

Leishmania donovani (DD8) promastigotes were routinely sub-cultured and maintained in Dulbecco's minimum essential medium (DMEM) with 10% heat inactivated fetal bovine serum, 40 μg/ml gentamicin antibiotic and 25 mM HEPES buffer at 26^0C. Axenic amastigotes were generated from promastigote stage by changing the pH of growth medium to 6.0, temperature 37^0C and providing 5% CO_2 (Sereno and Lemerse, 1997; Debrabant et al., 2004). Mouse macrophage (J774A.1) and HEK 293 were maintained in DMEM, 10% FBS, $NaHCO_3$ and 1% penicillin-streptomycin antibiotics.

4.3.3 In silico docking studies

Leishmania infantum TR structure (PDB ID 2JK6) was used for the docking study. Docking was done using AutoDock 4.2.2.1, implementing Lamarckian genetic algorithm, which is considered as one of the best docking methods available in AutoDock (Morris et al., 1998; Huey et al., 2007). Docking was performed after the removal of cofactors, SO_4^{2-} and water molecules from the protein manually. Polar hydrogens were added, Gasteiger charges were calculated, atom types were assigned using AutoDock tools interface (Shukla et al., 2010b; Venkatesan et al., 2011). The rotatable bonds and torsions of the ligand were set by TORSDOF, grid maps were generated using the AutoGrid utility with 120 × 120 × 102 points with a grid spacing of 0.375Å. The X, Y and Z coordinates were fixed at -1.0, 30.0 and 15.0 respectively, with the knowledge of the active site. ga_pop_size (initial population size), 300; ga_num_evals (number of energy evaluations),

TH-1101_08610603

2500000; and ga_run (number of GA runs), 100, the remaining docking parameters were set to default. The active site of receptor was kept rigid and non flexible docking was carried out because no significant conformational change was observed at the active site during the binding of native substrate in *T. cruzi* which shares a significant similarity with the TR of *Leishmania infantum* (Baiocco et al., 2009a). The docked confirmations of each ligand were clustered on the basis of Root Mean Square Deviation (RMSD). All the clusters were visually observed for their interaction with the active site residues. Ligplot was employed to make the hydrogen bonding and hydrophobic interactions map between the compound and active site residues (Wallace et al., 1995).

4.3.4 Preparation of Plant Extracts

Plant powder (50 g) was soaked in methanol (50 ml) and distilled water for 2-4 h to prepare methanolic and aqueous extracts respectively. Then this solution was subjected to sonication to disrupt the cell wall. After sonication, the extract was centrifuged (2500 rpm for 20 mins) and supernatant was collected. The pellet was again dissolved in methanol/water for subsequent extraction. The supernatant was lyophilized to get powdered extract. 1 mg/ml powder, dissolved in distilled water, was used further for TR activity assay.

4.3.5 Isolation of Iridoid glucosides

Iridoid glucosides were isolated from *Nyctanthes* seeds according to available protocol in literature (Rathore et al., 1989). Briefly, 2 kg seed kernel of plant was dried at room temperature and extracted in 50% ethanol by incubating overnight followed by sonication. After sonication, sample was centrifuged and supernatant was dried in vacuum to get powder (400 g). The extract was fractionated using n-hexane, chloroform and n-butanol subsequently. n-Butanol fraction (20 g) was subjected to column chromatography using silica gel 60-120 (300 g) and eluted with ethyl acetate and ethyl acetate-methanol (increasing MeOH content) which gave two fractions, fraction 1 (4 g) and fraction 2 (2.3 g). Fraction 1 was again subjected to column chromatography using 100 g Silica gel and eluted with $CHCl_3$–MeOH. 7% MeOH–$CHCl_3$ eluted compound a (white needles, m.p. 220–222^{0}C) and 10% MeOH–$CHCl_3$ eluted compound b (white amorphous powder, m.p. 200–202^{0}C). Fraction 2 was also further purified by column chromatography using 70 g silica gel and ethyl acetate-MeOH as eluents. 2% EtOAc–MeOH yielded compound c (colourless, m.p. 221–223^{0}C).

TH-1101_08610603

4.3.6 Enzyme inhibition studies

Inhibition parameters were calculated using Line-weaver Burk plots. Briefly, enzyme assay was carried out on a Tecan spectrophotometer using DTNB as an indicator for reduced thiol groups using method of Hamilton et al. (2003). For microplate assays, the final assay mixture (250 µl) contained TR (1 m unit), 40 mM HEPES (pH 7.5) , 15 mM NADPH, 1 mM EDTA, 25 µM DTNB and different concentrations of $T(S)_2$ ranging from 0.5 to 200 µM and 2.5 µl of plant extract or 5, 10 and 20 µM of iridoid glucosides. Enzyme mixture was pre-incubated with NADPH for 5 min at 26^0C, then the reaction was started by addition of substrate and inhibitor. Enzyme activity was monitored at 412 nm due to conversion of DTNB into yellow coloured TNB.

4.3.7 Calculation of IC_{50} values of compound a, b and c against TR

The IC_{50} values (concentration required for 50% inhibition) of all the three compounds were calculated in 96-well plate. The assay mixture contained TR (1 mU), 40 mM HEPES (pH 7.5), 0.15 mM NADPH, 1 mM ethylenediaminetetraacetic acid, 25 µM DTNB, 5 µM $T(S)_2$ as substrate and different concentrations of inhibitor 1, 2, 4, 8, 10 and 20 µM. The resulting slope of the (dAbs/dt) of absorbance versus time plot is the measure of enzyme activity (Hamilton et al., 2003). The enzyme inhibition was determined by taking the ratio of activity with drug and without drug (Cota et al., 2008). Thus the percentage inhibition can be calculated as following:

$$\textbf{Percent inhibition} = (1 - (\text{Activity})_{exp}/(\text{Activity})_{contr}) \times 100$$

4.3.8 Estimation of decrease in reduced thiol level

Inhibition of TR leads to a decrease in $T(SH)_2$ and it was estimated via microtitre plate assay using DTNB. *Leishmania* promastigotes and axenic amastigotes were grown in 1 ml culture medium for 48 h in presence of various concentrations of iridoid glucosides (1.562, 3.125, 6.25, 12.5, 25, 50 and 100 µM). Cells were centrifuged, dissolved in 10 mM Tris-HCl buffer (pH-2.5) and sonicated. Acidic pH was used during sonication to prevent oxidation of free thiol groups. Cell debris was removed by centrifugation. 100 µl of supernatant and 100 µl of 500 mM phosphate buffer (pH-7.5) were taken in each

TH-1101_08610603

microtitre well followed by addition of 20 µl of DTNB (1 mM) to each well. Absorbance was measured at 412 nm.

4.3.9 Measurement of ROS elevation in Leishmania promastigotes / axenic amastigotes

Intracellular ROS levels were measured in presence of iridoid glucosides using cell permeant probe CM-H_2DCFDA (Balasubramanyam et al., 2003). *Leishmania* cells were incubated with different concentrations of compound a, b and c (0, 5, 10 and 20 µM) for different time intervals (0, 3, 12, 24 and 48 h), centrifuged, washed and re-suspended in 10 mM Phosphate Buffer Saline (pH-7.4). These cells were loaded with 10 µM CM-H_2DCFDA probe in dark for 45 min. ROS levels were measured as an increase in fluorescence due to conversion of non-florescent dye to highly florescent 2', 7' dichlorofluorescein with an excitation at 488 nm and emission at 530 nm. Morphological changes of *Leishmania* cells as well as ROS levels were further investigated using flow cytometry (BD FACS caliber). After treatment of *Leishmania* promastigotes and axenic amastigotes with 20 µM of compound a, b and c, cells were stained with 10 µM CM-H_2DCFDA for 45 mins and flow cytometric analysis was done for both treated and untreated cells using 488 nm laser and 530 nm emission filter.

4.3.10 Flow cytometric determination of apoptosis using Annexin V-FITC PI kit

Apoptosis causes rapid alterations in phospholipids of cell membrane leading to exposure of phosphatidyl serine on cell surface (early apoptosis) which can be detected by using fluorescein isothiocyanate (FITC) conjugated Annexin V. When there is necrosis of cells, cell membrane ruptures and propidium iodide enters inside the cell to bind with DNA. Thus, necrotic cells bind with propidium iodide (PI) but also get stained with Annexin V-FITC. Therefore, apoptotis of cells can be measured using different filters (FL1 and FL2) in flow cytometer. Flow cytometric detection of apoptosis was performed in promastigotes using Annexin V-FITC apoptosis detection kit (Calbiochem) according to manufacturer's protocol (Paris et al., 2004; Debrabant et al., 2008; Das et al., 2008).

Briefly, promastigotes ($1x10^6$ cells/ml) were incubated with 20 µM of compound a, b and c for 24 h. Cells were centrifuged at 1000g for 5 min, washed twice with PBS, suspended in 0.5 ml 1X binding buffer followed by addition of 1.25 µl of Annexin V FITC for 15 min at room temperature. Again centrifuged and resuspended in binding buffer followed by addition of 10 µl Propidium Iodide. Flow cytometer (BDFACS caliber) was used with an argon laser (excitation wavelength 488 nm) for detection of

TH-1101_08610603

Annexin V FITC stained (early apoptotic) cells in FL1 filter (emission wavelength 518 nm) and PI stained (late apoptotic or necrotic) cells in FL2 filter (emission wavelength 620 nm).

4.3.11 Estimation of macrophage infectivity in presence of iridoid glucosides

For estimation of macrophage infectivity, initially infection of macrophages with *Leishmania* promastigotes was optimized. A mouse macrophage (J774A.1) suspension of density 10^6 cells/ml in DMEM with 20% FBS was prepared. Macrophage suspension and promastigotes were mixed in 1:10 ratio, transferred to 24-well cell culture plate and incubated at 35^{o}C. Promastigotes gained entry into macrophage in about 8 h, then the cells were washed thoroughly to remove non-entered promastigotes (Chang, 1980). These infected macrophages were incubated with increasing concentration of iridoid glucosides (0-100 µM) for 48 h. Fluorescent images were taken after staining with Ethidium bromide (EB) and acridine orange (AO) double stain (1:1) to differentiate between infected and non-infected macrophage (amastigotes appears as bright green spots in infected macrophages).

After 48 h, amastigotes were isolated as reported earlier (Chang, 1980). Briefly, infected macrophages (in PBS with 2 mM EDTA) were passed through a 27-gauge, 0.5 inch syringe thrice followed by centrifugation at 3500g for 5 min to rupture macrophages and remove intracellular amastigotes. The material was suspended in 45% percoll (in PBS) layered over a cushion of 1ml 100% percoll and then centrifuged at 3500g for 30 min. The amastigotes were isolated from the interface between 45% and 100% percoll and counted under microscope. Accordingly, % infectivity was calculated for all the three iridoid glucosides according to the following formula:

$$\% \text{ Infectivity} = \frac{N}{M} \times 100$$

Where, N is number of intracellular amastigotes in presence of drug and M is number of intracellular amastigotes without drug.

TH-1101_08610603

4.3.12 Calculation of IC_{50} values against Leishmania promastigotes / axenic amastigotes

MTT assay (Mosmann, 1983) was performed for the estimation of viability of promastigotes and axenic amastigotes in presence of different concentrations of iridoid glucosides. Both promastigotes ($2x10^6$ cells/ml) and axenic amastigotes ($1x10^6$ cells/ml) were incubated in presence of different concentrations of iridoid glucosides (1 µM-100 µM) for 48 h. The parasite without iridoid glucosides was considered as control. After addition of MTT for 4 h, purple coloured formazan complex was formed which was dissolved in DMSO. Absorbance was measured at 570 nm to calculate % viability of the parasite. Viability of control cells was considered as 100%. The absorbance is a measure of living cells and IC_{50} is the concentration of iridoid glucosides which causes death of 50% cells.

4.3.13 Differentiation of live and apoptotic cells by fluorescence microscopy

Leishmania promastigotes were incubated in 24 well plate with 200 µM compound a, b and c. The cells were taken out at 0, 12, 24, 36 and 48 h, centrifuged and dissolved in 25 µl PBS. 10 µl EB/AO mixture (100 µg/ml each) was added to the cells and examined by epi-fluorescent microscope in blue filter (470 nm/40x). Live cells get stained with acridine orange and fluoresce green whereas necrotic cells with ethidium bromide and fluoresce red (Darzynkiewicz, 1990).

4.3.14 Cytotoxicity measurement of iridoid glucosides on HEK-293 cells and mouse macrophage (J774.1A)

HEK-293 and mouse macrophage (J774A.1) cells were procured from National Centre for Cell Science, Pune, India. The cells were grown in DMEM containing 1.5 g/l $NaHCO_3$, 10% fetal bovine serum, penicillin (100 U/ml) and streptomycin (100U/ml) at 37^0C in 5% CO_2. The % cell viability was estimated using MTT assay in presence of iridoid glucosides as described above.

TH-1101_08610603

4.4 Results

Plants are like chemical factories synthesizing diverse set of highly complex compounds whose structures could escape from the imagination of even the most intelligent scientist. Iridoid glucosides from *Nyctanthes arbortristis* appear to be such compounds. Reports about antileishmanial activity of these compounds on animal model (Tandon et al., 1991) prompted us to understand molecular basis of their antileishmanial effect. In this direction, we have shown these compounds as inhibitors of TR of the parasite (Shukla et al., 2011a). Our current results clearly indicate that these compounds cause imbalance of redox homeostasis and increase in ROS level leading to parasite's death.

4.4.1 Iridoid glucosides have shown positive inhibition of TR in in silico docking studies

We carried out *in silico* docking studies of three compounds which are derivatives of iridoid glucosides (Table 4.1) and reported to be present in the seed kernel of the plant, these compounds show antileishmanial activity. The docking statistics of these compounds with TR of *Leishmania infantum* show that they can be potent inhibitors of TR, providing vital clues about their mode of action. These compounds bind to the residues of the TR substrate binding cleft and can be potential inhibitors of the enzyme. They also dock with higher docking energy to TR which signifies their selectivity towards the enzyme.

The residues which are involved in hydrogen bonding with the inhibitors, namely GLU466, GLU467, MET400 and LEU399, LYS61 aid in hydrogen bonding of the substrate and in orientation of the substrate towards the hydride transfer site respectively, whereas HIS461 aids in charge transfer by hydride transfer from FAD of the active site (Figure 4.2). The clusters formed at the active site are very discrete, indicating these molecules can bind to the active site in multiple orientations and also potentially exhibit synergistic role in inhibition of the enzyme. These *in-silico* docking results prompted us to carry out experimental validation on recombinant enzyme.

TH-1101_08610603

Table 4.1 Chemical structure and docking statistics of iridoid glucosides.

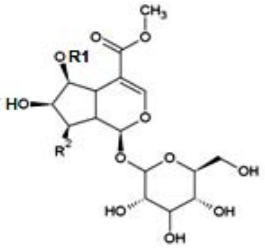

S. No	R^1	R^2	Binding energy to TryR	Hydrogen bonds
1. Compound a	Coumaroyl 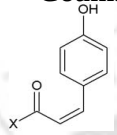	CH_3	-5.77	2jk6:A:GLU467:OEI 2jk6:A:LEU399:HN 2jk6:A:THR397:HN
2. Compound b	p-methoxy cinnamoyl 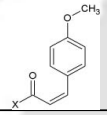	CH_3	-5.86	2jk6:B:LYS61;HZ2 2jk6:B:GLY49:O 2jk6:B:SER14:OG
3. Compound c	H	CH_3	-5.84	2jk6:A:GLU467:OEI 2jk6:A:SER464:OG 2jk6:A:MET400:HN 2jk6:A:GLU466:OE2

Table 4.2 Inhibition of trypanothione reductase by iridoid glucosides and other inhibitors from plants.

Sr. No.	Name of Compound	Source	Ki (µM)	IC_{50}	References
1.	Compound a	*Nyctanthus arbortristis*	3.24±0.05	2.29±0.03µM	Current study
2.	Compound b	*Nyctanthus arbortristis*	3.34±0.03	2.65±0.05µM	Current study
3.	Compound c	*Nyctanthus arbortristis*	6.49±0.05	4.74±0.05µM	Current study
4.	Spermidine analogue of Kukoamine A	*Lycium chinensis*	7.5	-	Ponasik et al., 1995
5.	*Altenusin	*Alternaria sp.*	-	43± 0.3	Cota et al., 2008a
6.	*Panepoxydone	*Lentinus strigosus*	-	38.9	Cota et al., 2008b
7.	* Arylfuran derivative of lignans	*Virola surinamensis*	-	48.5	Oliveira, et al., 2006

TH-1101_08610603

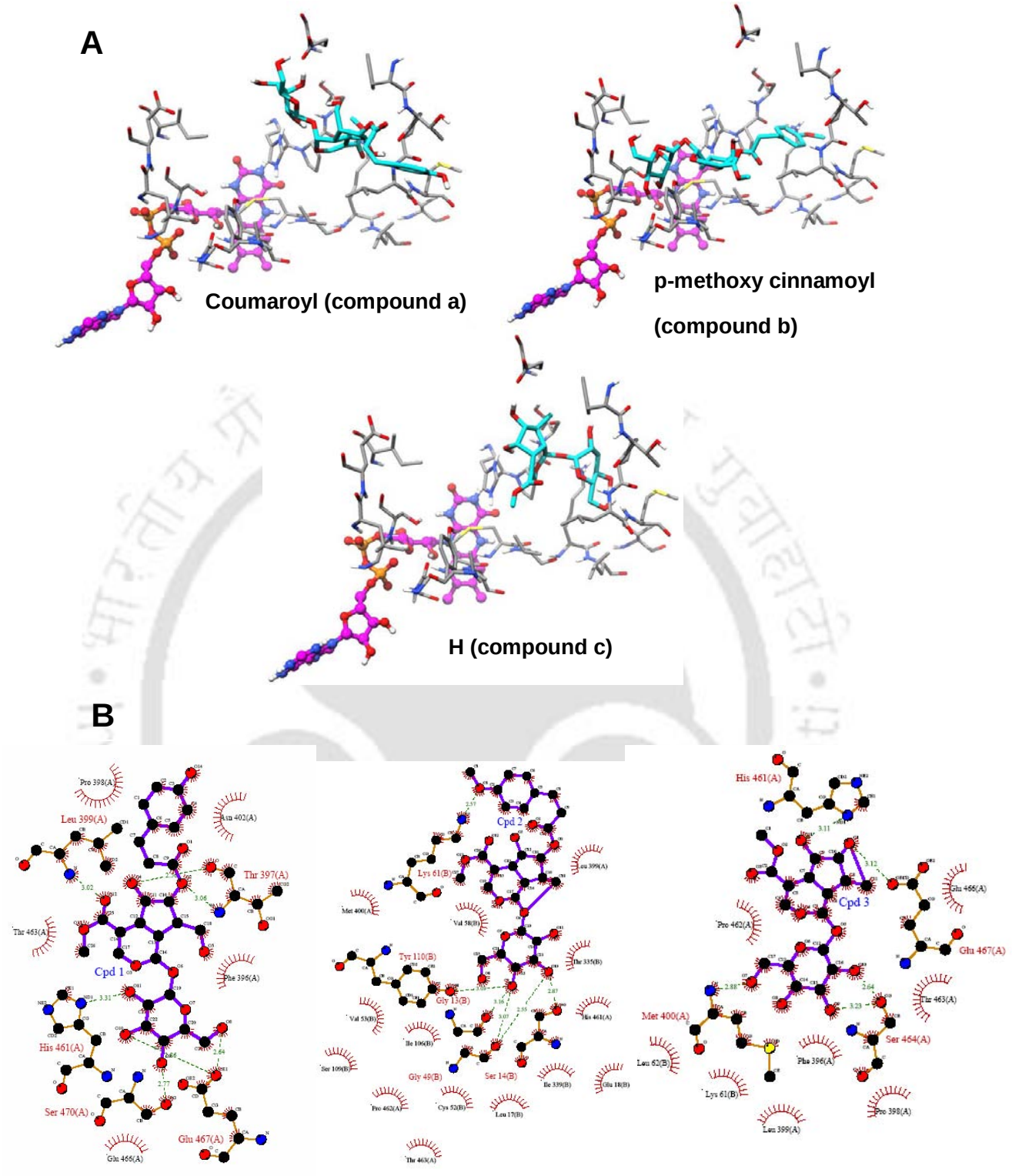

Figure 4.2 ***In silico*** **interactions of iridoid glucosides with TR: (A)** 3D binding modes of iridoid glucosides with TR. **(B)** 2D Ligplots showing the Hydrogen bonding and hydrophobic interaction map between the compounds and active site residues. From the modelled 2D interaction maps it is apparent that interactions (Hydrogen and Non-bonding) are conserved among all the three compounds that we studied.

TH-1101_08610603

4.4.2 Effect of plant extracts on trypanothione metabolism

Both the methanolic and aqueous extracts obtained from leaf, stem and flower have shown positive inhibition of TR with an increase in Michaelis constant (K_m value) from 5.44±0.05 µM to 21.73±0.15, 83.33±1.0, 33.34±1.0 µM for stem, leaf and flower respectively in case of methanolic extract and to 5.74±0.05, 6.66±0.08 and 8.33±0.05 µM for stem, leaf and flower in case of aqueous extract respectively. Therefore, some of the biological components present inside this medicinal plant have inhibition effect on trypanothione metabolism via inhibiting the TR and can be targeted as naturally occurring chemotherapeutic agents against Leishmaniasis. These results prompted us for further purification of compounds from the plant and assay their inhibitory effect against TR.

4.4.3 Calculation of inhibitory constant (K_i) and IC_{50} values of iridoid glucosides

All the three isolated iridoid glucosides (compounds a, b and c) have shown inhibition of TR with an increase of K_m value from 5.44 µM to 22.23 µM, 21.73 µM and 13.81 µM for compound a, b and c respectively (with 10 µM of inhibitor concentrations). Thus, these three isolated glucosides have shown very high competitive inhibition of TR with K_i values of 3.24±0.05 µM, 3.34±0.04 µM and 6.49±0.05 µM, respectively. As V_{max} of the enzymatic reaction does not change, the compounds are likely to be competitive inhibitors (Figure 4.3). Additionally, IC_{50} values are also calculated and given in Table 4.2. It is worth mentioning that TR (from *Trypanosoma cruzi*) inhibitor of plant origin is reported in the literature (Cota et al., 2008).

Therefore these iridoid glucosides can be targeted as naturally occurring chemotherapeutic agents against Leishmaniasis. This is the first report of iridoid glucosides as inhibitors for this class of enzyme. It is interesting to note that the structure of these iridoid glucosides is completely distinct from the peptide backbone of the $T(SH)_2$ substrate. As the TR activity is required for parasite's survival, inhibition of the enzyme will result in parasite's death (Sharma et al., 2012). Moreover, we have also worked on effects of these compounds on redox-homeostasis of the parasite as TR has key role in redox balance.

TH-1101_08610603

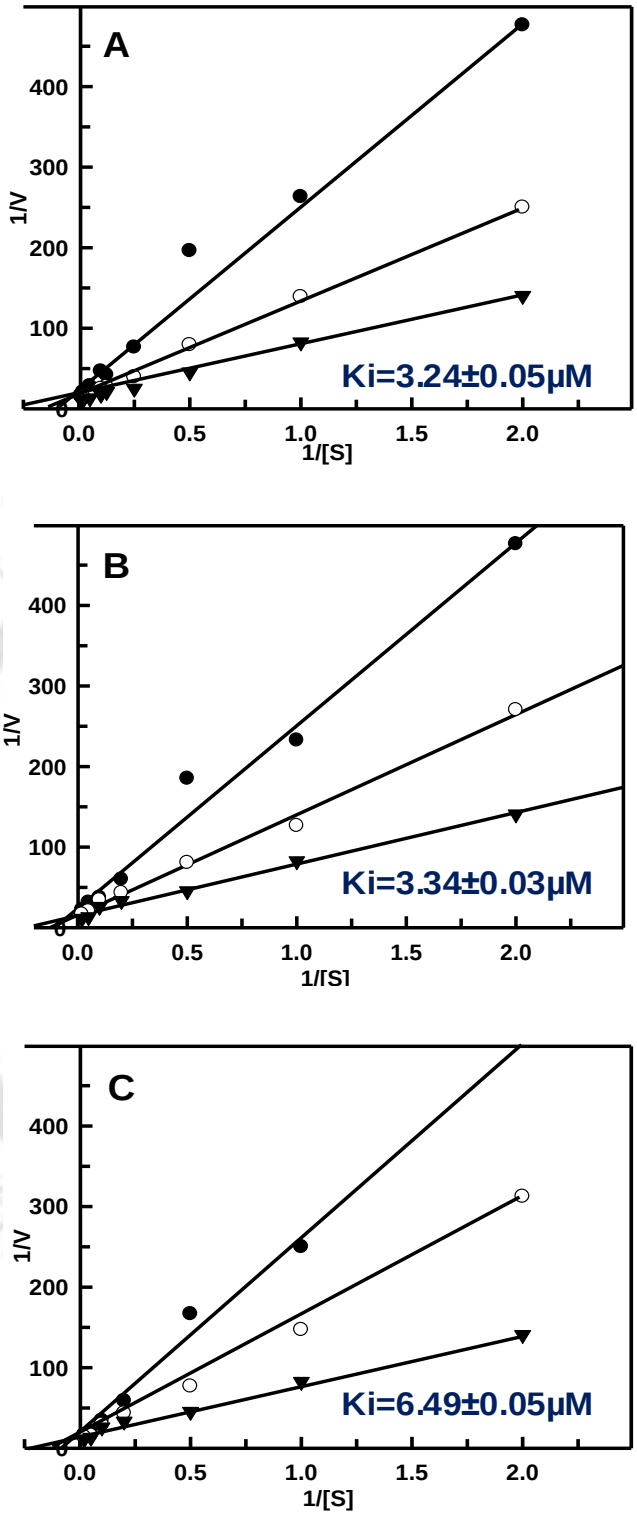

Figure 4.3 Enzymatic assay of TR in presence of iridoid glucosides: **(A)** In presence of Compound a, **(B)** In presence of compound b and **(C)** In presence of compound c. Triangle, circle and dot represents data with 0μM, 5μM and 10μM inhibitor concentration respectively..

TH-1101_08610603

4.4.4 Iridoid glucosides induce decrease in total reduced thiol

When promastigotes and axenic amastigotes were incubated with different concentrations of compound a, b and c for 12, 24, 36 and 48 h, the lowest concentration (3.125 µM) showed a decrease in reduced thiol level up to 92.54±2.87%, 92.58±3.65% and 95.30±2.87% respectively after 12 h. After 48 h, the decrease was 63.72±1.87%, 67.87 ±1.43% and 78.87±1.65% for the same concentration of each compound. The highest concentration (100 µM) showed a decrease up to 60.09±3.21%, 63.63±1.65% and 62.67 ±1.33% after 12 h and 33.82±2.87%, 41.87 ±2.66% and 46.87±3.00% after 48 h. Similarly, in case of axenic amastigotes, 3.125 µM concentration showed a decrease in reduced thiol level up to 97.87±1.43%, 96.88±3.87% and 97.66±2.76% after 12 h and 73.43±2.65%, 77.53±2.1% and 82.76±3.12% after 48 h. 100 µM showed a decrease up to 65.77±1.84%, 67.87±2.76% and 67.76±2.62% after 12 h and 41.87±1.52%, 46.87 ±2.76% and 51.66±2.43% after 48 h (Figure 4.4). These results indicate imbalance in redox homeostasis which causes decrease in total reduced thiol levels.

4.4.5 Iridoid glucosides cause elevation in ROS level

Intracellular ROS measurements using CM-H_2DCFDA probe have shown that ROS levels were significantly increased with increasing concentration of any of these compounds (Figure 4.5). The effect was maximal after 48 hs of incubation. Moreover there was no prominent difference in effect on promastigote or amastigotes forms of parasite and both forms appear to be equally responsive. Furthermore, morphological changes took place inside the parasite due to elevation in ROS level which was estimated by flow cytometry. We have used acquisition dot plot between side scatter (SSC) and FL1 (specific for CM-H_2DCFDA) and histogram plot using FL1 to evaluate changes in surface morphology as well as increase in oxidative stress due to elevated level of ROS. Flow cytometric analysis, using excitation of 488 nm argon laser and 530 nm emission filter (FL1), showed high population of cells compared to control on density plot which further confirmed an increase in ROS (Figure 4.6). Oxidative stress in the parasite leads to morphological changes in the cells. SSC-H is a measure of cell surface topology i.e. when cell is under stress condition, its surface becomes rough and SSC-H increases. FL1 parameter indicates the intensity of fluorescence of probe due to ROS. SSC-H was found to increase substantially in treated promastigotes and amastigotes compared to control, which indicated that cell surface became rough due to oxidative stress. On the other hand, the FL1 intensity was observed to be greatly increased in treated promastigotes and

TH-1101_08610603

axenic amastigotes compared to control cells which in turn confirms significant increase in ROS levels inside the parasite on treatment with iridoid glucosides. These results indicate that *Leishmania* cells are prone to apoptotic death due to increased level of ROS which was further proved by apoptotic assay.

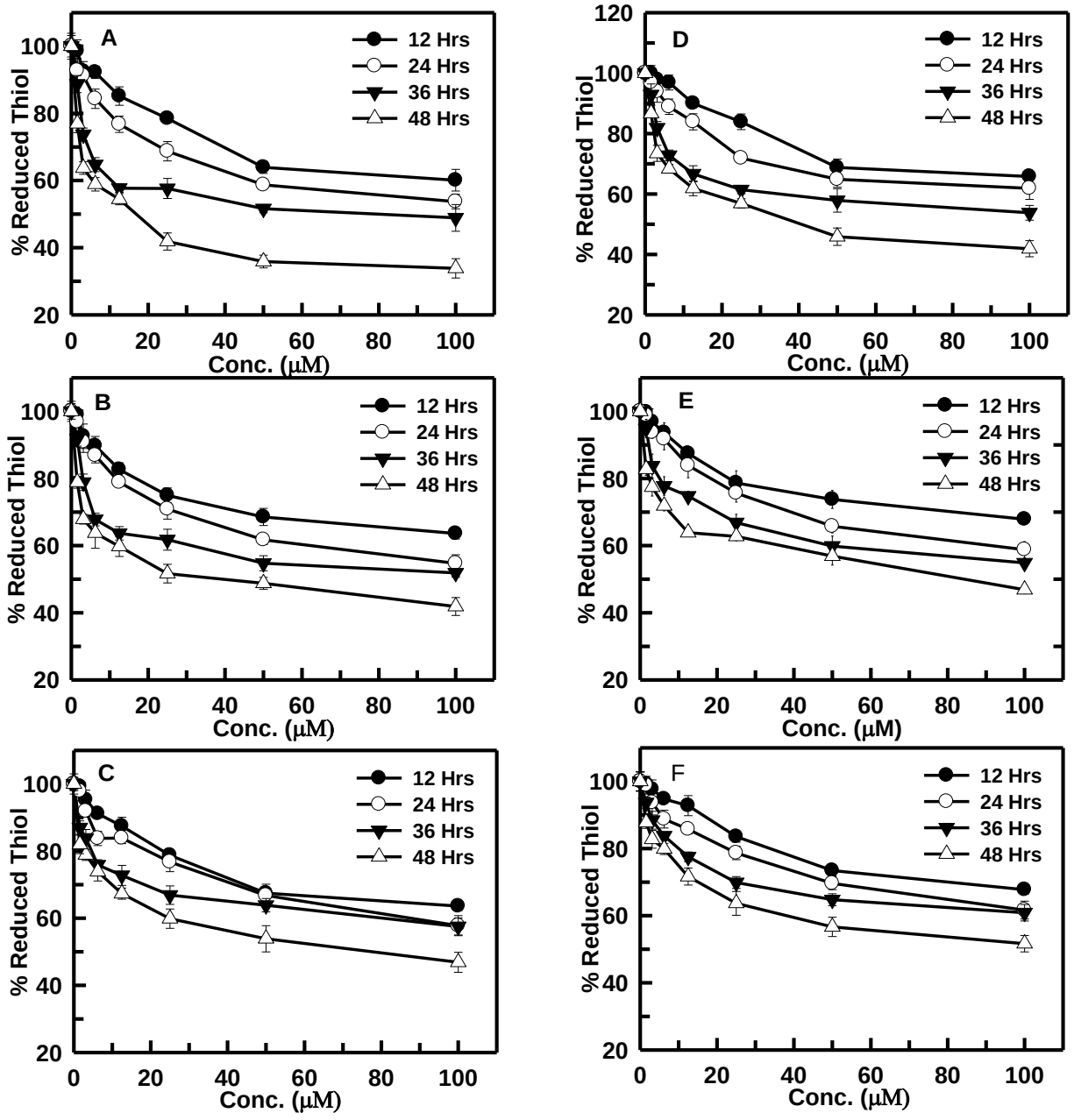

Figure 4.4 **Estimation of decrease in thiol levels: (A), (B)** and **(C)** represent graphs showing decreased thiol levels inside *Leishmania* promastigotes and **(D), (E)** and **(F)** inside amastigotes after treatment for 12, 24, 36 and 48 h in different concentrations of compound a, b and c respectively.

TH-1101_08610603

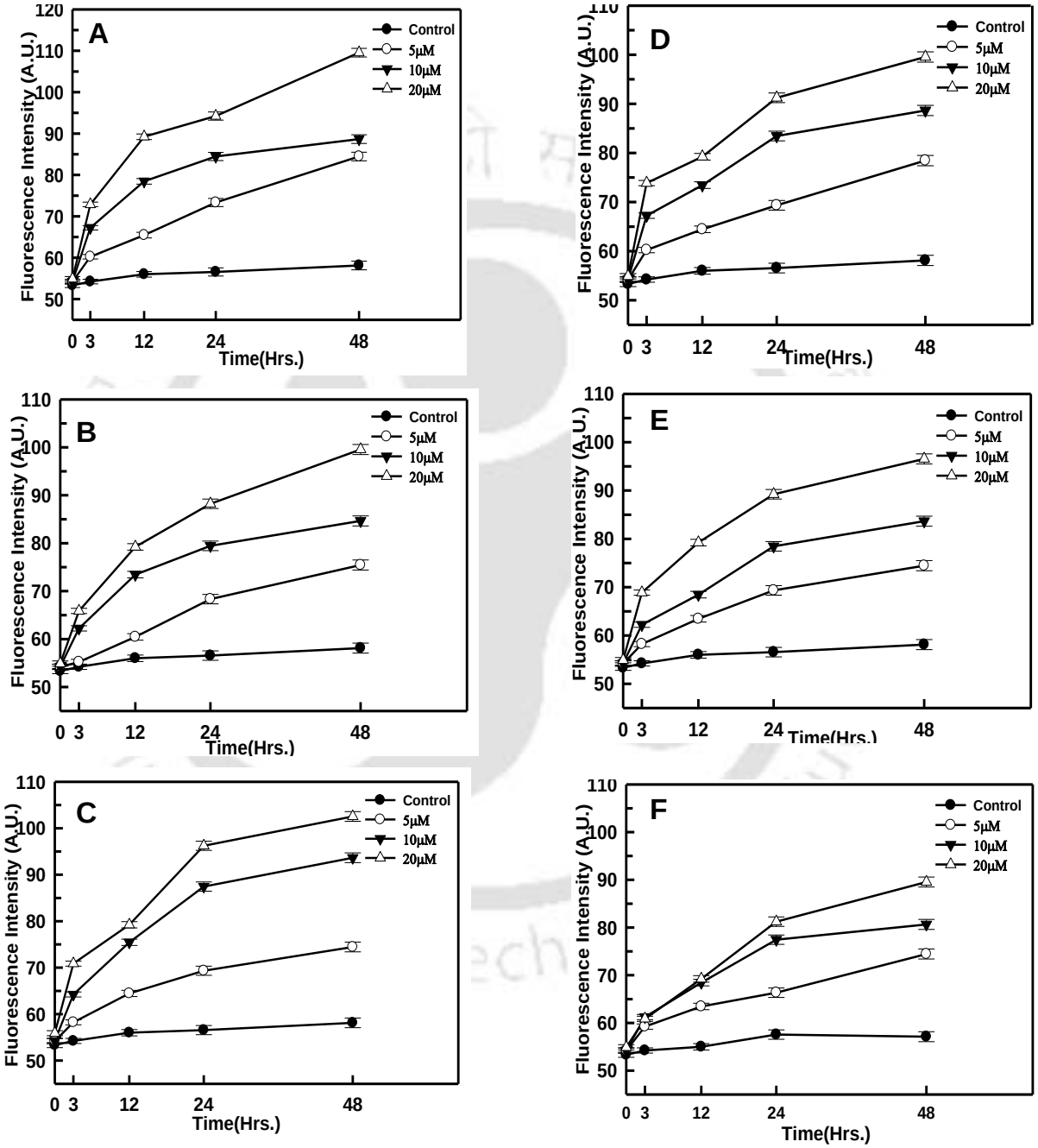

Figure 4.5 Measurements of intracellular ROS levels: **(A)**, **(B)** and **(C)** fluorescence intensity measurements at 488/530 nm in promastigotes in presence of compound a, b and c respectively. **(D), (E)** and **(F)** fluorescence intensity measurements at 488/530 nm in amastigotes in presence of compound a, b and c respectively.

TH-1101_08610603

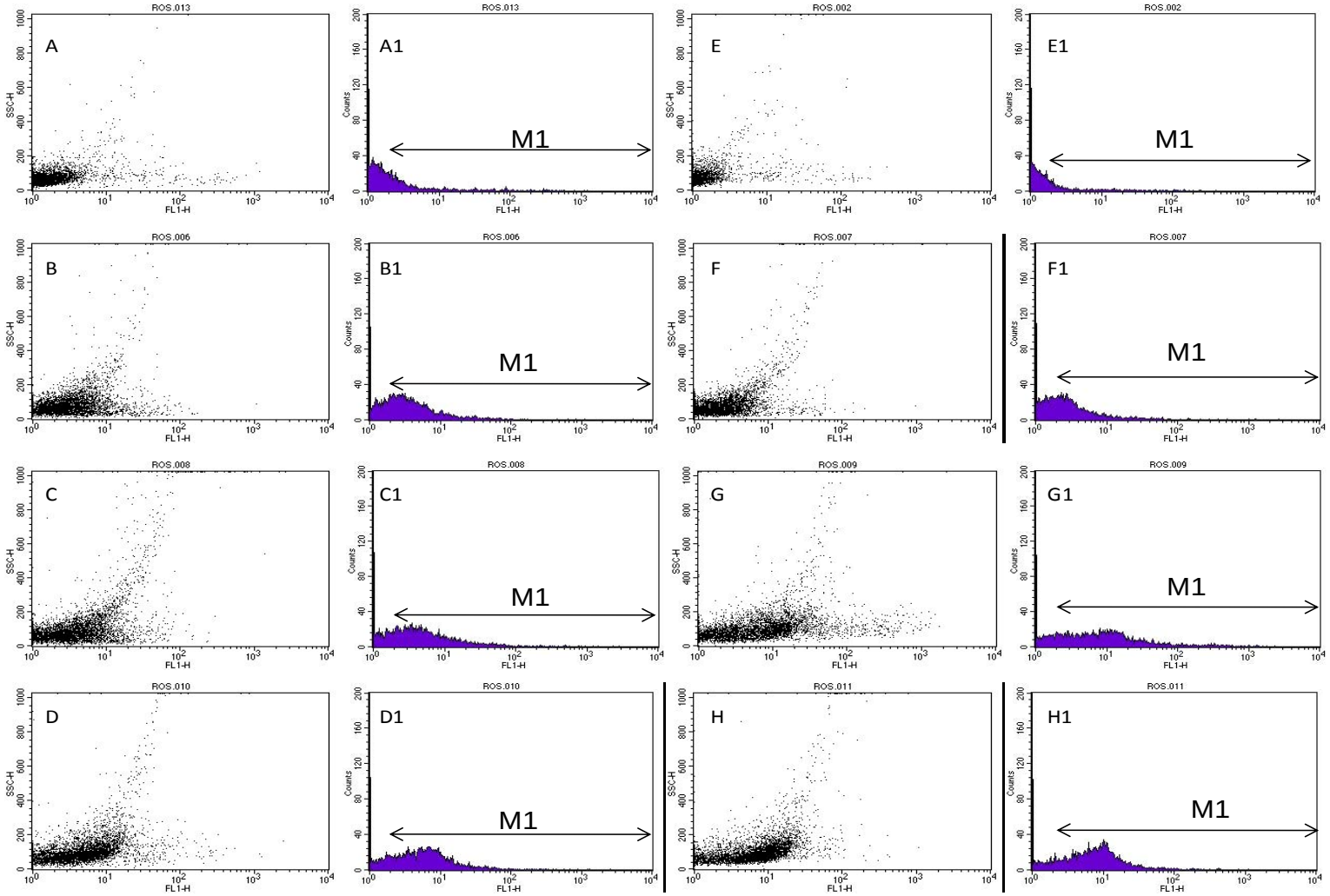

Figure 4.6: Flow cytometric analysis in *Leishmania* promastigotes and axenic amastigotes: **(A), (B), (C)** and **(D)** acquisition dot plots (FSC vs. FL1) of control and treated promastigotes with 20 µM of compound a, b and c respectively, whereas **(A1), (B1), (C1)** and **(D1)** represent histogram plot (FL1 vs. FSC) of control and treated *Leishmania* promastigotes. Similarly **(E), (F), (G)** and **(H)** and **(E1), (F1), (G1)** and **(H1)** represent histogram plot of untreated and treated amastigotes.

TH-1101_08610603

4.4.6 Iridoid glucosides cause death of promatigotes and axenic amastigotes

Compounds a, b and c have shown significant inhibition of growth when tested *in vitro* against *Leishmania donovani* promastigotes and amastigotes via MTT cell viability assay. IC_{50} values of compound a, b and c against promastigotes and axenic amastigotes were found to be 3.264±.05, 3.504±.04, 5.016±.05 µM and 7.26±.05, 7.63±.05, 9.00±.03 µM respectively (Figure 4.7). All these values are very small which signifies these compounds to be very potent inhibitor of cell growth via interfering with the trypanothione metabolism which leads to oxidative stress and death of parasite.

This data is further substantiated by the fluorescent imaging of *Leishmania* promastigotes stained with double dye (EB/AO). Images showed the progressive death of treated *Leishmania* parasite (200 µM of compound a, b and c) compared to untreated with increasing time. Compound a was found to be the most effective in killing promastigotes (Figure 4.8).

4.4.7 Iridoid glucosides cause hindered growth of intracellular amastigotes

Mouse macrophages (J774A.1) were successfully infected by *Leishmania donovani DD8* with an optimal infectivity time of 8-10 h. Microscopic images clearly showed that in absence of the drug, infected macrophage were damaged and ruptured releasing amastigotes, whereas in presence of 10 µM concentration of each compound, macrophages were non-ruptured and confluent. Also, macrophages were highly confluent and healthy when 100 µM concentration of compound a, b and c was present (Figure 4.9). It depicts that the growth of intracellular amastigotes is hindered inside the macrophage along with maintaining viability of macrophages in presence of these iridoid glucosides. Epifluorescent images indicated the presence of intracellular amastigotes inside the macrophage as bright green spots (Figure 4.10A-D). Percentage (%) infectivity was significantly decreased with increasing concentration of each iridoid glucoside as measured by counting the number of isolated amastigotes (Figure 4.10E). This indicates that iridoid glucosides inhibit the multiplication of intracellular amastigotes.

TH-1101_08610603

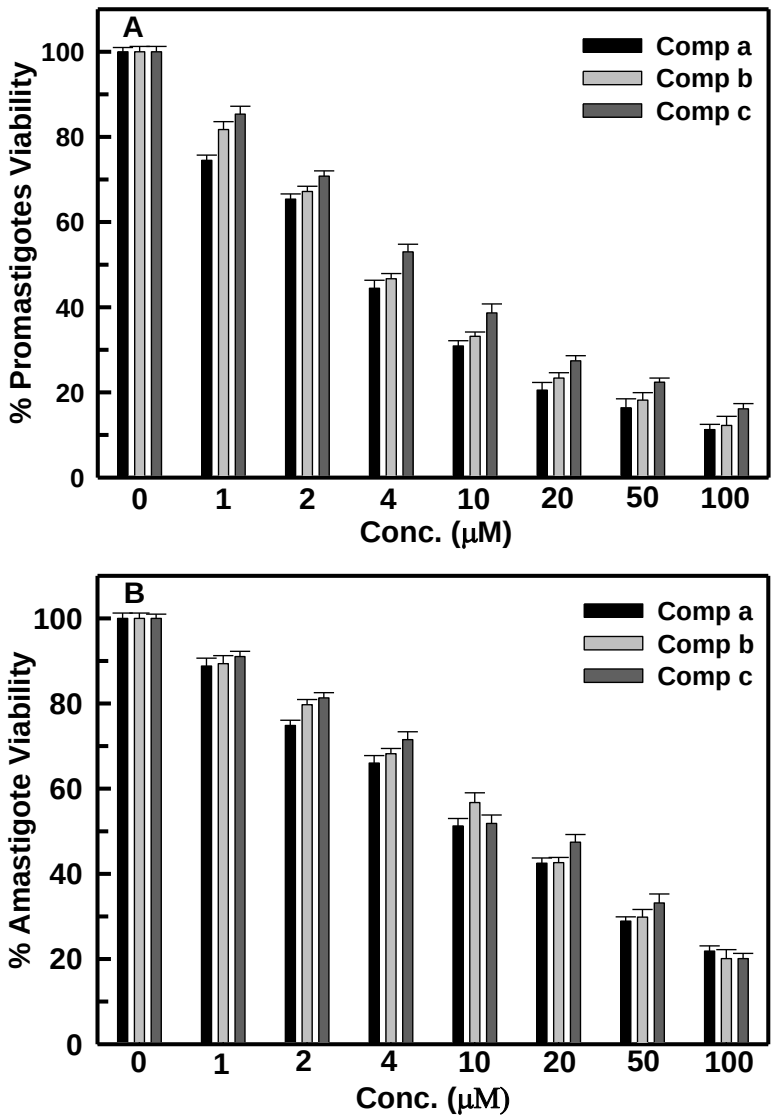

Figure 4.7 MTT assay of iridoid glucosides: **(A)** *Leishmania* promastigotes and **(B)** *Leishmania* axenic amastigotes with different concentration (0, 1, 2, 4, 10, 20, 50 and 100 μM) of compound a, b and c respectively. IC_{50} values of compound a, b and c against promastigotes and axenic amastigotes were found to be 3.264±.05 μM, 3.504±.04 μM, 5.016±.05 μM and 7.26±.05 μM, 7.63±.05 μM, 9.00±.03 μM respectively. Control cells were considered as 100% viable.

TH-1101_08610603

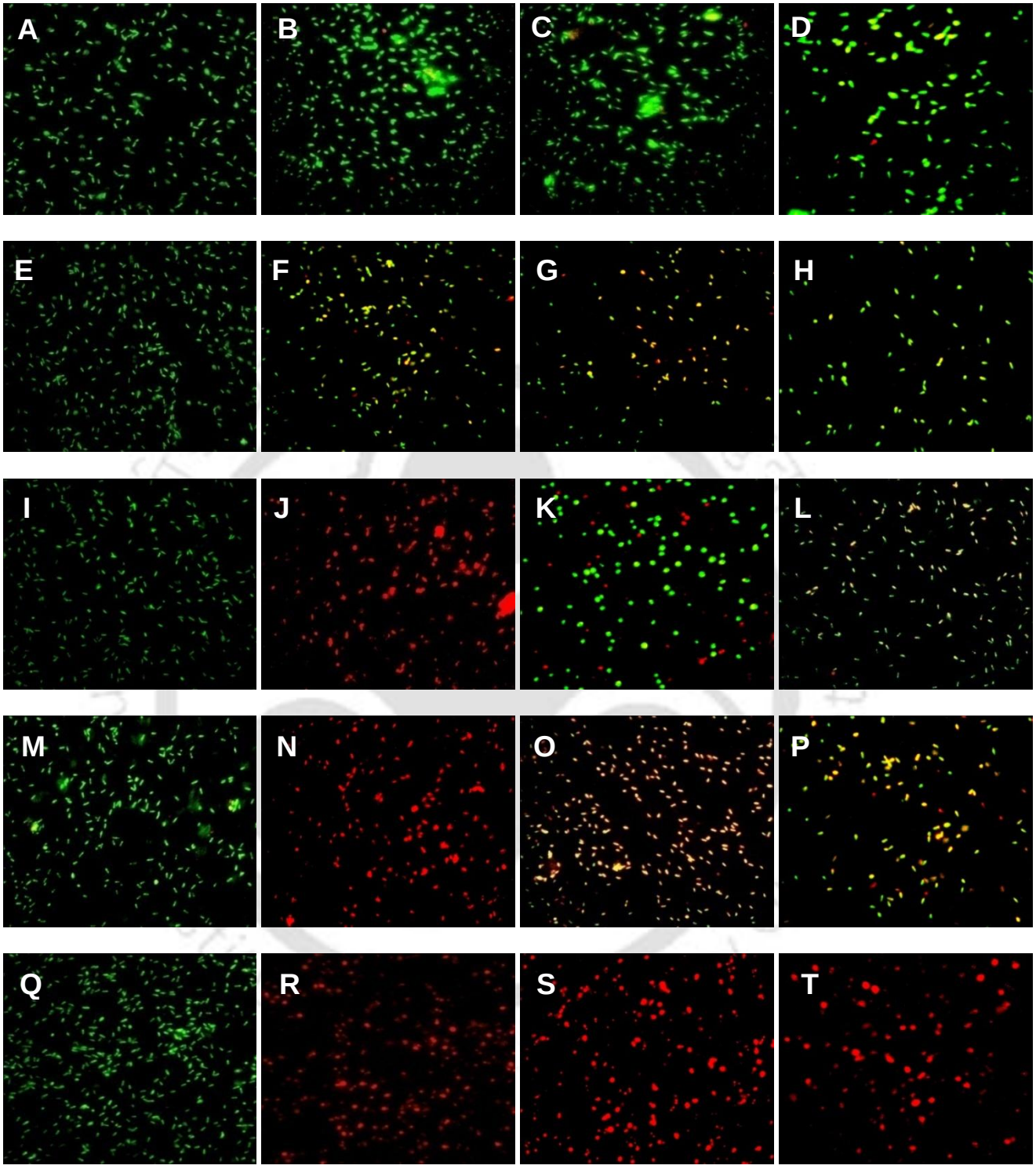

Figure 4.8 **Fluorescent images of AO/EB stained *Leishmania* promastigotes in presence of 200 µM of iridoid glucosides: (A)** to **(D)** control promastigotes and promastigotes in presence of compound a, b and c at 0 h. Similarly, **(E)** to **(H)** at 12 h, **(I)** to **(L)** at 24 h, **(M)** to **(P)** at 36 h, **(Q)** to **(T)** at 48 h. Figures shows that compounds cause death of *Leishmania* parasite and compound a is most potent in killing.

TH-1101_08610603

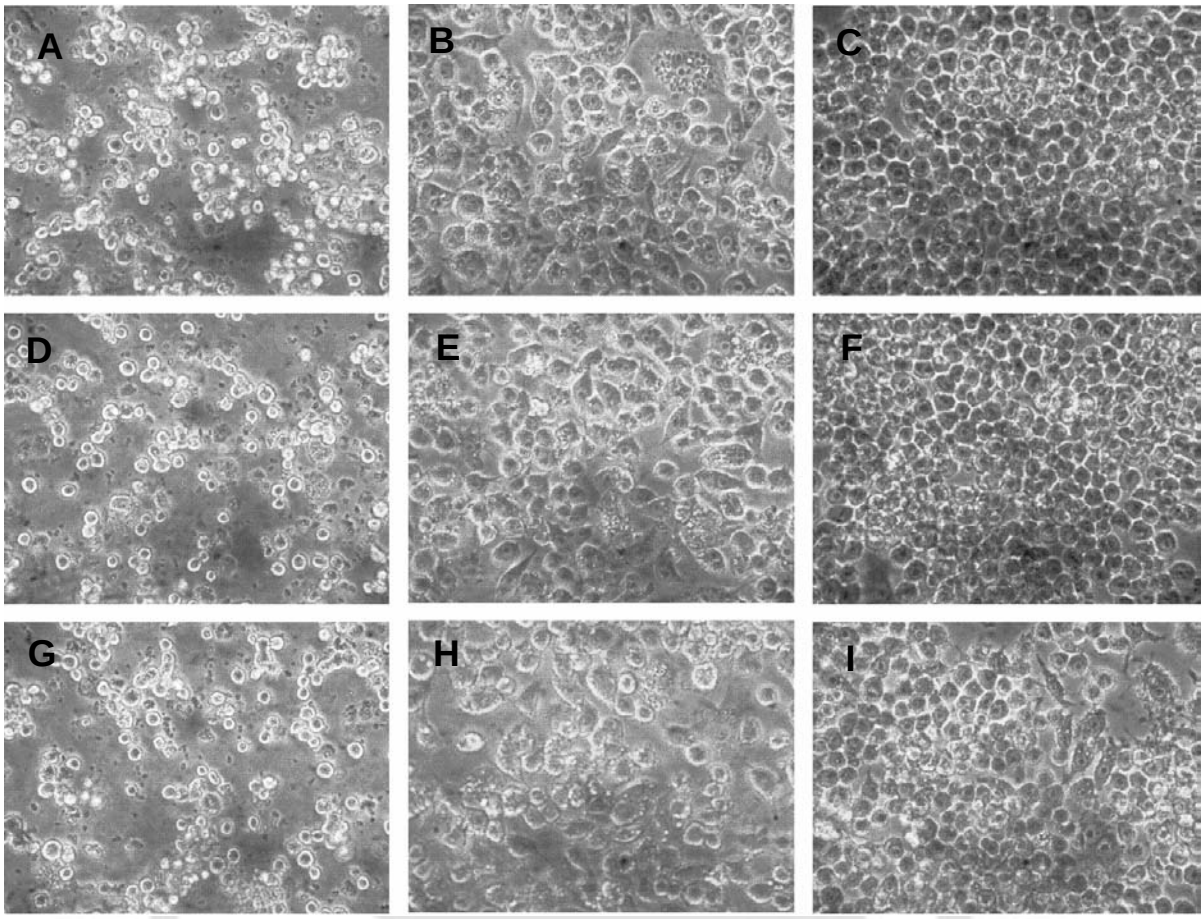

Figure 4.9 Microscopic images of infected macrophage at different concentration of iridoids: (A), (B) and (C) at 0, 10 and 100 µM of compound a respectively. (D), (E) and (F) at 0, 10 and 100 µM of comp b respectively. (G), (H) and (I) at 0, 10 and 100 µM of comp c respectively (Magnification 100X). Images indicate that macrophages are health and least infected in presence of 100 µM compounds whereas macrophages without compounds are unhealthy, ruptures and amastigotes are also release outside.

4.4.8 Iridoid glucosides treated Leishmania promastigotes exhibit apoptosis-like death mechanism

Annexin V, a calcium dependent phospholipid binding protein interacts with externalized PS (phosphatidyl serine) by apoptotic cells. Cell impermeable dye PI (propidium iodide) was used to differentiate between necrotic cells and apoptotic cells as Annexin V also labels necrotic cells but PI does not permeate cells until membrane integrity is lost i.e. necrosis of cell occurs. Acquisition dot plot shows quadrant {LL=live cells (both Annexin V and PI Negative), LR= apoptotic cells (Annexin V positive only), UR= necrotic cells (both Annexin V and PI positive) and UL= normally dead cells}. Figure 4.11 clearly demonstrates that % of apoptotic cells is quite higher in treated cells compared to control cells which may be due to increased ROS level.

TH-1101_08610603

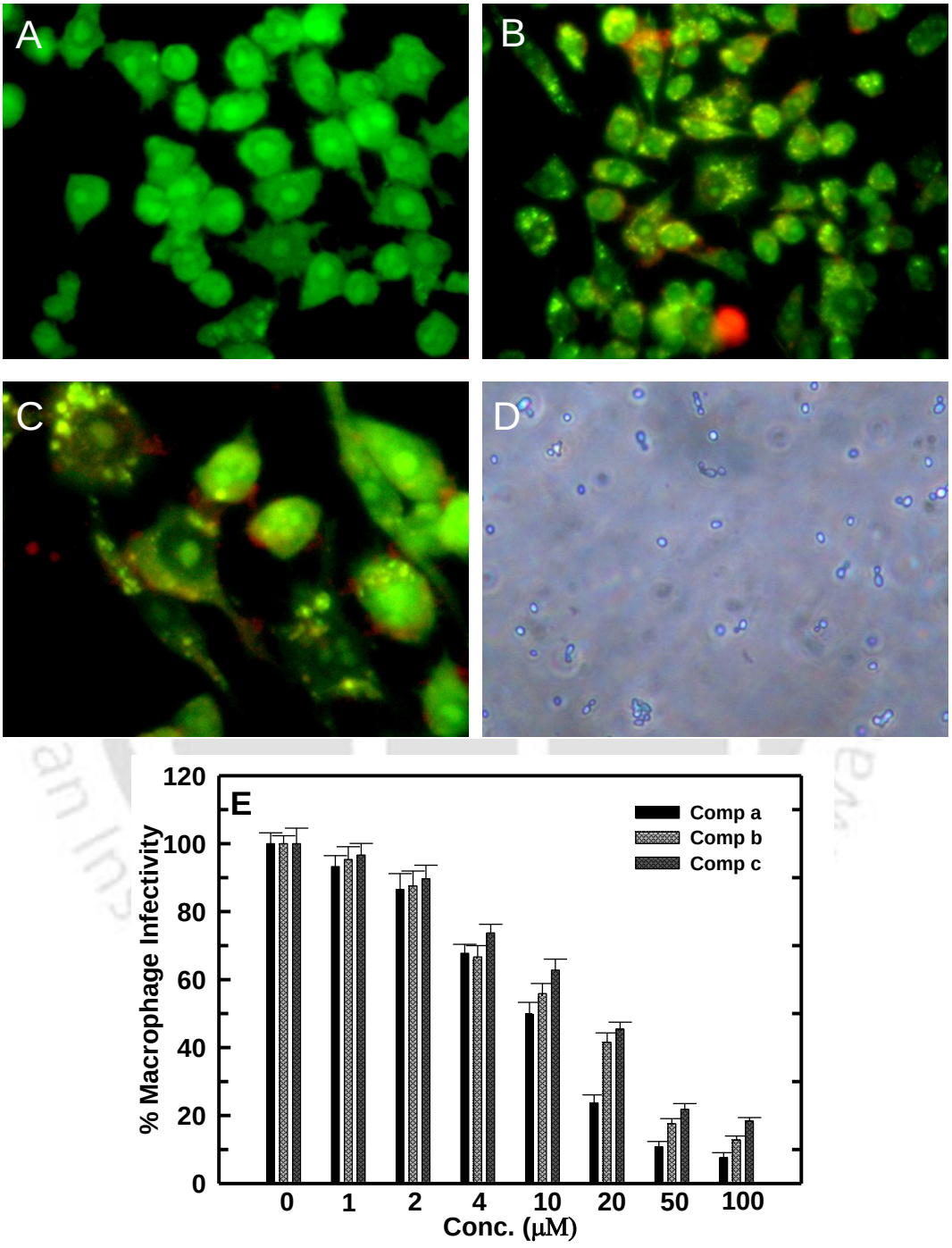

Figure 4.10 Fluorescent images of AO/EB stained mouse macrophages (J774.1A): (A) Non-infected macrophages. **(B)** & **(C)** *Leishmania* infected macrophages. **(D)** Amastigotes isolated from infected macrophages. **(E)** Macrophage infectivity in different concentration of iridoid glucosides. Bright green amastigotes are visible inside infected macrophages. % infectivity decreases with increasing concentration of iridoid glucosides.

TH-1101_08610603

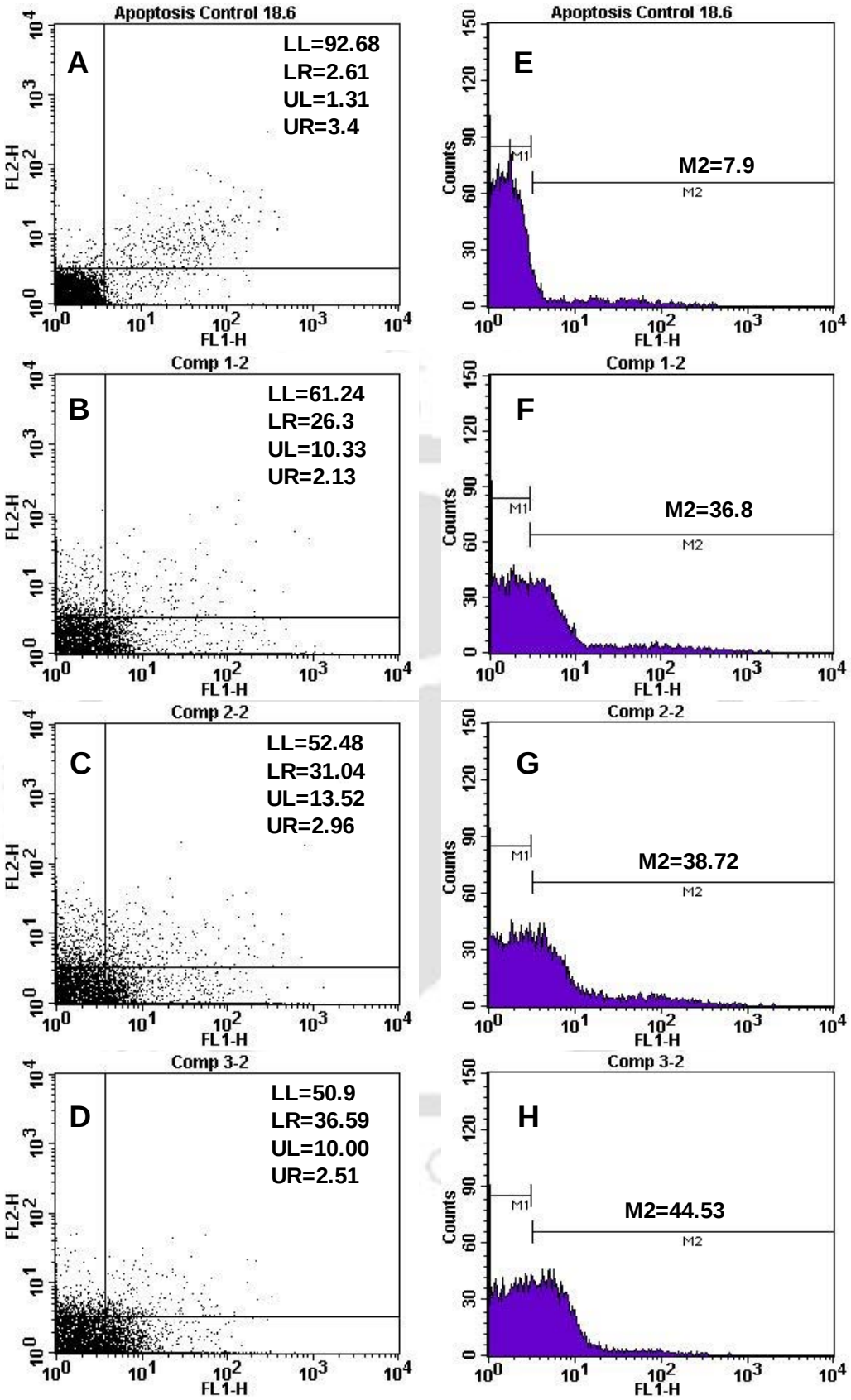

Figure 4.11 Apoptosis assay using Annexin V-FITC & PI (A), (B), (C) & **(D)** Acquisition dot plots (FL1vs FL2) of control promastigotes and promastigotes treated with compound a, b and c respectively. **(E), (F), (G)** & **(H)** Histogram plots (FL1 vs Counts) of control and promastigotes treated with compound a, b and c respectively. Increase in LR quadrant and FL1 indicates apoptosis of cells.

TH-1101_08610603

4.4.9 Iridoid glucosides are not toxic

Iridoid glucosides have shown negligible toxicity on both mouse macrophage (J774.1A) and human embryonic kidney cells (HEK 293). The results showed that these compounds have accepted toxicity if given in limited doses (Figure 4.12). High concentrations of iridoid glucosides (compared to their IC_{50} values) show slight toxicity on HEK 293 cells.

In case of RBC haemolysis assay, after 24 h 3.8%, 3.7% and 4.2% haemolysis was found with 32xIC_{50} of compound a, b and c respectively. Whereas, after 1 h 0% haemolysis with 1xIC_{50} of all the three compounds was found. In case of cytotoxicity studies, the % cell viability of HEK 293 cell lines was found to be 89.91±1.62, 86.63±2.53 and 74.25±2.45 with 10 µM of compound a, b and c respectively. Whereas, the % viability of mouse macrophage was found to be 92.87±1.52, 94.84±2.67 and 90.11±2.41 with 10 µM concentration of compound a, b and c respectively. Therefore, these small values indicate that iridoid glucosides obtained from *Nyctanthes arbortristis* are quite safe to be used as antileishmanial drugs.

As the drug reaches to kidney cells after complete absorption and assimilation process so, even if high initial concentrations of these drugs are given, only a small fraction will reach to kidney cells which will be well within its toxic threshold. Thus, these compounds are safe with respect to human health and have high potential to be developed as antileishmanial drugs. Furthermore, there is no adverse effect of these compounds on macrophages, the home of the parasite which will lead to decrease in infectivity by *Leishmania*. Taken altogether, these observations point towards the importance of thiol redox state for the survival of *Leishmania* parasite and potential application of these compounds as anti-leishmanials.

TH-1101_08610603

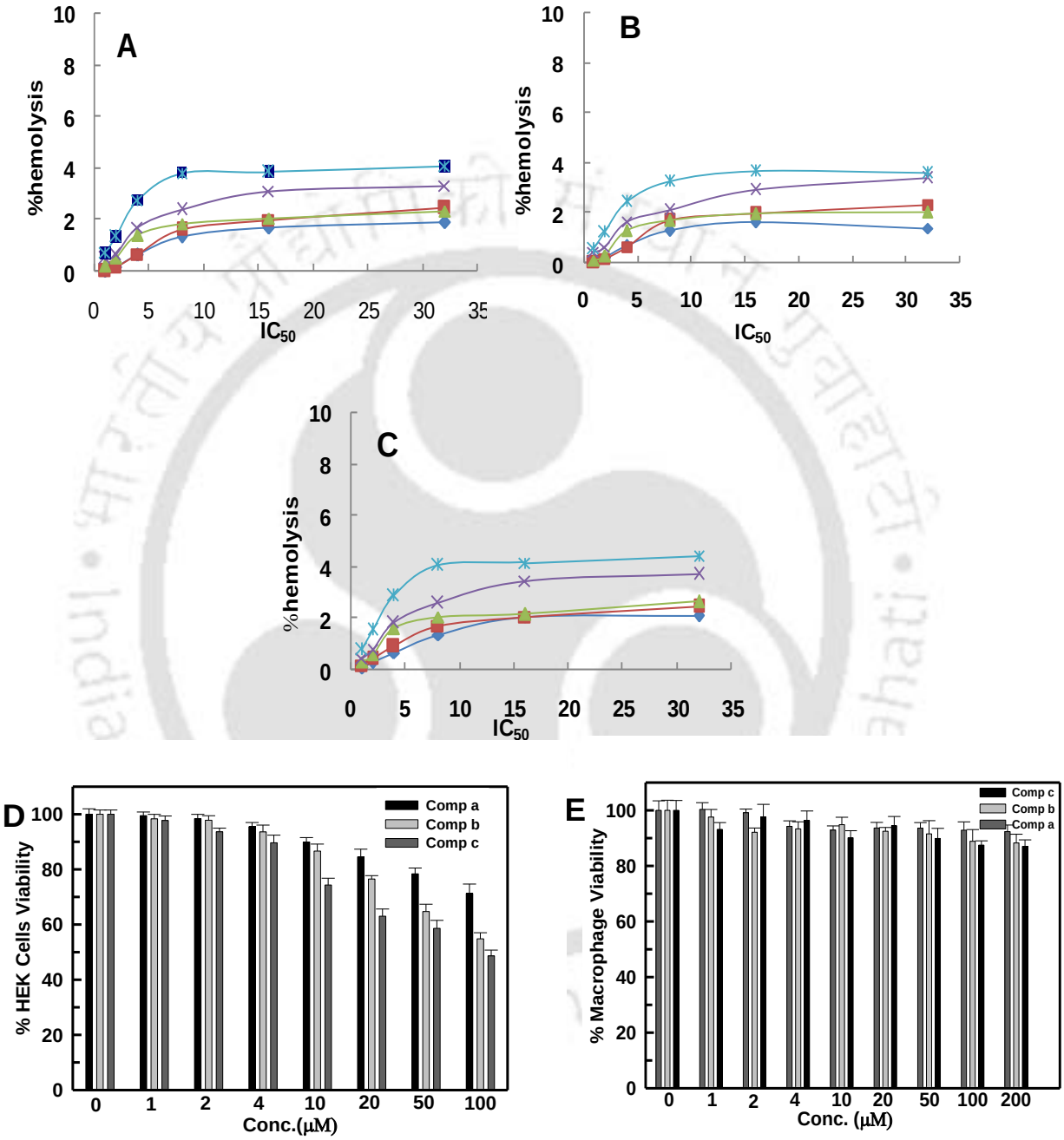

Figure 4.12 **RBC haemolysis assay and cytotoxicity assay on HEK 293 and MQ: (A), (B) & (C)** RBC haemolysis assay with compound a, compound b and compound c. at 0, 12, 24, 36 & 48 h. D) and E) MTT assay on HEK 293 cells and macrophages. They were incubated with different concentration of compound a, b and c (0, 1, 2, 4, 10, 20, 50, 100 and 200 µM). 4 µM of compound a, b and c showed 95.46±1.95%, 93.62±1.50% and 89.63±2.46% cell viability while very high concentration i.e. 100 µM showed 71.25±97%, 54.83±1.60 % and 48.62±2.35% cell viability. All the three iridoids have shown negligible toxicity on macrophage, the home of the parasite.

TH-1101_08610603

4.5 Discussion

Redox homeostasis is crucial for numerous biological events to occur such as enzyme activation, DNA synthesis and cell cycle regulation. As redox imbalance is correlated with increase in ROS, it is likely that the compounds are interfering with some enzyme (s) of $T(SH)_2$ metabolism involved in removal of oxidative stress. Our preliminary studies establish these compounds as inhibitors of trypanothione reductase (Shukla et al., 2011a). However, their effect on other enzymes/proteins involved in transfer of reducing equivalents to Glutathione peroxidase type enzyme (Px) cannot be ruled out. All aerobic organisms which derive their energy from reduction of oxygen are quite sensitive to intracellular ROS levels. Small variation in the basal level of intracellular ROS modulates the cell metabolism, gene expression, as well as post-translational modification of proteins (Darzynkiewicz, 1990). Mammalian cells possess well defined defense mechanisms to detoxify radicals. Catalase or Glutathione peroxidase (GPx) are involved in reduction of hydrogen peroxide into water. *Leishmania* parasite does not have catalase as well as Glutathione peroxidase (GPx) system. However, they have an analogous enzyme called Glutathione peroxidase type enzyme (Px) which carries out the same function (Sies, 1991; Krauth-Seigel and Comini, 2008). Reducing equivalence is provided to Px through cascade of reactions involving several proteins (like trypanothione reductase, thioredoxin and tryparedoxin). Our results so far, point out that these iridoid glucosides inhibit trypanothione reductase and thus stop flow of reducing equivalence to Px. This results in increased level of ROS and oxidative stress in parasitic cell, followed by apoptosis and inhibition of DNA synthesis.

4.6 Conclusion

In summary, we have reported that iridoid glucosides, isolated from *Nyctanthes arbortristis*, are competitive inhibitors of TR enzyme of *Leishmania* parasite. These compounds elevate oxidative stress inside the parasite leading to its death via apoptosis like death mechanism. All the three isolated glucosides have inhibitory effect on macrophage infection by the parasite Their toxicity is minimal on HEK293 and macrophages. Thus, these compounds may be developed as unique and novel therapeutics for the treatment of Leishmaniasis and other trypanosomal disease.

TH-1101_08610603

Chapter V

Biophysical and Folding Parameters of Trypanothione Reductase from *Leishmania infantum**.

5.1 Abstract

Out of various tropical diseases caused by trypanosomatids, Leishmaniasis is a life threatening disease caused by *Leishmania* parasite. We are targeting thiol metabolic pathway of the parasite for drug development and trypanothione reductase (TR) is a key enzyme of this pathway. It is important to gather significant knowledge about biophysical and intrinsic properties of this enzyme which will be helpful in better understanding of this drug-target enzyme. We report here the modulation of activity and stability of TR *Leishmania infantum* in presence of various denaturants and pH. The enzyme is quite stable under extreme conditions and high concentration of denaturants and showed better stability compared to TR of *Leishmania donovani* which differs at only one position (Ala343→Gly) in amino acid sequence. Structural basis of the destabilizing effects is also discussed.

---

* Part of the work has been published in *Applied Biochemistry and Biotechnology*, **2011**, 165, 13-23

TH-1101_08610603

5.2 Introduction

Trypanothione reductase (TR) is a dimeric disulphide oxidoreductase protein having two glutathionyl moieties linked together by spermidine linkage (Fairlamb et al., 1992). TR is involved in the unique thiol metabolism of trypanosomatids such as *Leishmania* and *Trypanosoma*. These trypanosomatids are causative agents of several medicinally challenged infectious diseases such as African sleeping sickness (*Trypanosoma brucei*), chagas disease (*Trypanosoma cruzi*), kala azar or visceral Leishmaniasis (*Leishmania donovani* and *Leishmania infantum*) and oriental sore or cutaneous Leishmaniasis (*Leishmania major*) in tropical and subtropical regions of the world (Zhang et. al., 1996).

According to current WHO statistics, 12 million people living in 88 countries, mainly on 5 continents i.e. Asia, Europe, Africa, South America and North America, are infected with Leishmaniasis with an annual increase of 1.5-2 million new cases (Desjeux et al., 1992). This disease is still common in rural areas and is endemic in Central and South American countries (Tempone et al., 2005). The treatment of this disease is mainly based upon chemotherapy and most of the drugs are having toxicity, high cost and have low efficacy (Delgado et al., 1999; Shukla et al., 2010). These protozoan parasites have entirely different thiol metabolism to tackle with oxidative stress compared to their insect (Phlebotamine sand fly) and mammalian hosts. TR is a member of NADPH dependant flavoprotein oxidoreductase and functional analogue of glutathione reductase (GR) which is present in mammalian host (Krauth-Seigel et al., 1987).

The activity of several proteins is altered in presence of denaturants like urea and guanidine hydrochloride (GuHCl) due to modulation of their conformations (Sarkar et al., 2009). In last few years, focus has been mainly restricted towards studying the mechanism of interaction of GuHCl and urea denaturants with proteins to get insights about folding and stability (Pompea et al., 2002). In view of its important role in oxidative stress removal and unique nature, TR becomes an interesting target for chemotherapy of Leishmaniasis. We have attempted here to focus on biophysical properties of TR to evaluate its stability and activity parameters in presence of different denaturants such as urea and GuHCl and pH. Solvent denaturation curves using urea and GuHCl can provide information about conformational stability of proteins (Pace, 1975). Unfolding results are reported on TR from a different species of *Leishmania* i.e. *Leishmania donovani* (Rai et al., 2009). Interestingly, we found that TR of *Leishmania infantum* is more stable and

TH-1101_08610603

active in extreme conditions compared to that of *Leishmania donovani*. Sequence analysis of these proteins shows that TR of *Leishmania donovani* differs from the enzyme of *Leishmania infantum* at only one position (Ala343→Gly). The structural basis of the stability effect was interpreted. Moreover, differences in folding/unfolding patterns of TR from these two species are also discussed.

5.3 Materials & Methods

5.3.1 Materials

Trypanothione was purchased from BACHEM, Switzerland. TR gene inserted in the NdeI-HindIII unique sites of pET28b Novagen, in frame with N-terminal His-tag was generously donated by Dr. Andrea Ilari and Gianni Colotti, Università "La Sapienza" Rome, Italy. Thrombin, 8-Anilionaphthalene 1-suphonic acid (ANS), Urea, Guanidine hydrochloride (GuHCl) and all other chemicals of analytical grade were procured from Sigma Aldrich, USA.

5.3.2 Measurement of fluorescence

All fluorescence spectroscopic measurements were done using Varian fluorescence spectrophotometer and 10 mm path length quartz cuvette. FAD fluorescence was monitored by exciting at 460 nm and emission recorded between 480-600 nm. Tryptophan fluorescence was monitored by exciting at 290 nm and emission recorded between 300-400 nm (Pompea et. al., 2002). Both the changes in fluorescence intensity and wavelength maxima were plotted against denaturant concentration to reveal unfolding pattern.

5.3.3 ANS binding experiments

ANS binding experiment was performed by incubation of native and denaturant treated samples with 50 μM ANS for 30 mins. The ANS fluorescence was monitored by exciting the sample at 380 nm and recoding the emission between 400-600 nm (Schonbrunn et al., 2000).

5.3.4 Estimation of denaturation by urea and GuHCl

TR (7 μM) enzyme was incubated in presence of different concentrations of urea and GuHCl (ranging from 0.2 M to 8 M of urea and 0.2 M to 6 M of GuHCl) overnight at room temperature. After the incubation, fluorescence spectra for FAD, tryptophan and

TH-1101_08610603

ANS were measured as previously discussed. Enzyme inactivation by urea and GuHCl was studied by incubating the samples for 1 h and 24 h. We have chosen longer time of incubation as there was no significant effect on enzyme activity after incubation for 1 h.

5.3.5 Circular dichroism measurements

CD measurements were performed using Jasco J715 spectropolarimeter equipped with constant temperature cell holder. CD spectra were collected in the range of 200 to 250 nm using a quartz cuvette of 1 mm path length and scan speed of 40 nm/min. Final protein concentration was kept at 5 μM. Protein secondary structure prediction was done using K2D2 online server.

5.3.6 Estimation of sulfhydryl groups in native and denatured TR

DTNB (Ellman's reagent) works as an indicator for the reduced thiol groups present in the protein. It is converted to colored TNB molecule by reduced thiol group which gives yellow colour and its absorbance can be measured at 412 nm. Enzyme mixture containing 7 μM native TR, NADPH reduced TR, urea denatured TR and urea denatured cum NADPH reduced TR, 1 mM EDTA in 100 mM Tris buffer (pH-8.2) was incubated with 100 μM DTNB in four different microtitre wells and absorbance was monitored at 412 nm. 300 μM NADPH was used for reduction of TR enzyme.

5.3.7 Estimation of renaturation of TR

To estimate the renaturation capability of TR, firstly enzyme was denatured in presence of different urea and GuHCl concentrations for 24 h and then the mixture was dialyzed extensively to remove the denaturant. The enzyme activity was measured after incubation of 1 h at room temperature. Fluorescence spectra were also similar to the native TR.

5.3.8 Estimation of effect of pH on TR stability and activity

Native TR was incubated in buffers of different pH range (0.5 to 12.5) namely 50 mM KCl-HCl (pH-1.0-1.5), 50 mM glycine-HCl (pH-2.0-3.5), 50 mM sodium acetate (pH-4.0-5.5), 50 mM sodium phosphate buffer (pH-6.0-7.5), 50 mM tris-HCl (pH-8.0-10.5) and 50 mM glycine-NaOH (pH-11-12.5) respectively for 24 h at room temperature followed by estimation of enzyme activity, tryptophan and FAD fluorescence.

TH-1101_08610603

5.4 Results

5.4.1 Structural features of native TR

Tryptophan fluorescence spectrum of TR i.e. excitation at 290 nm and emission between 300-400 nm shows a typical peak at 334 nm of tryptophan residue embedded inside the protein (Figure 5.1A). Native TR when excited at 460 nm and emission recorded between 480-600 nm, gave emission maxima at 525 nm which is the characteristic of FAD group present in the protein (Figure 5.1B). Far UV Circular dichroism spectra of the native protein shows typical α/β helix pattern with 57.3±0.4% α helix and 6.1±0.2% β strands as calculated (Figure 5.1C).

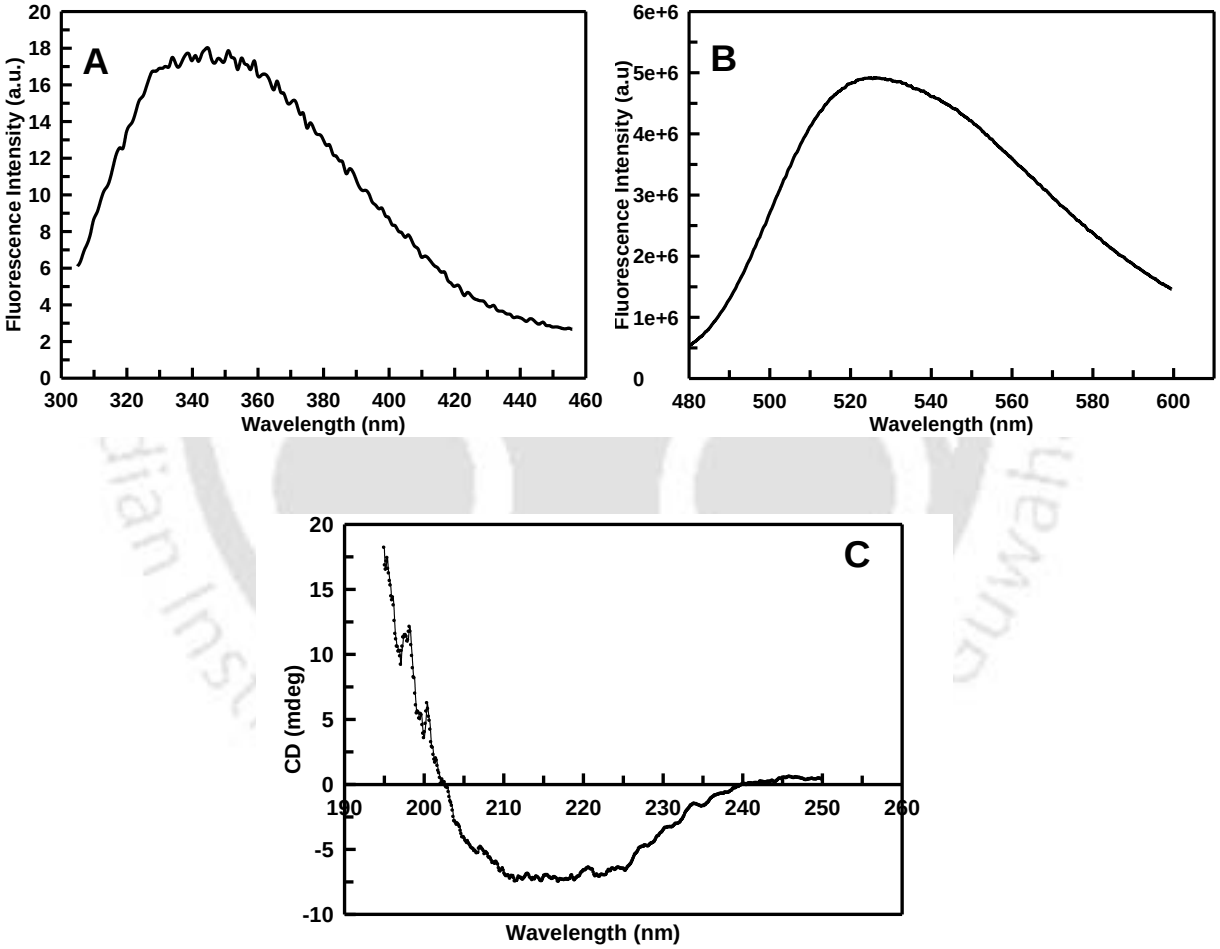

Figure 5.1 Spectroscopic characterization of *Leishmania infantum* TR: (A) Tryptophan fluorescence **(B)** FAD fluorescence, **(C)** Far UV-CD spectrum. Tryptophan and FAD fluorescence maxima were obtained at 334 nm and 525 nm respectively, indicating that they are embedded inside the protein. CD spectra showed typical α/β barrel protein pattern.

TH-1101_08610603

5.4.2 Urea induced unfolding of TR

Urea induced changes are given in Figure 5.2. The unfolding transitions by urea show biphasic nature (Figure 5.2A and Figure 5.2C). The tryptophan fluorescence emission spectra of TR shows emission maxima at 334 nm for native state which shifts to 358 nm upon denaturation by 8 M urea (Figure 5.2A). Fluorescence intensity was also more in presence of urea compared to native state. The emission fluorescence maxima around 334 nm is the characteristic of tryptophan residues buried inside the hydrophobic core of TR whereas emission maxima above 350 nm shows that all the tryptophan residues are exposed to polar environment after denaturation. The FAD fluorescence intensity does not change upto 3M urea and then increases linearly upto saturation after 6 M urea (Figure 5.2C). The 3 M concentration of urea is insufficient for unfolding the protein so that at urea concentration above 6 M, the FAD group is not exposed to aqueous environment. Beyond this concentrations of denaturant /unfolding agent, the protein unfolds and the FAD group now comes in contact with aqueous environment and hence, a linear increase in FAD fluorescence intensity with concentration was observed. FAD is tightly bound to N-terminal domain through hydrogen bonds (Zhang et. al., 1996).

ANS (8-anilio-1-naphthalene sulfonate) is an extrinsic fluorescence dye which is widely used for probing conformational changes in proteins. ANS non-covalently binds with hydrophobic core of proteins and has low fluorescence in polar environment. It is widely used in protein folding/unfolding experiments and biological membranes (Semisotnov et al., 1991). We found a sharp decrease in emission maxima and enhanced ANS fluorescence at ~4 M urea concentration This pattern indicates the formation of molten globule like intermediate state at this concentration (Figure 5.2D). This is further substantiated by biphasic unfolding transition of urea (Figure 5.2A; Figure 5.2C). Through our inactivation studies we found that TR retains its activity for longer time and denaturation is reversible. TR of *Leishmania infantum* retains 76.02±2.9% and 41.17±2.4% activity in presence of 2M urea after 1 h and 24 h respectively (Figure 5.2E) . This result indicates that TR from *Leishmania infantum* is active for longer time compared to reported complete inactivation of TR from *Leishmania donovani* only after 1 h (Rai et. al., 2009).

TH-1101_08610603

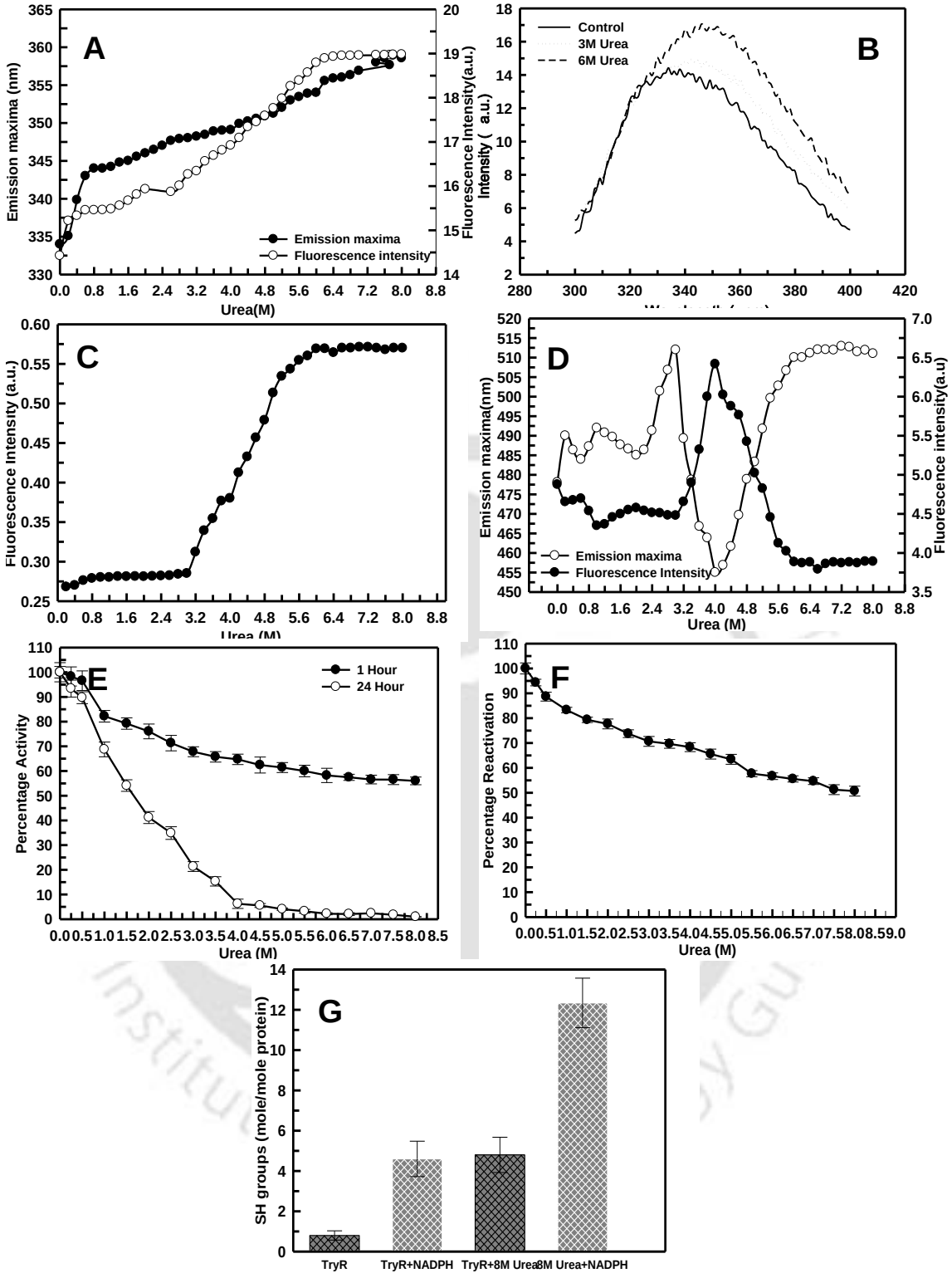

Figure 5.2 Urea induced unfolding of TR: **(A)** Changes in tryptophan emission maxima and fluorescence intensity at emission maxima. **(B)** Tryptophan fluorescence at 0 M, 3 M and 6 M urea concentration **(C)** Changes in FAD fluorescence intensity at 525 nm. **(D)** Changes in ANS-fluorescence intensity and emission maxima. **(E)** Enzyme inactivation profile **(F)** Reactivation of denatured TR **(G)** Sulfhydryl group estimation

TH-1101_08610603

Denaturation of TR by urea is partially reversible (Figure 2F). It regains activity upto 54.91±2.2% after denaturation with 8 M urea. We have estimated the amount of sulfhydryl groups present in different native and denature states of TR (Figure 2G). Native TR had 0.8±0.23 mole/mole of protein sulfhydryl content whereas TR reduced by NADPH, urea denatured TR and urea denatured cum NADPH reduced TR had 4.6±0.87, 4.8±0.83 and 12.34±1.23 mole/mole of protein sulfhydryl content respectively.

5.4.3 GuHCl induced unfolding of TR

GuHCl induced changes are given in Figure 5.3. The unfolding transitions via GuHCl also show biphasic nature (Figure 5.3A, Figure 5.3C). The tryptophan fluorescence emission spectra of TR shifts from 334 nm to 386 nm and fluorescence intensity increased from 5.4 Au to 16.24 Au when denatured by 6 M GuHCl (Figure 5.3A). The FAD fluorescence intensity does not change upto 2 M GuHCl and then increases linearly upto 3.2 M before it becomes stable. It shows that exposure of FAD to polar environment starts at 2 M and it is completed at 3.2 M GuHCl. This result also shows that TR is more prone to denaturation by GuHCl compared to urea. In case of our ANS binding experiments at different concentrations of GuHCl, we found a sharp decrease in emission maxima and enhanced ANS fluorescence at ~1 M GuHCl concentration (Figure 5.3D). It shows that unfolding of TR via GuHCl also involves formation of intermediate state at lower GuHCl concentration compared to urea.

We interestingly found that TR from *Leishmania infantum* is active even after 24 h of GuHCl treatment and contains 74.67±2.2% and 13.33±2.9% activity in 2 M GuHCl after 1 h and 24 h respectively (Figure 5.3E). Here, we also found that TR inactivation is also reversible when denatured by GuHCl whereas TR activity from *Leishmania donovani* is reported to be irreversible after denaturation with GuHCl (Figure 5.3F). It regains 45.73±2.11% activity after denaturation with 6M GuHCl. Figure 5.3G shows the amount of sulfhydryl groups present in different native and denatured states of TR. Native TR has 0.8±0.22 mole/mole protein sulfhydryl content whereas TR reduced by NADPH, GuHCl denatured TR and GuHCl denatured cum NADPH reduced TR has 4.7±0.99, 6.9±1.00 and 13.21±1.89 mole/mole protein sulfhydryl content respectively.

TH-1101_08610603

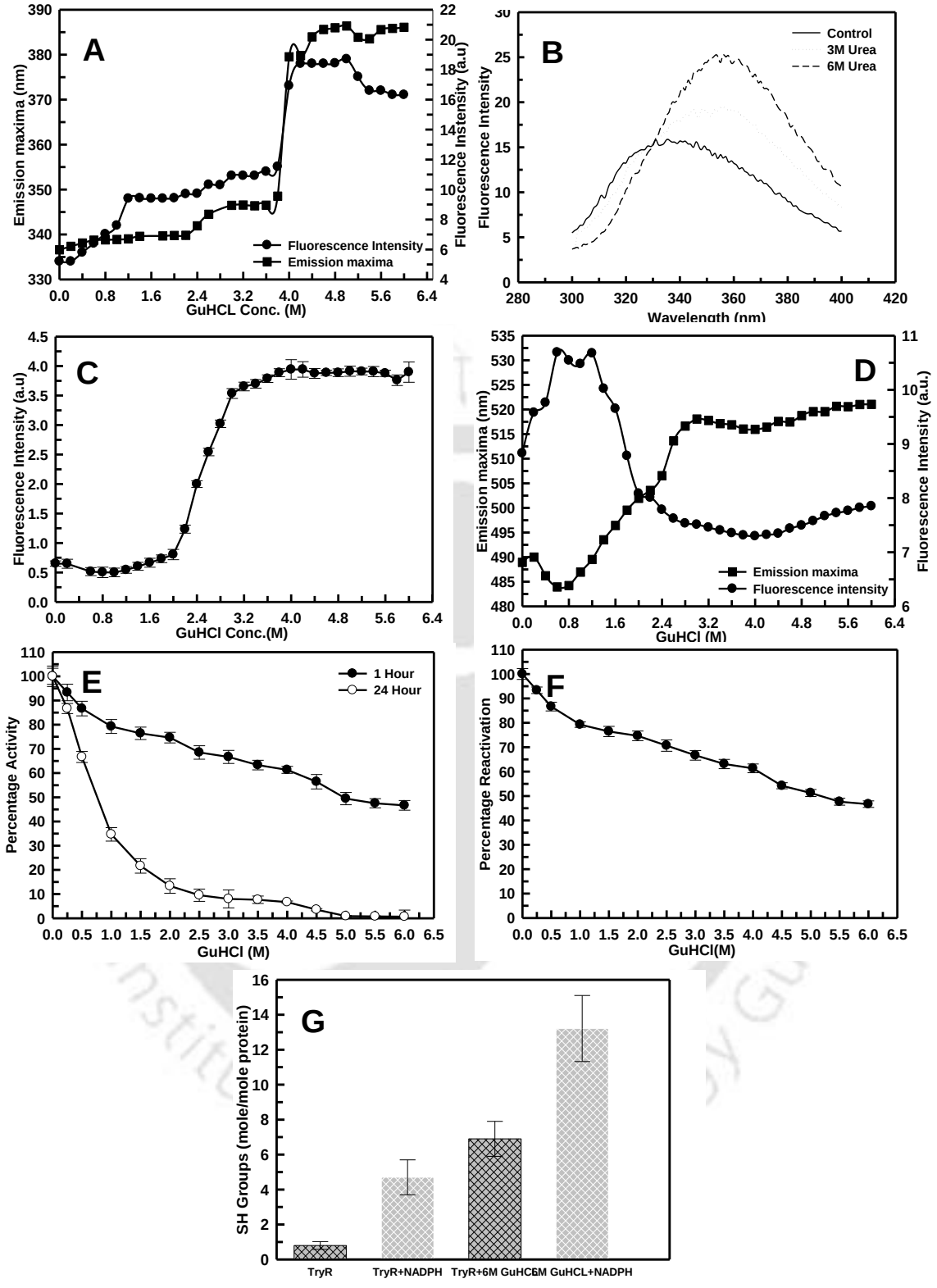

Figure 5.3 GuHCl induced unfolding of TR: **(A)** Changes in tryptophan emission maxima and fluorescence intensity at emission maxima. **(B)** Tryptophan fluorescence at 0 M, 3 M and 6 M GuHCl concentration **(C)** Changes in FAD fluorescence intensity at 525 nm**. (D)** Changes in ANS-fluorescence intensity and emission maxima**. (E)** Enzyme inactivation profile **(F)** Reactivation of denatured Try R (G) Sulfhydryl group estimation

TH-1101_08610603

5.4.4 pH induced changes in enzyme activity and fluorescence properties

pH induced changes of TR are shown in Figure 5.4. Change in tryptophan and FAD fluorescence as function of pH indicates distortion in the protein structure which leads to unfolding and inactivation of TR. Moreover, our results show that TR is active in the pH range 6.0 to 11.0 showing maximum activity at pH-7.5.

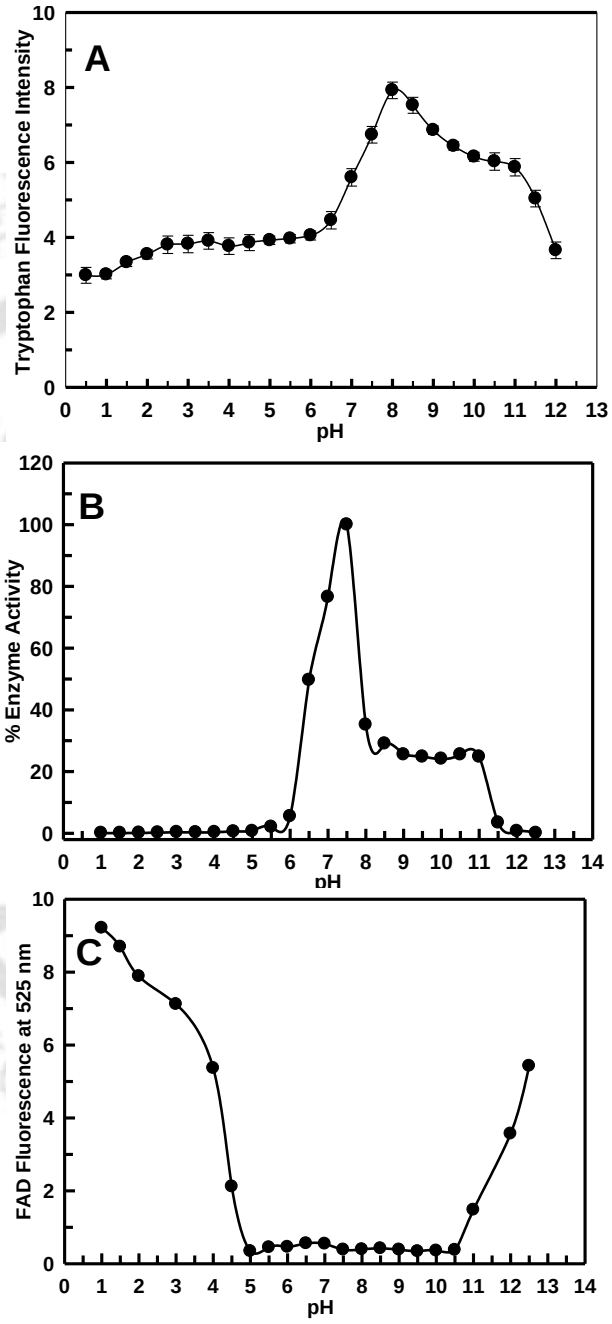

Figure 5.4 **Effect of pH on properties of TR: (A)** modulation of tryptophan fluorescence, **(B)** modulation of FAD fluorescence and **(C)** effect on enzymatic activity. All the datas were collected in the pH range 0.5 to 12.5. The results indicate that TR is stable between pH-6 to pH-11.5 with optimum activity at pH-7.5.

TH-1101_08610603

5.5 Discussion

The biological function of a protein depends upon the correct folding pattern of the protein. Denaturants like urea and GuHCl affect intrinsic properties of protein such as secondary structure, function and stability. Urea and GuHCl have almost same structure with a difference of positive charge on GuHCl. It is assumed that GuHCl is preferentially adsorbed on the protein surface due to interaction with H- bonding groups (Nandi et al., 1984; Mayo et al., 1993). This may be the reason why GuHCl is more potent denaturant compared to urea. In our study as well, protein conformation is distorted in presence of ≥ 3 M urea concentration while the same effect was observed in presence of ≥2 M GuHCl. Equilibrium unfolding of TR indicates that this dimeric protein is quite stable at high concentrations of denaturants and extreme pH range and unfolding pathway involves formation of intermediate states as indicated by decrease in fluorescence intensity of ANS.

In our current study, we proved that TR of *Leishmania infantum* is more stable and active in denaturing environment of denaturants urea and GuHCl as compared to TR of *Leishmania donovani*. The main aim of our current study was to explore the differences in activity and stability of TR from two *Leishmania* species i.e. *Leishmania infantum* and *Leishmania donovani*. We have done experimental analysis on TR of L infantum (Li-TR) whereas folding and stability parameters of TR of *Leishmania donovani* (Ld-TR) are already reported (Rai et al., 2009). Interestingly, we found that Li-TR is less prone to equilibrium unfolding and inactivation compared to Ld-TR.

Li-TR retains about 70% activity after 1 h and about 20% activity after 24 h in presence of 3 M urea concentration while the activity of Ld-TR is completely lost only after 1 h of 3 M urea treatment. Li-TR does not lose more than 40% activity even at 8 M urea concentration after 1 h. There is a sharp decrease in ANS emission maxima at 2 M concentration with Ld-TR while the same is at 3 M urea concentration with Li-TR i.e. Ld-TR tends towards the intermediate formation step at lower concentration of urea compared to Li-TR. Tryptophan and FAD fluorescence patterns also differ between these two species as there is sharp increase in emission maxima of both tryptophan and FAD fluorescence in Ld-TR while this increase is quite gradual in case of Li-TR which shows immediate unfolding of Ld-TR but, gradual unfolding of Li-TR.

TH-1101_08610603

During denaturation with GuHCl, Ld-TR shows comparatively very high instability and inactivation as only 200mM GuHCl inactivates it completely after 1 h. Whereas, Li-TR retains 95% activity after 1 h and 86% activity after 24 h and doesnot looses more than 50% activity even at very high concentration of GuHCl (6M after 1 h). FAD fluorescence intensity is increased after 1 M of GuHCl in Ld-TR while it is increased after 2 M GuHCl in Li-TR i.e. FAD is exposed to polar solvent at higher concentration of GuHCl in Li-TR. Also, Tryptophan fluorescence emission maxima sharply increases just after 1 M GuHCl in Ld-TR while, it is almost stable upto 3.6 M GuHCl and then increases. Thus all these experimental results lead us to conclude that Li-TR is more stable and active in higher concentration of urea and GuHCl compared to Ld-TR.

To understand structural basis of better stability of TR form *Leishmania infantum*, crystal structure of the enzyme was analyzed (Figure 5.5). The only difference between the proteins from these two *Leishmania* species is Ala343 in *Leishmania infantum* is replaced by Gly residue in *Leishmania donovani*. Position 343 in the crystal structure of the protein (PDB ID: 2JK6) appears to be part of an interface with molecule B. In particular, Val B440 may pack against Ala A343 via Vander Waals interaction. Thus, Gly substitution in case of TR from *Leishmania donovani* would disrupt this Vander Waals packing (i.e. leaving a hole). As TR is a dimer in solution, a part of the overall stabilization energy is associated with this dimerization. Thus, the Gly mutation may destabilize the overall dimer due to interface disruption which leads to overall loss of stability. In other words, Ala substitution at position 343 in case of *Leishmania infantum* contributes to improved stability due to better packing at dimer interface.

Additionally, Gly substitution increases the entropy of the denatured state (i.e. stabilizes it) but often has little effect on the entropy of the native state. Thus the effect is destabilization due to unfolded state considerations. Gly is typically utilized in positions where the side chain Cβ is eclipsed (i.e. strained) with local main chain atoms. This situation arises in turns, where the main chain makes a substantial change in direction. Thus, Gly is found at certain turn positions (and stabilizes the turn by eliminating the bad contact with side chain Cβ). In this case, the secondary structure is not a turn but a β-strand. Ala is not the best residue for stabilizing β-strand, but Gly would be worse (due to the above mentioned entropy considerations and loss of Vander Waals contacts with the main chain.

TH-1101_08610603

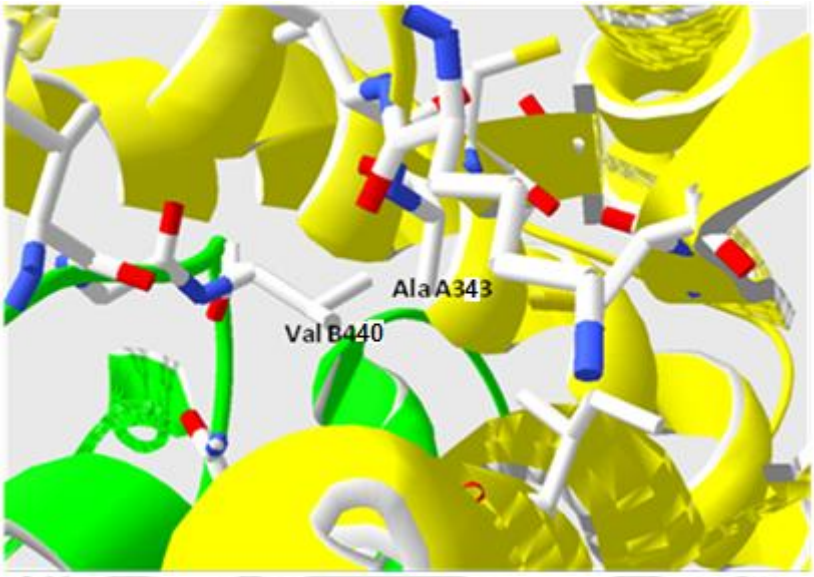

Figure 5.5 Figure showing packing of Ala A343 against Val B440 at dimeric interface of TR for *Leishmania infantum* (PDB ID: 2JK6).

5.6 Conclusion

Unfolding and biophysical studies carried out on TR from *Leishmania infantum* showed significant differences in stability and activity between TR from two different species i.e *Leishmania infantum* and *Leishmania donovani*. Comparative studies on the effects of urea and GuHCl on the structural and functional properties of *Leishmania infantum* TR demonstrated that the enzyme is stable and active even at high concentrations of both these denaturants. Rather, enzyme showed biphasic unfolding pattern with formation of molten globule like intermediate state. Additionally, TR from *Leishmania infantum* showed inactivation by denaturants with reversible activity. It was found to be resistant to unfolding and active site disulfides remain intact in presence of urea and GuHCl. These differences in activity and stability of enzymes from two different species are probably due to Gly to Ala substitution at 343 position as estimated by integrated computational analysis.

TH-1101_08610603

Chapter VI

Summary

Human Leishmaniasis is not a disease, but a group of diseases. It is a wide spread tropical disease caused by protozoan parasite *Leishmania* which belongs to order kinetoplastida and family trypanosomatidae. This parasite is transmitted by sandfly. Two genera of sandfly transmit *Leishmania* to humans- *Lutzomyia* in the New World and *Phlebotomous* in the Old World. 12 million people are affected by Leishmaniasis and 1.5-2 million new cases of Leishmaniasis estimated to occur annually. No effective vaccine is yet available against this parasite and its control relies primarily on pentavalent antimonials. The search for new strategies to overcome toxicity, parasitic resistance and enhanced uptake of drug still remains as the current goal.

Trypanothione reductase (TR) is the key enzyme of thiol metabolism in trypanosomatids (e.g. *Leishmania sp*. and *Trypanosoma sp.)* consisting of two glutathione moieties linked together by spermidine linkage. It reduces trypanothione, an abundant thiol of the parasite, and helps in maintaining redox balance by detoxification of hydroperoxides into water and alcohol and DNA replication by providing reducing equivalents to ribonucleotide reductase for synthesis of dNPxs via tryparedoxin protein. Our current research focuses on identifying best inhibitor of trypanothione reductase from *Leishmania sp.* We identified few antitumor agents (doxorubicin and mitomycin C),

TH-1101_08610603

isolated iridoid glucosides from an Indian medicinal plant, *Nyctanthes arbortristis* and estimated their inhibitory effect against TR of *Leishmania sp.* We have also estimated increase in oxidative stress, decrease in thiol level, invitro antileishmanial activity, apoptosis assay and measurement of cytotoxicity of these compounds on human cell-lines. Furthermore, we have also formulated biodegradable nanoparticles based delivery methods of these drugs for specific delivery to macrophages with increased efficiency, long-exposure and deliberate intracellular release. Finally, we carried out experiments to investigate intrinsic properties of TR from *Leishmania infantum* like unfolding studies in presence of urea and guanidine hydrochloride as denaturants, stability and activity measurements at different pH conditions.

Chapter 1

Leishmania sp. a trypanosomatid, causes a lethal tropical disease known as Leishmaniasis which exists in three forms i.e. cutaneous, mucocutaneous and lethal visceral Leishmaniasis. The different metabolic pathways of leishmania parasite involve several key enzymes which may be ideal targets for antileishmanial drug design. One such enzyme is TR, a key enzyme in redox homeostasis, which helps in removal of reactive oxygen species (ROS) and DNA synthesis (dNPxs synthesis) through a cascade of reactions. Although, glutathione reductase of human is analogous to trypanothione reductase and performs same physiological function, yet there are several differences in active site of these two enzymes. Thus TR can be targeted for drug development against Leishmaniasis without interfering with the function of GR. Our prime focus was to target thiol metabolism of the parasite for discovery of potential anti-leishmanial agents.[1]

Chapter 2

Additionally, after extensive computational analysis, we found some antitumor agents (Doxorubicin and Mitomycin C) showing significant inhibition of TR activity. Recombinant TR was expressed in *E. coli* (BL21) and purified using Ni-affinity chromatography. In vitro inhibition studies indicated these compounds to be competitive inhibitors and subversive substrates of TR enzyme and subvert biological function of enzyme by making it pro-oxidant from anti-oxidant. This mechanism was investigated using various methods like FT-IR analysis and enzyme activity. Further, effect of generation of superoxide free radical and oxidative stress in parasite was also investigated. These candidate drugs were further screened for their mode of action

TH-1101_08610603

(inhibition studies, ROS generation, cytotoxicity studies on parasite and human cell lines etc.). The study points out potential application of Doxorubicin and Mitomycin C as antileishmanials. [2, 3]

Chapter 3

Numerous techniques (liposomal formulations, micelles, emulsions and nanoparticles) have been implicated to administer drugs to several target tissues and have met with failures because of their characteristic of being identified by polymorphonuclear cells and macrophages which leads to their phagocytosis. However, this phagocytosis mechanism facilitates drug delivery to target site in case of Leishmaniasis i.e. macrophage itself. The biodegradable diblock co-polymer MPEG-PLA {methoxypoly (ethylene glycol)-b-poly (lactic acid)} nanoparticles are most appropriate for antileishmanial drug delivery due to their amphiphilic, biodegradable behavior and increased half life in blood stream. Doxorubicin and mitomycin C loaded polymeric MPEG-PLA nanoparticles were prepared by nanoprecipitation method. The mean diameter of spherical drug carriers was found to be 70-200 nm with a surface area of 14.491 m^2/g as characterized by TEM, FESEM and BET surface area analyzer. *In vitro* release profile of drugs suggested fairly slow release of drug. These polymeric nanoparticles were efficiently capable of delivering drug at low pace inside macrophages which was monitored by Epifluorescent microscopy using intrinsic fluorescence of doxorubicin. Cytotoxicity profile suggested that encapsulation of doxorubicin and mitomycin C into NPs decreases cellular toxicity on HEK-293 and macrophages itself.

Chapter 4

Further, we explored TR for inhibition studies and isolated iridoid glucosides from seed kernel of *Nyctanthes arbortristis*, a widely used medicinal plant. Docking studies revealed that iridoid glucosides bind at the active site of TR with high docking energy. Therefore, further evaluation of inhibition parameters like anti-lieshmanial activity (via MTT assay), ROS generation (fluorescense studies and flow cytometry using CM-H_2DCFDA dye), safety evaluation (on HEK 293, J774A.1 celllines) and *in vitro* experiments (apoptosis mechanism and killing of intra-macrophageal amastigotes) were performed. Therefore, these compounds may be developed as affordable drugs with higher efficiency and low toxicity.[4]

TH-1101_08610603

Chapter 5

In this part of our research we have focused on structural properties of cloned TR and modulation of structure and function by different denaturants like urea and guanidine hydrochloride. We have investigated fluorescence spectroscopic properties of native and denatured TR with respect to FAD fluorescence, Tryptophan florescence. Along with these experiments other experiments have also been performed such as Circular Dichroism to investigate secondary structure of protein, ANS binding for unfolding pattern, chemical denaturation, Sulphahydryl group estimation, etc. Experiments were carried out to gather significant knowledge about biophysical and intrinsic properties of this enzyme (unfolding studies, activity modulation in presence of denaturants and at different pH) for better understanding of drug-target interactions.[5]

---

1. Shukla et al. *Applied Biochemistry and Biotechnology* , 2010, 160, 2208–2218. **2**. Shukla et al. *Journal of Computational Chemistry,* 2010, 31, 2463-2472. **3.** Shukla et al. *Molecular and Cellular Biochemistry,* 2011, 352, 261–270**. 4.** Shukla et al. *Journal of Ethnopharmacology* 134, 2011, 996–998. **5.** Shukla et al. *Applied Biochemistry and Biotechnology*, 2011, 165, 13-23.

TH-1101_08610603

Bibliography

Akendengue B, Roblot F, Loiseau PM, Bories C, Ngou-Milama E, Laurens A. Klaivanolide, an antiprotozoal lactone from *Uvaria klaineana* . *Phytochemistry* 59, 885 (2002).

Alphey MS, Bond CS, Tataud E, Fairlamb AH, Hunter WN. The structure of reduced tryparedoxin peroxidase reveals a decamer, an insight into reactivity of 2-Cys-peroxiredoxins . *Journal of Molecular Biology* 300, 903–916 (2000).

Alphey MS, Leonard GA, Gourley DG, Tetaud E, Fairlamb AH, Hunter WN. The high resolution crystal structure of recombinant *Crithidia fasciculata* tryparedoxin-I. *The Journal of Biological Chemistry* 274, 25613-25622 (1999).

Alvar J, Yactayo S, Bren C. Leishmaniasis and poverty. *Trends in Parasitology* 2, 552–557 (2006).

Aronow B, Kaur K, McCartan K, Ullman B. Two high affinity nucleoside transporters in *Leishmania donovani*. *Molecular and Biochemical Parasitology* 22, 29–37 (1987).

Baiocco P, Colotti G, Franceschini S, Ilari A. Molecular basis of antimony treatment in Leishmaniasis. *Journal of Medicinal Chemistry* 52, 2603-2612 (2009a).

Baiocco P, Franceschini S, Ilari A, Colotti G. Trypanothione reductase from *Leishmania infantum*: cloning, expression, purification, crystallization and preliminary X-ray data analysis. *Protein and Peptide Letters* 16, 196-200 (2009b).

Balasubramanyam M, Koteswari AA, Kumar RS, Monickaraj SF, Maheswari JU, Mohan V. Curcumin-induced inhibition of cellular reactive oxygen species generation. *Journal of Biosciences* 28, 715–721 (2003).

TH-1101_08610603

Bally MB, Lim H, Cullis PR, Mayer LD. Controlling the drug delivery attributes of lipid-based drug formulations. *Journal of Liposome Research* 8, 299-335 (1998).

Benson TJ, Mckie JH, Garforth J, Borges A, Fairlamb AH, Douglas KT. Rationally designed selective inhibitors of Trypanothione reductase: Phenothiazines and related tricyclics as lead structures. *Journal of Biochemistry* 286, 9–11 (1992).

Berman J. Current treatment approaches to *Leishmania*. *Current Opinion in Infectious Diseases* 16, 397 (2003).

Bhaumik S, Basu R, Sen S, Naskar K, Roy S. KMP-11 DNA immunization significantly protects against *Leishmania donovani* infection but requires exogenous IL-12 as an adjuvant for comparable protection against *L. major*.*Vaccine* 27, 1306-16 (2009).

Bonse S, Santelli-Rouvier C, Barbe J, Krauth-Siegel RL. Inhibition of *Trypanosoma cruzi* trypanothione reductase by acridines: kinetic studies and structure-activity relationships. *Journal of Medicinal Chemistry* 42, 5448–5454 (1999).

Bora D. Epidemiology of visceral Leishmaniasis in India. *National Medical Journal of India* 12, 62–68 (1999).

Borges A, Cunningham ML, Tovar J, Fairlamb AH. Site-directed mutagenesis of the redox-active cysteines of *Trypanosoma cruzi* trypanothione reductase. *European Journal of Biochemistry* 228, 745-752 (1995).

Brigger I, Dubernet C, Couvreur P. Nanoparticles in cancer therapy and diagnosis. *Advanced Drug Delivery Reviews* 54, 631-651 (2002).

Bringaud F, Rivière L, Coustou V. Energy metabolism of trypanosomatids: adaptation to available carbon sources. *Molecular and Biochemical Parasitology* 149, 1–9 (2006).

Camacho MR, Kirby GC, Warhurst DC, Croft SL, Phillipson JD. Oxoaporphine Alkaloids and Quinones from *Stephania dinklagei* and Evaluation of Their Antiprotozoal Activities. . *Planta Medica* 66, 478 (2002).

Chang KP. Human cutaneous Leishmaniasis in mouse macrophage line: propagation and isolation of intracellular parasite. *Science* 209, 1240-1242 (1980).

Chen M, Zhai L, Christensen SB, Theander TG, Kharazmi A. Inhibition of fumarate reductase in *Leishmania major* and *Leishmania donovani* by chalcones. *Antimicrobial Agents and Chemotherapy* 45, 2023–2029 (2001).

Cheng J, Teply BA, Sherifi I, Sung J, Luther G, Gu FX, Levy-Nissenbaum E, Radovic-Moreno AF, Langer R, Farokhzad OC. Formulation of functionalized PLGA–PEG NPs for *in vivo* targeted drug delivery. *Biomaterials.* 28, 869-876 (2007).

Chowdhury AR, Mandal S, Mittra B, Sharma S, Mukhopadhyay S, Majumder HK. Betulinic acid, a potent inhibitor of eukaryotic topoisomerase I: identification of the inhibitory step, the major functional group responsible and development of more potent derivatives. *Medical Science Monitor* 8, BR254–BR265 (2002).

TH-1101_08610603

Chowdhury AR, Sharma S, Mandal S, Goswami A, Mukhopadhyay S, Majumder HK. Luteolin, an emerging anti-cancer flavonoid, poisons eukaryotic DNA topoisomerase I. *Biochemical Journal* 366, 653–661 (2002).

Colucci MA, Moody CJ, Couch GD. Natural and synthetic quinones and their reduction by the quinone reductase enzyme NQO1, from synthetic organic chemistry to compounds with anticancer potential. *Organic and Biomolecular Chemistry* 5, 3665–3673 (2008).

Cota BB, Rosa LH, Caligiorne RB, Rabello ALT, Almeida Alves TM, Zani CS. Altenusin, a biphenyl isolated from the endophytic fungus *Alternaria sp.*, inhibits trypanothione reductase from *Trypanosoma cruzi*. *FEMS Microbiology Letters* 285, 177–182 (2008).

Croft SL, Coombs GH. Leishmaniasis-current chemotherapy and recent advances in the search for novel drugs. *Trends in Parasitology* 19, 502–508 (2003).

Croft SL. Recent developments in the chemotherapy of Leishmaniasis. *Trends in Pharmacolgical Sciences* 9, 376–81(1988).

Da Silva LJ. Vianna and the discovery of *Leishmania braziliensis*: the role of Brazilian parasitologists in the identification of Bauru's ulcer as American Leishmaniasis. *Parassitologia* 47, 335-341 (1915)

Darzynkiewicz Z. Differential staining of DNA and RNA in intact cells and isolated cell nuclei with acridine orange. *Methods in Cell Biology* 33, 285-98 (1990).

Das R, Roy A, Dutta N, Majumdar HK. Reactive oxygen species and imbalance of calcium homeostasis contributes to curcumin induced programmed cell death in *Leishmania donovani*. *Apoptosis* 13, 867-882 (2008).

Datta AK, Datta R, Sen B. Antiparasitic chemotherapy: tinkering with the purine salvage pathway. *Advances in Experimental Medicine and Biology* 625, 116–132 (2008).

Debrabant A, Joshi MB, Pimenta PFP, Dwyer DM. Generation of *Leishmania donovani* axenic amastigotes: their growth and biological characteristics. *International Journal of Parasitology* 34, 205-217 (2004).

Debrabant A, Lee N, Bertholet S, Duncan R, Nakhasi HL. Programmed cell death in trypanosomatids and other unicellular organisms. *International Journal of Parasitology* 33, 257–267 (2008).

Del RCM, Phillipson JD, Croft SL, Yardley V, Solis PN. *In vitro* Antiprotozoal and cytotoxic activities of some alkaloids, quinones, flavonoids, and coumarins. *Planta Medica* 70, 70 (2004).

Delfin DA, Morgan ER, Zhu X, Werbovetz AK. Redox-active dinitrodiphenylthioethers against *Leishmania*: Synthesis, structure–activity relationships and mechanism of action studies. *Bioorganic & Medicinal Chemistry*, 17, 820–829 (2009).

TH-1101_08610603

Delgado J, Macias J, Pineda JA, Corzo JE, Gonzalez-Moreno MP, de la Rosa R. High frequency of serious side effects from meglumine antimoniate given without an upper limit dose for the treatment of visceral Leishmaniasis in human immunodeficiency virus type-1-infected patients. *American Journal of Tropical Medicine and Hygiene* 61, 766-769 (1999).

Delorenzi JC, Attias M, Gattass CR, Andrade M, Rezende C, daCunha Pinto A, Henriques AT, Bou-Habib DC, Saraiva EM. Antileishmanial activity of an indole alkaloid from *Peschiera australis. Antimicrobial Agents and Chemotherapy* 45, 1349–1354 (2001).

Desai MP, Labhasetwar V, Walter E, Levi RJ, Amidon GL. The mechanism of uptake of biodegradable microparticles in CaCO-2 cells is size dependant. *Pharmaceutiacl Research* 14, 1568-1573 (1997).

Desjeux P. Human Leishmaniasis: epidemiology and public health aspects. *World Health Statistics* 45, 267-275 (1992).

Di Cristina G, Caronia G. Treatment of visceral Leishmaniasis. *Journal of Tropical Medicine and Hygiene* 18, 118-119 (1915)

Dirix LY, Libura M, Libura J, Vermeulen PB, Bruijn D, Ernst A, Van O, Allan T. *In vitro* toxicity studies with mitomycins and bleomycin on endothelial cells. *Anticancer Drugs* 8, 859-868 (1997).

Dixon MJ, Maurer RI, Biggi C, Oyarzabal J, Essex JW, Bradley M. Mechanism and structure-activity relationships of nonspermidine-based peptidic inhibitors of trypanothione reductase. *Bioorganic and Medicinal Chemistry* 13, 4513–4526 (2005).

Dong Y, Feng SS. Methoxy poly (ethylene glycol)-poly (lactide) (MPEG-PLA) nanoparticles for controlled delivery of anticancer drug. *Biomaterials* 25, 2843-2849 (2004).

Dujardin JC, Campino L, Cañavate C, Dedet JP, Gradoni L, Soteriadou K, Mazeris A, Ozbel Y, Boelaert M. Spread of vector borne diseases and neglect of Leishmaniasis, Europe. *Emerging Infectious Diseases* 14, 1013–1018 (2008).

Dumas C, Ouellette M, Tovar J, Cunningham MJ, Fairlamb AH, Tamar S, Olivier M, Papadopoulou B. Disruption of the trypanothione reductase gene of *Leishmania* decreases its ability to survive oxidative stress in macrophages. *EMBO Journal* 16, 2590–2598 (1997).

El-On J Jacobs GP Witztum E Greenblatt CL. Development of topical treatment for cutaneous Leishmaniasis caused by *Leishmania major* in experimental animals. *Antimicrobial Agents and Chemotherapy* 26, 745 (1984).

Fairlamb AH, Blackburn P, Ulrich P, Chait BT, Cerami A. Trypanothione: a novel bis(glutathionyl)spermidine cofactor for glutathione reductase in trypanosomatids. *Science* 227, 1485–7(1985).

Fairlamb AH, Cerami A. Metabolism and functions of trypanothione in the kinetoplastida. *Annual Reviews in Microbiology* 46, 695-729 (1992).

TH-1101_08610603

Fessi H, Puisieux F, Devissaguet JP, Ammoury N, Benita S. Nanocapsules formation by interfacial polymer deposition following solvent displacement. *International Journal of Pharmacy* 55, 25-28 (1989).

Fevrier A, Ferreira ME, Fournet A, Yaluff G, Inchausti A, Rojas de Arias A. Acetogenins and other compounds from *Rollinia emargi*. *Planta Medica* 65, 47 (1999).

Flohe L, Hecht HJ, Steinert P. Glutathione and trypanothione in parasitic hydroperoxide metabolism. *Free Radical Biology & Medicine* 27, 966–984 (1999).

Fournet A, Barrios AA, Munoz V, Hocquemiller R, Cave A, Bruneton J. 2-substituted quinoline alkaloids as potential antileishmanial drugs. *Antimicrobial Agents and Chemotherapy* 37, 859–863(1993).

Fournet A, De Arias RA, Ferreira ME. Efficacy of the bisbenzylisoquinoline alkaloids in acute and chronic *Trypanosoma cruzi* murine model. *International Journal of Antimicrobial Agents* 13, 189–195 (2000).

Fournet A, Muñoz V. Natural products as trypanocidal, antileishmanial and antimalarial drugs. *Current Topics in Medicinal Chemistry* 2, 1215-37 (2002).

Frank G, Langer R, Farokhzad OC. Precise engineering of targeted nanoparticles by using self assembled biointegrated block copolymers. *Proceedings of the National Academy of Sciences of the United States of America* 105, 2586-2591 (2008).

Fyfe PK, Oza SL, Fairlamb AH, Hunter WN. *Leishmania* trypanothione synthetase-amidase structure reveals a basis for regulation of conflicting synthetic and hydrolytic activities. *The Journal of Biological Chemistry* 283, 17672–17680 (2008).

Garforth J, Yin H, McKie JH, Douglas KT, Fairlamb AH. Rational design of selective ligands for trypanothione reductase from *Trypanosoma cruzi*. Structural effects on the inhibition by dibenzazepines based on imipramine. *Journal of Enzyme Inhibition* 12, 161–173 (1997).

Ghisla SK and Massey V. Mechanism of flavoprotein-catalyzed reactions. *European Journal of Biochemistry* 181, 1-17 (1989).

Glew RH, Saha AK, Das S, Remaley A. Biochemistry of the *Leishmania* species. *Microbiological Reviews* 52, 412–432 (1988).

Gordon S. The macrophage. *BioEssays* 17, 977-986 (1995).

Gref R, Domb A, Quellec P, Blink T, Muller RH, Verbavatz JM Langer R. The controlled intravenous delivery of drugs using PEG-ciated sterically stabilized nanospheres. *Advanced Drug Delivery Reviews* 16, 215-233 (1994).

Grogl M, Thomason TN, Franke ED. Drug resistance in Leishmaniasis: its implication in systemic chemotherapy of cutaneous and mucocutaneous disease. *The American Journal of Tropical Medicine and Hygiene* 47, 117–26 (1992).

Grosjean NL, Vrable RA, Murphy AJ, Mansfield LS. Seroprevalence of antibodies against *Leishmania spp.* among dogs in the United States. *Journal of the American Veterinary Medical Association* 222, 603–606 (2003).

TH-1101_08610603

Gupta S, Pal A, Vyas SP. Drug delivery strategies for therapy of visceral Leishmaniasis. *Expert Opinion in Drug Delivery* 7, 371-402 (2010).

Haanstra JR, Tuil AV, Kesseler P, Reijnders W, Michels PAM, Westerhoff HV, Parsons M, Bakker BM. Compartmentation prevents a lethal turbo-explosion of glycolysis in trypanosomes. *Proceedings of the National Academy of Sciences of the United States of America* 105, 17718–17723 (2008).

Hamilton CJ, Saravanamuthu A, Eggleston IM, Fairlamb AH. Ellman's-reagent-mediated regeneration of trypanothione *in situ*, substrate economical microplate and time-dependent inhibition assays for trypanothione reductase. *Biochemistry* 369, 529–537 (2003)

Handman E. Leishmanisis: Current Status of Vaccine Development. *Clinical Microbiology Reviews* 14, 229-243 (2001).

Heby O, Roberts SC, Ulman B. Polyamine biosynthetic enzymes as drug targets in parasitic protozoa. *Biochemical Society Transactions* 31, 415–419 (2005).

Henderson GB, Fairlamb AH, Cerami A. Trypanothione dependent peroxide metabolism in *Crithidia fasciculata* and *Trypanosoma brucei*. *Molecular and Biochemical Parasitology* 24, 39-45 (1987a).

Henderson GB, Fairlamb AH, Ulrich P, Cerami A. Substrate specificity of the flavoprotein trypanothione disulfide reductase from *Crithidia fasciculate*. *Biochemistry* 26, 3023–3027 (1987b).

Hoet S, Stevigny C, Block S, Opperdoes F, Colson P, Baldeyrou B. Alkaloids from *Cassytha filiformis* and related aporphines: Antitrypanosomal activity, cytotoxicity, and interaction with DNA and topoisomerases. *Planta Medica* 70, 407 (2004).

Huey R, Morris GM, Olson AJ, Goodsell DS. A semi empirical free energy force field with charge-based desolvation. *Journal of Computational Chemistry* 28, 1145–1152 (2007).

Hunter WN, Bailey S, Habash J, Harrop SJ, Helliwell JR, Aboagye-Kwarteng T, Smith K, Fairlamb AH. Active site of trypanothione reductase. A target for rational drug design. *Journal of Molecular Biology* 227, 322–33 (1992).

Jones MC, Leroux JC. Polymeric micelle-a new generation of colloidal drug carriers. *European Journal of Pharmaceutics and Biopharmaceutics* 48, 101-111 (1999).

Kazi YF, Parton R, Memon BA. Haemolytic assay for the detection of adenylate cyclase toxin for *Bordetella pertussis*. *Pakistan Journal of Pharmaceutical Sciences* 7, 55–59 (1994).

Kedzierski L, Zhu Y, Handman E. Leishmania Vaccines: Progress and problems. *Parasitology* 133, S87-S112 (2006).

Khan M. Trypanothione Reductase: A viable chemotherapeutic target for antitrypanosomal and antileishmanial drug design. *Drug Target Insights* 1, 129–146 (2007).

TH-1101_08610603

Khatune NA, Mosaddik MA, Haque ME. Antibacterial activity and cytotoxicity of *Nyctanthes arbor-tristis* flowers. *Fitoterapia* 72, 412-414 (2001).

Kole L, Das L, Das PK. Synergistic effect of interferon-δ and mannosylated liposome-incorporated doxorubicin in the therapy of experimental visceral Leishmaniasis. *Journal of Infectious Diseases* 180, 811–820 (1999).

Krauth-Siegel RL, Comini MA. Redox control in trypanosomatids, parasitic protozoa with trypanothione-based thiol metabolism. *Biochimica et Biophysica Acta* 1780, 1236–1248 (2008).

Krauth-Siegel RL, Enders B, Henderson GB, Fairlamb AH, Schirmer RH. Trypanothione reductase from *Trypanosoma cruzi*. Purification and characterization of the crystalline enzyme. *European Journal of Biochemistry* 164(1), 123-128 (1987).

Lafon SW, Nelson DJ, Berens RL, Marr JJ. Inosine analogs: their metabolism in mouse L cells and in *Leishmania donovani*. *Journal of Biological Chemistry* 260, 9660–9665 (1985).

Lindsay DS and Zajac AM. Leishmaniasis in American foxhounds: An emerging zoonosis? *Compedium* 24, 304-313 (2002)

Lundberg B, Griffiths G, Hansen HJ. Cellular association and cytotoxicity of anti-CD74-targeted lipid drug-carriers in B lymphoma cells. *Journal of Controlled Release* 94, 155-161 (2004).

Marles RJ, Farnsworth NR, Neill DA. Isolation of a novel cytotoxic polyacetylene from a traditional anthelmintic medicinal plant, *Minquartia guianensis*. *Journal of Natural Products* 52, 261(1989).

Mattock N. Public/private partnership: developing an oral treatment for visceral Leishmaniasis. *TDR News* 60, 1-2 (1999).

Mayo SL, Baldwin RL. Guanidinium chloride induction of partial unfolding in amide proton exchange in RNase A. *Science* 262, 873-876 (1993).

Mbwambo ZH, Apers S, Moshi MJ, Kapingu MC, VanMiert S, Claeys M.. Anthranoid Compounds with Antiprotozoal Activity from *Vismia orientalis. Planta Medica* 70, 706 (2004).

McLennan IJ, Lenkinski RE, Yanuka Y. A nuclear magnetic resonance study of the self association of adriamycin and daunomycin in aqueous solution. *Canadian Journal of Chemistry* 63, 1233-1238 (1985).

Meiering S, Inhoff O, Mies J, Vincek A, Garcia G, Kramer B, Dormeyer M, Krauth-Siegel RL. Inhibitors of Tryapnosoma cruzi trypanothione reductase by virtual screening and parallel synthesis. *Journal of Medicinal Chemistry* 48, 4793–4802 (2005).

Meister A. Glutathione; Chemical, Biochemical and Medical Aspects (Dolphin, D., Poulson, R. and Avramovic, O., (eds). *John Wiley, New York*, 367-474.

Menozzi M, Valentini L, Vannini E, Arcamone F. Self association of doxorubicin and related compounds in aqueous solution. *Journal of Pharmaceutical Sciences* 73,766-770 (1984).

TH-1101_08610603

Michels PAM, Bringaud F, Herman M, Hannaert M, Hannaert V. Metabolic functions of glycosomes in trypanosomatids. *Biochimica et Biophysica Acta* 1763, 1463–1477 (2006).

Mishra P, Khaliq T, Reddy KP, Gupta S, Kant R, Maulik PR. Rational approaches for drug designing against Leishmaniasis. *Journal of Antimicrobial Chemotherapy* 62, 998–1002 (2008).

Montenegro H, Gutierrez M, Romero LI, Ortega-Barria E, Capson TL, Rios LC. Aporphine alkaloids from *Guatteria spp.* with Leishmanicidal activity. *Planta Medica*, 69, 677 (2003).

Moretti C, Sauvain M, Lavaud C, Massiot G, Bravo J, Munoz V. A Novel Antiprotozoal Aminosteroid from *Saracha punctata*. *Journal of Natural Products* 61, 1390 (1998)

Morris GM, Goodsell DS, Halliday RS, Huey R, Hart WE, Belew RK, Olson AJ. Automated docking using a Lamarckian genetic algorithm and an empirical binding free energy function. *Journal of Computational Chemistry* 19, 1639–1662 (1998).

Mosmann T. Rapid colorimetric assay for cellular growth and survival, application to proliferation and cytotoxicity assays. *Journal of Immunological Methods* 65, 55-63 (1983).

Muhammad I, Bedir E, Khan SI, Tekwani BL, Khan IA, Takamatsu S. A new antimalarial quassinoid from *Simaba orinocensis*. *Journal of Natural Products* 67, 772 (2004).

Mukherjee S, Das L, Kole L, Karmakar S, Datta N, Das PK. Targeting of parasite-specific immunoliposome-encapsulated doxorubicin in the treatment of experimental visceral Leishmaniasis. *Journal of Infectious Diseases* 189, 1024–1034 (2004).

Muriel P, Abdelkader L, Hatem F. Pentamidine loaded poly (D, L-lactide) nanoparticles: adsorption and drug release. *Drug Delivery Research* 43, 98-104 (1998).

Murray HW. Kala Azar- Progress against a neglected disease. *New England Journal of Medicine* 347, 1793–1794 (2002).

Murthy ASN, Balasubramanian A, Rao CNR, Kasturi TR. Spectroscopic studies of keto-enol equilibria. *Canadian Journal of Chemistry* 10, 2267–2271 (1962).

Myler PJ, Fasel N. Leishmania after the genome: biology and control. Wymondham, UK*: Caister Academic Press* (2008).

Nandi PK, Robinson DR. Effects of urea and guanidine hydrochloride on peptide and nonpolar groups. *Biochemistry*, 23, 6661-6668 (1984).

Ngure PK, Tonui WK, Ingonga J, Mutai C, Kigondu E, Nganga Z, Rukunga G , Kimutai A. *In vitro* antileishmanial activity of *Warburgia ugandensis* (Family cancellaceae), a Kenyan medicinal plant. *Journal of Medicinal Plants Research*, 3, 61–66 (2009).

TH-1101_08610603

Ofek I, Goldhar J, Keisari Y, Sharon N. Non-opsonic phagocytosis of microorganisms. *Annual Reviews in Microbiology* 49, 239-276 (1995).

O'Sullivan MC, Zhou Q, Li Z, Durham TB, Rattendi D, Lane S, Bacchi CJ. Polyamine derivatives as inhibitors of trypanothione reductase and assessment of their trypanocidal activities. *Bioorganic and Medicinal Chemistry* 5, 2145-55 (1997).

Pace CN. The stability of globular proteins. *CRC Critical Reviews in Biochemistry* 3, 1-43 (1975).

Panyam J, Labhasetwar V. Biodegradable nanoparticles for drug and gene delivery to cells and tissues. *Advanced Drug Delivery Reviews* 55, 329-347 (2003).

Paris C, Loiseau PM, Bories C, Breard J. Miltefosine induces apoptosis-like death in *Leishmania donovani* promastigotes. *Antimicrobial Agents and Chemotherapy*, 48, 852-859 (2004).

Parveen S, Khan MOF, Austin SE, Croft SL, Yardley V, Rock P, Douglas KT. Antitrypanosomal, antileishmanial and antimalarial activities of quaternary arylalkylammonium-2-amino-4-chloropjenyl phenyl sulfides, a new class of trypanothione reductase inhibitor, and of N-acyl derivatives of 2-amino-4-chlorophenyl phenyl sulfide. *Journal of Medicinal Chemistry* 48, 8087–8097 (2005).

Pearson RD, de Queiroz Souza A. Clinical spectrum of Leishmaniasis. *Clinical Infectious Diseases*, 22, 1–13 (1996).

Pineyro MD, Pizarro JC, Lema F, Pritsch O, Cayota A, Bentley GA, Robello C. Crystal structure of the tryparedoxin peroxidase from the human parasite *Trypanosoma cruzi*. *Journal of Structural Biology* 150, 11-22 (2005).

Plock A, Beyer G, Hiller K, Grundemann E, Krause E, Nimtz M. Application of MS and NMR to the structure elucidation of complex sugar moieties of natural products: exemplified by the steroidal saponin from *Yucca filamentosa* L. *Phytochemistry* 57, 489 (2001).

Pompea DV, Giuseppe G, Vincenzo G, Guido B, Luigi M, Mose R, et al. Denaturing action of urea and guanidine hydrochloride towards two thermophilic esterases. *Biochem J*, 367, 857-863 (2002).

Puri A, Saxena R, Saxena RP, Saxena KC, Srivastava V, Tandon JS. Immunostimulant activity of *Nyctanthes arbortristis* L. *Journal of Ethnopharmacology* 42, 31-37 (1994).

Rai S, Dwivedi UN, Goyal N. *Leishmania donovani* trypanothione reductase: role of urea and guanidine hydrochloride in modulation of functional and structural properties. *Biochimica et Biophysica Acta* 1794, 1474-1484 (2009).

Rathore A, Srivastava V, Srivastava KC, Tandon JS. Iridoid glucosides from *Nyctathes arbortristis*. *Phytochemistry* 29, 1917-1920 (1990).

Rathore A, Juneja RK, Tandon JS. An iridoid glucoside from *Nyctanthus arbortristis*. *Phytochemistry* 24, 1913-1917 (1989).

TH-1101_08610603

Ray S, Hazra B, Mittra B, Das A, Majumder HK. Diospyrin, a bisnaphthoquinone: a novel inhibitor of type I DNA topoisomerase of Leishmania donovani. *Molecular Pharmacology* 54, 994 (1998).

Reithinger R, Dujardin JC, Louzir H, Pirmez C, Alexander B, Brooker S. Cutaneous Leishmaniasis. *The Lancet Infectious Diseases* 7, 581-96 (2007)

Righetti PG. Charge-state and charge-continuum models in electrophoresis and isoelectric focusing of genetic variants. *Journal of Chromatography* 173(1), 1-5 (1979).

Rocha LG, Almeida JRGS, Macedo RO, Barbosa-Filho JM. A review of natural products with antileishmanial activity. *Phytomedicine* 12, 514–535 (2005).

Ross MR. Note on the bodies recently described by Leishman and Donovan. *The British Medical Journal*, 1261-1262 (1903).

Roy A, Ganguly A, BoseDasgupta S, Das BB, Pal C, Jaisankar P. Mitochondria-dependent reactive oxygen species-mediated programmed cell death induced by 3,3´-diindolylmethane through inhibition of F^0F^1-apx synthase in unicellular protozoan parasite *Leishmania donovani*. *Molecular Pharmacology* 74, 1292–1307 (2008).

Saeidnia S, Gohari AR, Uchiyama N, Ito M, Honda G, Kiuchi F. Two new monoterpene glycosides and trypanocidal terpenoids from *Dracocephalum kotschyi*. *Chemical and Pharmaceutical Bulletin* 52, 1249 (2004).

Saleheen D, Ali SA, Yasinzai MM. Antileishmanial activity of aqueous onion extract *in vitro*. *Fitoterapia* 75, 9–13 (2004).

Salem MM, Werbovetz KA. Antiprotozoal compounds from *Psorothamnus polydenius*. *Journal of Natural Products* 68, 108-11 (2005).

Salem MM, Werbovetz KA. Natural products from plants as drug candidates and lead compounds against Leishmaniasis and Trypanosomiasis. *Current Medicinal Chemistry*, 13, 2571-2598 (2006).

Saravanan P, Venkatesan SK, Mohan CG, Patra S, Dubey VK. Mitogen-activated protein kinase 4 of *Leishmania* parasite as a therapeutic target. *European Journal of Medicinal Chemistry* 45, 5662–5670 (2010).

Sarkar N, Singh AN, Dubey VK. Effect of curcumin on amyloidogenic property of molten globule-like intermediate state of 2,5-diketo-D-gluconate reductase A. *The Journal of Biological Chemistry* 390, 1057-1061(2009).

Saxena RS, Gupta B, Lata S. Tranquilizing, antihistaminic and purgative activity of *Nyctanthes arbortristis* leaf extract. *Journal of Ethnopharmacology* 81, 321-325 (2002).

Schirmer RH, Mueller JG, Krauth-Siegel RL. Disulfide-reductase inhibitors as chemotherapeutic agents: the design of drugs for trypanosomiasis and malaria. *Angewandte Chemie International Edition* 34,141–54 (1995).

TH-1101_08610603

Schonbrunn E, Eschenburg S, Luger K, Kabsch W, Amrhein, N. Structural basis for the interaction of the fluorescence probe 8-anilino-1-naphthalene sulfonate (ANS) with the antibiotic target MurA. *Proceedings of the National Academy of Sciences of the United States of America* 97, 6345-6349 (2000).

Semisotnov GV, Rodionova NA, Razgulyaev OI, Uversky VN, Gripas AF, Gilmanshin RI. Study of the "molten globule" intermediate state in protein folding by a hydrophobic fluorescent probe. *Biopolymers* 31, 119-128 (1991).

Sereno D, Lemerse JL. Axenically cultured amastigote forms as an *in vitro* model for investigation of antileishmanial agents. *Antimicrobial Agents and Chemotherapy* 41, 972–976 (1997).

Service RF. Nanotechnology takes aim at cancer. *Science* 310, 1132-1134 (2005).

Sett R, Basu N, Ghosh A, Das PK. Potential of doxorubicin as an antileishmanial agent. *Journal of Parasitology* 78, 350–354 (1992).

Shames SL, Fairlamb AH, Cerami A. Purification and characterization of trypanothione reductase from *Crithidia fasciculata*, a newly discovered member of the family of disulfide-containing flavoprotein reductases. *Biochemistry* 25, 3519–26 (1986).

Sharma N, Shukla AK, Das M and Dubey VK. Evaluation of plumbagin and its derivative as potential modulator of redox thiol metabolism of *Leishmania* parasite. *Parasitology Research* 110. 341-348 (2012).

Shukla AK, Singh BK, Patra S, Dubey VK. Rational approaches for drug designing against Leishmaniasis. *Applied Biochemistry and Biotechnology* 160, 2208–2218 (2010a).

Shukla AK[¥], Venkatesan SK[¥], Dubey VK. Molecular docking studies of selected tricyclic and quinone derivatives on trypanothione reductase of *Leishmania infantum*. *Journal of Computational Chemistry* 31, 2463-2472 (2010b) ([¥]Equal author).

Shukla AK, Patra S, Dubey VK. Deciphering molecular mechanism underlying antileishmanial activity of *Nyctanthes arbortristis*, an Indian medicinal plant. *Journal of Ethnopharmacology* 34, 996-998 (2011a).

Shukla AK, Patra S, Dubey VK. Evaluation of selected antitumor agents as subversive substrate and potential inhibitor of trypanothione reductase: an alternative chemotherapy of Leishmaniasis. *Molecular and Cellular Biochemistry* 352, 261-270 (2011b).

Shukla AK, Patra S, Dubey VK. Biophysical and Folding parameters of trypanothione reductase from *Leishmania infantum*. *Applied Biochemistry and Biotechnology* 165, 13-23 (2011c).

Sies H. Oxidative stress: oxidant and antioxidants. London: Academic Press, (1991).

Singh BK, Sarkar N, Jagannadham MV, Dubey VK. Modeled structure of trypanothione reductase of *Leishmania infantum*. *BMB Reports* 41, 444–447 (2008).

TH-1101_08610603

Singh BK, Dubey VK. *In silico* studies on tryparedoxin peroxidase of *Leishmania infantum*: structural aspects. *Current Pharmaceutical Biotechnology* 10, 626–630 (2009)

Singh BK, Sarkar N, Dubey VK. Modeled structure of trypanothione synthetase of *Leishmania infantum* for development of novel therapeutics for Leishmaniasis. *Current Trends in Biotechnology and Pharmacy* 2, 390–395 (2008).

Singh G, Dey CS. Induction of apoptosis-like cell death by pentamidine and doxorubicin through differential inhibition of topoisomerase II in arsenite-resistant *Leishmania donovani*. *Acta Tropica* 103, 172–185 (2007).

Singh N, Gupta R, Jaiswal AK, Sundar S, Dube A. Transgenic *Leishmania donovani* clinical isolates expressing green fluorescent protein constitutively for rapid and reliable *ex vivo* drug screening. *Journal of Antimicrobial Chemotherapy* 64, 370–374 (2009).

Singh N, Mishra PK, Kapil A, Arya KR, Maurya R, Dube A. Efficacy of *Desmodium gangeticum* extract and its fractions against experimental visceral Leishmaniasis. *Journal of Ethnopharmacology* 98, 83–88 (2005).

Sinha PK, Ranjan A, Singh VP, Das VN, Pandey K, Kumar N, Verma N, Lal CS, Sur D, Manna B, Bhattacharya SK. Visceral Leishmaniasis (Kala-Azar) the Bihar (India) perspective. *Journal of Infection* 53, 60–64 (2006).

Slappendel RJ, Ferrer L. In: C. E. Greene (Ed.), Infectious diseases of the dog and cat (pp. 450–458). Philadelphia: *WB Saunders Co* (1998).

Sundar S, Jha TK, Thakur CP, Sinha PK, Bhattacharya SK. Injectable paromomycin for visceral Leishmaniasis in India . *New England Journal of Medicine* 356, 2571–2581 (2007).

Takahashi M, Fuchino H, Satake M, Agatsuma Y, Sekita S. *In vitro* screening of leishmanicidal activity in myanmar timber extracts. *Biological and Pharmaceutical Bulletin* 27, 921(2004).

Tandon JS, Srivastava V, Guru PY. Iridoids: A new class of leishmanicidal agents from *Nyctanthes arbortristis*. *Journal of Natural Products* 54, 1102-1104 (1991).

Tardi PG, Boman NL, Cullis PR. Liposomal doxorubicin. *Journal of Drug Targeting* 4, 129–140 (1996).

Tempone AG, Borboremab SE, de Andrade HF, Amorim Gualda NC, Yogi A, Carvalho CS, Bachiega D, Lupo FN, Bonottoc SV, Fischer DC. Antiprotozoal activity of Brazilian plant extracts from isoquinoline alkaloid-producing families. *Phytomedicine* 12, 382–390 (2005).

Thiem DA, Sneden AT, Khan SI, Tekwani BL. Bisnortriterpenes from *Salacia madagascariensis. Journal of Natural Products* 68, 251 (2005).

Thouvenel C, Hocquemiller R, Fournet A. Leishmanicidal activity of two canthin-6-one alkaloids, two major constituents of *Zanthoxylum chiloperone* var. *angustifolium. Journal of Ethnopharmacology* 80, 199–202 (2002).

TH-1101_08610603

Thronalley PJ, Ladan MJ, Ridgway SJS, Kang Y. Antitumor activity of s-(p-bromobenzyl) glutathione diesters *in vitro*: a structure-activity study. *Journal of Medicinal Chemistry* 39, 3409–3411(1996).

Torchilin VP, Trubetskoy VS. Which polymers can make nanoparticulate drug carriers long-circulating? *Advanced Drug Delivery Reviews* 16, 141-155 (1995).

Torres-Santos EC, Sampaio-Santos MI, Buckner FS, Yokoyama K, Gelb M, Urbina JA, Rossi-Bergmann B. Altered sterol profile induced in Leishmania amazonensis by a natural dihydroxymethoxylated chalcone. *Journal of Antimicrobial Chemotherapy* 63, 469–472 (2009).

Tromelin A, Moutiez M, Meziane-Cherif D, Aumercier M, Tartar A, Sergheraert C. Synthesis of non reducible inhibitors for trypanothione reductase from *Trypanosoma cruzi*. *Bioorganic and Medicinal Chemistry* 3, 1971–1976 (1993).

Venkatesan SK, Saudagar P, Shukla AK, Dubey VK. Screening natural products database for identification of potential antileishmanial chemotherapeutic agents. *Interdisciplinary Sciences: Computational Life Sciences* 3, 1-15 (2011).

Vickers TJ, Greig N, Fairlamb AH. A trypanothione dependant glyoxylase-I with a prokaryotic ancestry in *Leishmania major*. *Proceedings of the National Academy of Sciences of the United States of America* 101, 13186–13191 (2004).

Wallace AC, Laskowski RA, Thornton JM. LIGPLOT, A program to generate schematic diagrams of protein-ligand interactions. *Protein Engineering, Design and Selection* 8, 127–134 (1995).

WHO/TDR/Crump. Progress report on elimination of neglected tropical diseases. *WHO Bulletin review* (2010).

WHO/TRS/949. Control of the Leishmaniasis: report of a meeting of the WHO Expert Committee on the control of Leishmaniasis, Geneva, 2010.

Williams and Jr CH. Lipoamide dehydrogenase, glutathione reductase, thioredoxin reductase and mercuric ion reductase. A family of flavoenzyme transhydrogenase. *Chemistry and Biochemistry of flavoenzymes* 3, 121-211 (1992)

Xiao R Z, Zeng ZW, Zhou G L, Wang JJ, Li FZ, Wang AM. Recent advances in PEG–PLA block copolymer nanoparticles. *International Journal of Nanomedicine* 5, 1057-1065 (2010).

Yi Y, Kim JH, Kang HW, Oh HS, Kim SW, Seo MH. A Polymeric NP Consisting of mPEG-PLA-Toco and PLMA-COONa as a drug carrier: Improvements in cellular uptake and biodistribution. *Pharmaceutical Research* 22, 200-208 (2005).

Yokoyama M, Fukushima S, Uchara R, Okamoto K. Characterization of physical entrapment and chemical conjugation of adriamycin in polymeric micelles and their design for in vivo delivery to a solid tumor. *Journal of Controlled Release* 50, 79-92 (1998).

TH-1101_08610603

Zhang Y, Bond CS, Bailey S, Cunningham ML, Fairlamb AH, Hunter WN. The crystal structure of trypanothione reductase from the human pathogen Trypanosoma cruzi at 2.3 A resolution. *Protein Science* 5, 52-61(1996).

Zheng X, Kan B, Gou M, Fu S, Zhang J, Men K, Chen L, Luo F, Zhao Y, Zhao X, Wei Y, Qian Z. Preparation of MPEG-PLA nanoparticle for honokiol delivery *in vitro*. *International Journal of Pharmaceutics* 386, 262-267 (2010).

Website: http://pfs.med.stu.edu.cn/

WHO/TDR/Crump: website-http://www.who.int/tdr/news/2010/ntd-elimination/en/

Website: http://www.dpd.cdc.gov/dpdx

TH-1101_08610603

Publications

A. Publications (In Peer Reviewed Journals)

Published/ Accepted

1. **Anil Kumar Shukla**, Sanjukta Patra and Vikash Kumar Dubey. PEGylated nanospheres encapsulating antileishmanial drugs for their specific macrophage targeting, reduced toxicity and deliberate intracellular release. Vector Borne and Zoonotic Diseases, 2012, Accepted.

2. **Anil Kumar Shukla,** Sanjukta Patra and Vikash Kumar Dubey. Iridoid glucosides from *Nyctanthes arbortristis* result in increased Reactive Oxygen Species (ROS) and cellular redox homeostasis imbalance in Leishmania parasite. European Journal of Medicinal Biochemistry, 10.1016/j.ejmech.2012.04.034.

3. **Anil Kumar Shukla**, Sanjukta Patra and Vikash Kumar Dubey. Evaluation of selected antitumor agents as subversive substrate and potential inhibitor of trypanothione reductase: An alternative approach for chemotherapy of Leishmaniasis. Molecular and Cellular Biochemistry, 2011, 352, 261-70. ***Research Highlight of the article published in Nature India***

4. **Anil Kumar Shukla**, Sanjukta Patra and Vikash Kumar Dubey. Deciphering molecular mechanism underlying antileishmanial activity of *Nyctanthes arbortristis*, an Indian medicinal plant. Journal of Ethnopharmacology, 2011, 134, 996-998.

5. **Anil Kumar Shukla**, Sanjukta Patra and Vikash Kumar Dubey. Biophysical and Folding parameters of Trypanothione reductase from *Leishmania infantum*. Applied Biochemistry and Biotechnology 2011, 165, 13-23.

6. **Anil Kumar Shukla**[#], Santhosh K Venkatesan[#] and Vikash Kumar Dubey. Molecular docking studies of selected tricyclic and quinone derivatives on trypanothione reductase of *Leishmania infantum*. Journal of Computational Chemistry. 2010, 31, 2463-2472 ([#]Equal contribution). ***Research Highlight of the article published in Nature India***

7. **Anil Kumar Shukla**, Bishal Kumar Singh and Vikash Kumar Dubey. Rational approaches for drug designing against Leishmaniasis. Applied Biochemistry and Biotechnology, 2010, 160, 2208-2218.

8. **Anil Kumar Shukla**, Utpal Bora and Vikash Kumar Dubey. Functional Adaptations in Fibroblast Growth Factor (FGFs) Family. Journal of Proteins and Proteomics, 2009, 1, 11-13.

9. Neha Sharma, **Anil Kumar Shukla**, Mousumi Das and Vikash Kumar Dubey. Evaluation of plumbagin and its derivative as potential modulator of redox thiol metabolism of *Leishmania* parasite. Parasitology Research. 2012, 110. 341-348.

10. Santhosh K Venkatesan, Prakash Saudagar, **Anil Kumar Shukla** and Vikash Kumar Dubey. Screening natural products database for identification of potential antileishmanial chemotherapeutic agents. Interdisciplinary Sciences: Computational Life Sciences, 2011, 3, 1-15.

11. Syed Baquer Rizvi, **Anil Kumar Shukla** and Vikash Kumar Dubey. A simple method based on multiple alignment and phylogeny to derive a correlation between the protein fold and sequence via motif search. Interdisciplinary Sciences: Computational Life Sciences, 2009, 1, 235-243.

12. Abhay Narain Singh, **Anil Kumar Shukla**, M.V. Jagannadham and Vikash Kumar Dubey. Purification of a novel cysteine protease, procerain B, from *Calotropis procera* with distinct characteristics compared to procerain. Process Biochemistry, 2010, 45, 399-406.

TH-1101_08610603

B. Conferences/Workshops

1. **Anil Kumar Shukla,** Sanjukta Patra and Vikash Kumar Dubey. Redox metabolism of Leishmania parasite: Ideal target for drug development against leishmaniasis.15th International Congress on Infectious Diseases at Centara Grand, Bangkok, Thailand, Jun. 13-16, 2012

2. **Anil Kumar Shukla** and Vikash Kumar Dubey. Science and Communication Workshop (SciComm) organized by Wellcome Trust-DBT India Alliance at Golkonda Resorts, Hyderabad, India, Mar. 28-30, 2012

3. **Anil Kumar Shukla,** Sanjukta Patra and Vikash Kumar Dubey. Targeting redox system of Leishmania parasite for drug discovery.18th International Conference of ISCB-2012 at IASST Guwahati, India, Jan. 28-30, 2012

4. **Anil Kumar Shukla** and Vikash Kumar Dubey. Teaching and Research in Leading Indian Institutes: Scope of Improvements. Young Researchers Conclave-2011 at IIT Gandhinagar, India, Dec. 27-28, 2011

5. **Anil Kumar Shukla** and Vikash Kumar Dubey. Synthesis of PEGylated Nanospheres encapsulating doxorubicin and mitomycin C for their specific macrophage targeting, reduced toxicity and enhanced antileishmanial activity. European Molecular Biology Organization (EMBO) meeting 2011 at Vienna, Austria, Sept. 10-13, 2011

6. **Anil Kumar Shukla** and Vikash Kumar Dubey. Underlying the Anti-leishmanial activity of *Nyctanthes arbortristis*. 4th International conference on 'Current trends in drug discovery research. Central Drug Research Institute, Lucknow. Feb. 17-21, 2010.

7. **Anil Kumar Shukla**, Santhosh Kannan V. and Vikash Kumar Dubey. Studies on Trypanothione Reductase from *Leishmania infantum*. 78th Annual Meeting of Society of Biological Chemists, India held at National Centre for Cell Science and University of Pune, Oct. 30-Nov. 1, 2009.

8. **Anil Kumar Shukla** and Vikash Kumar Dubey. Studies of biochemical properties of Trypanothione reductase from *Leishmania infantum*. IncoFIBS-2010, NIT Rourkela, Oct. 1-3, 2010.

9. Vikash Kumar Dubey, **Anil Kumar Shukla** and Saudagar Prakash. Current trends in anti-leishmanial drug discovery. International conference on new horizons in biotechnology (BRSI). Trivandram, Nov. 21-24, 2011 (Invited talk).

10. Ruchika Bharadwaj, **Anil Kumar Shukla** and Vikash Kumar Dubey. Synthesis of Chitosan-PEG coated gold nanoparticles entrapping doxorubicin for evaluation of antileishmanial activity and targeted delivery to macrophages. 80th Annual Meeting of Society of Biological Chemists, India held at CIMAP, Lucknow, Nov. 12-15, 2011.

11. Neha Sharma, **Anil Kumar Shukla** and Vikash Kumar Dubey.Evaluation of Plumbagin and its derivative as potential modulator of redox thiol metabolism of *Leishmania* parasite World Congress on Biotechnology, Hyderabad, Mar. 21-23, 2011

12. Santhosh Kannan V, **Anil Kumar Shukla** and Vikash Kumar Dubey*. Structure based virtual screening approach to identify potential inhibitors of Trypanothione reductase from Leishmania infantum. 78th Annual Meeting of Society of Biological Chemists, India held at National Centre for Cell Science, Oct. 30-Nov. 1, 2009.

13. Abhay Narain Singh, **Anil Kumar Shukla** and Vikash Kumar Dubey*. Procerain B a novel cysteine protease from the latex of medicinal plant *Calotropis procera*. 78th Annual Meeting of Society of Biological Chemists, India held at National Centre for Cell Science, Oct. 30-Nov. 1, 2009.

TH-1101_08610603

C. Patent

1. Vikash Kumar Dubey, Sanjukta Patra, **Anil Kumar Shukla** and Santhosh Kannan. Iridoid glucosides from *Nyctanthes arbortristis* as new class of inhibitor of Trypanothione reductase of *Leishmania* parasite. (306/KOL/2010)

TH-1101_08610603